الجمهورية الجزائرية الديمقراطية الشعبية

MINISTRY OF HIGHER EDUCATION AND SCIENTIFIC RESEARCH

YAHIA FARES UNIVERSITY OF MEDEA

CENTER FOR DEVELOPMENT OF ADVANCED TECHNOLOGIES

FACULTY OF TECHNOLOGY

Department of Electrical Engineering

Master's Final Project

Field of study: Telecommunications

Specialty: Telecommunications Systems

Modeling and Simulation of a New Electromagnetic Absorbing Material: Application in Anechoic Chambers

Presented by:

LAROUSSI Manel
BENKESSIRAT Khadidja

Proposed and Directed by:

Dr. MENASRI Wahiba

Dr. ZOUBIRI Bachir

Promotion 2025

ACKNOWLEDGEMENT

First and foremost, our deepest gratitude goes to God, the Almighty and Most Merciful, for granting us the strength and perseverance to complete this work.

We extend our sincere thanks to our supervisors, **Mrs. Menasri Wahiba** and **Mr**. **Zoubiri Bachir**, for their continuous guidance, support, and encouragement throughout this project.

We also express our heartfelt appreciation to the **faculty of science and technology** at **Yahia Fares University** for the knowledge and education provided over the course of our academic journey.

A special thanks goes to the **CDTA** for giving us the opportunity to carry out this work within its facilities, and for providing a professional and resource rich environment.

Lastly, we are grateful to everyone who contributed to this project through valuable information, documentation, or support. We are proud to have completed this work and truly appreciative of all those who helped make it possible.

Dedication

Je n'aurais jamais imaginé arriver là où je suis aujourd'hui. La route est encore longue, mais le chemin déjà parcouru me rend fière.

Toute ma gratitude va d'abord à Dieu, le tout puissant, pour m'avoir donné la force, la patience et la foi nécessaires pour avancer.

To my father, my guardian angel, my number one supporter, the best dad I could ever ask for, à ma mamounette, je ne pourrai jamais vous rendre tout ce que vous avez fait pour moi, pour nous tous.

A mes frères et soeurs, je suis aussi fière de vous que vous l'êtes de moi. Je vous aime très fort. A mamaya, papano, mes chères tantes et oncle, et mimine merci d'avoir été là pour me remonter le moral quand j'en avais besoin.

To Hanan, my favorite cousin I purple you.

To Eya and Alaa, my lovely ladies thank you for being part of this journey. Without you and your support, I don't think I could've made it through.

A Khadidja, mon binôme, ma soeur d'amour: WE MADE IT.

Last but not least, I wanna thank me, I wanna thank me for believing in me, I wanna thank me for doing all this hard work, I wanna thank me for having no days off, I wanna thank me for never quitting, I wanna thank me for always being a giver and trying to give more than I receive, I wanna thank me for trying to do more right than wrong. I wanna thank me for just being me at all times.

MEOWS

LAROUSSI MANEL.

Dedication

I dedicate this work first to God, for the most precious gift "life"and the opportunity to leave something meaningful behind.

To the little girl I once was uncertain, quiet, and full of doubt thank you for not giving up. You made it here.

To my parents, for their unconditional love, support, and countless sacrifices. Every step I took was possible because of the strength you gave me.

To my brother and my sister, thank you for your constant encouragement and presence, which have meant more than words can say.

To my binome, who became more than just a teammate you became a sister to me in every sense. Thank you for walking beside me through this journey.To the family who raised her, and who welcomed me as one of their own your warmth and kindness will always stay with me.

To Alaa, my dear friend and constant source of happiness your laughter and light brought balance to even the toughest days.

To Minouche, my little cat, my silent comfort, who made even the hardest days feel softer just by being there.

This work carries a part of each of you. With all my heart thank you.

BENKESSIRAT KHADIDJA.

ملخص

يعرض هذا العمل تصميم ومحاكاة والتحقق التجريبي من ممتصات كهرومغناطيسية واسعة النطاق تعمل ضمن المجال 2–18GHz ، والموجهة لتطبيقات غرف عديمة الصدى. تم نمذجة عدة أشكال (هرمي، مخروطي، هجين، وطرف دائري) باستخدام برنامجCST Studio Suite ، وتقييمها بثلاث مواد: الحديد الكربونيلي، الفرايتNiZn ، والجرافيت. تم اختبار تسعة تركيبات من الارتفاع والحجم القاعدي لكل شكل من أجل تحديد المعلمات الهندسية التي توفر أفضل أداء في الامتصاص. أظهرت المحاكاة أن البنى الهرمية قدّمت أداءً أفضل بشكل عام، خاصة عند استخدام الجرافيت في الترددات العالية. كما أظهر الممتص الهجين الذي يجمع بين الفرايت والحديد الكربونيلي نتائج واعدة. وقد أكدت القياسات التجريبية باستخدام دليل موجي مملوء بالجرافيت الاتجاهات التي أظهرتها المحاكاة .يشكّل هذا العمل أساسًا لعمليات تحسين مستقبلية وتصنيع أولي للممتصات .

الكلمات المفتاحية: غرفة عديمة الصدى، ممتص كهرومغناطيسي، نطاق واسع، مادة ماصة، قياس دليل موجي.

ABSTRACT

This work presents the design, simulation, and experimental validation of broadband electromagnetic absorbers for the 2-18GHz range, targeting applications in anechoic chambers. Several geometries (pyramidal, conical, hybrid, and rounded tip) were modeled using CST Studio Suite and evaluated with three materials: carbonyl iron, NiZn ferrite, and graphite. For each shape, nine combinations of height and base size were tested to identify the geometric parameters that provide the best absorption performance. Simulations showed that pyramidal structures generally provided better performance, especially with graphite at higher frequencies. A hybrid absorber combining ferrite and carbonyl iron also showed promising results. Experimental measurements using a graphite filled waveguide confirmed the simulation trends. This work provides a foundation for future absorber optimization and physical prototyping.

Keywords: Anechoic chamber, electromagnetic absorber, broadband, absorbing material, waveguide measurement.

RESUME

Ce travail présente la conception, la simulation et la validation expérimentale d'absorbeurs électromagnétiques à large bande pour la plage 2–18 GHz, destinés aux chambres anéchoïques. Plusieurs géométries (pyramidale, conique, hybride et à sommet arrondi) ont été modélisées à l'aide de CST Studio Suite et évaluées avec trois matériaux : carbonyle de fer, ferrite NiZn et graphite. Pour chaque géométrie, neuf combinaisons de hauteur et de base ont été testées afin d'identifier les paramètres géométriques offrant la meilleure absorption. Les simulations ont montré que les structures pyramidales offraient généralement de meilleures performances, notamment avec le graphite à haute fréquence. Un absorbeur hybride combinant la ferrite et le carbonyle de fer a également montré des résultats prometteurs. Des mesures expérimentales, réalisées avec un guide d'onde rempli de graphite, ont confirmé les tendances de simulation. Ce travail constitue une base pour l'optimisation future des absorbeurs et leur prototypage physique.

Mots-clés : Chambre anéchoïque, absorbeur électromagnétique, large bande, matériau absorbant, mesure en guide d'onde.

List of figures

CHAPTER1: OVERVIEW OF ANECHOIC CHAMBER

Figure 1.1: Radio frequency anechoic chamber. 4

Figure 1.2: Fully anechoic chamber. 5

Figure 1.3: Semi-anechoic chamber. 6

Figure 1.4: An example setup for antenna radiation measurement. 8

Figure 1.5: Schematic representation of the electromagnetic wave absorption and reflection. 10

CHAPTER2: ELECTROMAGNETIC ABSORBERS

Figure 2.1: Ferrite tiles. 18

Figure 2.2: Mounted ferrite tile. 19

Figure 2.3: Foam pyramid absorbers. 20

Figure 2.4: Reflections in pyramidal absorbers. 21

Figure 2.5: Transformation of energy into heat. 21

Figure 2.6: An infinite 2D array of pyramidal absorbers is modeled using periodic boundary conditions on the sides of one unit cell. 24

Figure 2.7: Foam based wedge absorber. 25

Figure 2.8: Conical absorber. 25

Figure 2.9: Basic characteristics of electromagnetic wave inside the anechoic chamber. 29

CHAPTER3: RESULTS and DISCUSSION

Figure 3.1: Material definition for carbonyl iron (left) and NiZn ferrite (right). 35

Figure 3.2: Material definition for graphite. 36

Figure 3.3: 3D geometry of the pyramidal absorber. 36

Figure 3.4: Close-up view of the pyramidal absorber tip and excitation port. 37

Figure 3.5: Carbonyl Iron pyramidal absorbers. 38

Figure 3.6: Simulated S11 curves for all carbonyl iron based pyramidal absorbers. 39

Figure 3.7: Reflection coefficient S11 curves of the three best performing configurations. 39

Figure 3.8: NiZn ferrite pyramidal absorbers geometries combined. 40

Figure 3.9: Simulated S11 curves for all NiZn ferrite based pyramidal absorbers. 40

Figure 3.10: Best performing NiZn absorbers based on S11 results. 41

Figure 3.11: Pyramidal absorber geometries with graphite. 41

Figure 3.12: S11 curves for the graphite pyramidal absorbers. 42

Figure 3.13: S11 curves for the three best performing graphite absorber geometries. 42

Figure 3.14: S11 curves of the best absorber configurations: three per material. 43

Figure 3.15: S11 curves comparison at 2GHz. 43

Figure 3.16: S11 curves comparison at 8GHz. 44

Figure 3.17: S11 curves comparison at 10GHz and beyond. 44

Figure 3.18: 3D geometry of the conical absorber. 45

Figure 3.19: Close-up view of the conical absorber tip and excitation port. 45

Figure 3.20: Carbonyl iron conical absorbers with all height base combinations. 46

Figure 3.21: S11 curves for the nine carbonyl iron conical absorber configurations. 46

Figure 3.22: S11 curves of the top three performing conical absorbers. 47

Figure 3.23: NiZn ferrite conical absorbers geometries combines. 47

Figure 3.24: S11 results for the nine NiZn ferrite conical absorbers. 48

Figure 3.25: Top performing NiZn ferrite absorbers. 48

Figure 3.26: Conical absorber geometries with graphite. 49

Figure 3.27: S11 results of the graphite based conical absorbers. 49

Figure 3.28: Top three S11 curves for graphite based conical absorbers. 50

Figure 3.29: S11 curves of the best pyramidal absorber configurations: three per material. 50

Figure 3.30: S11 curves response at 2GHz (top) and 8GHz (bottom). 51

Figure 3.31: S11 curves response at 14GHz. 51

Figure 3.32: S11 curves response at 18GHz. 52

Figure 3.33: 3D geometry of the hybrid pyramidal absorber. 52

Figure 3.34: Comparison of S11 curves for carbonyl iron and NiZn ferrite absorbers. 53

Figure 3.35: Comparison between S11 performances of NiZn ferrite, carbonyl iron, and hybrid pyramidal absorbers. 53

Figure 3.36: Geometrical comparison between standard tip (left) and rounded tip (right) pyramidal absorbers. 54

Figure 3.37: S11 comparison carbonyl iron based pyramidal absorber : rounded tip vs standard tip. 54

Figure 3.38: S11 comparison NiZn based pyramidal absorber : rounded tip vs standard tip. 55

Figure 3.39: S11 comparison graphite based pyramidal absorber : rounded tip vs standard tip. 55

Figure 3.40: Geometry comparison between conical (left) and pyramidal (right) absorber structures. 56

Figure 3.41: Comparison of top performing pyramid, conical absorbers carbonyl iron based. 56

Figure 3.42: Comparison of top performing pyramid, conical absorbers NiZn ferrite based. 57

Figure 3.43: Comparison of top performing pyramid, conical absorbers graphite based. 57

Figure 3.44: Graphite in its two forms. 59

Figure 3.45: Graphite holder. 59

Figure 3.46: Multiple side views of the waveguide. 60

Figure 3.47: Full 3D view of the waveguide model used for simulation. 60

Figure 3.48: Close-up view of the SMA connector. 61

Figure 3.49: Waveguides S11 and S21 results. 61

Figure 3.50: Analog measurement setup. 62

Figure 3.51: VNA measurement setups : empty PLA holder (left), graphite filled holder (right). 63

Figure 3.52: Measured S11 and S21 for the empty PLA holder. 63

Figure 3.53: CST model of the graphite block between waveguides. 64

Figure 3.54: Comparison of S11 and S21 CST vs VNA. 64

List of tables

CHAPTER2: ELECTROMAGNETIC ABSORBERS

Table 2.1: Comparison between material composition of absorbers. 23

Table 2.2: Comparative overview of typical absorber geometries..... 28

CHAPTER3: RESULTS and DISCUSSION

Table 3.1: Labeled configurations of carbonyl iron based pyramidal absorbers. 38

Table 3.2: Summary of top performing configurations by shape and material..... 58

List of acronyms and symbols

Acronyms

3D: 3 Dimension.

5G: 5^{th} Generation.

AC: Anechoic Chamber.

CST: Computer Simulation Technology.

dB: decibel.

EM: Electromagnetic.

EMC: Electromagnetic Compatibility.

EMI: Electromagnetic Interference.

GHz: Giga Hertz.

MHz: Mega Hertz.

NiZn: Nickel-Zinc.

PEC: Perfect Electrical Conductor.

PLA: Polylactic Acid.

RCS: Radar Cross Sections.

RF: Radio Frequency.

SE: Shielding Effectiveness.

S-parameter: Scattering parameters.

SMA: SubMiniature version A.

VNA: Vector Network Analyzer.

Symbols

f: Frequency (Hz)

ε: Absolute permittivity (F/m)

μ: Absolute permeability (H/m)

ε_o: Permittivity of free space $\approx 8.854 \times 10^{-12}$ (F/m)

μ_o: Permeability of free space $\approx 4\pi \times 10^{-7}$ (H/m)

ε_r: Relative permittivity

μ_r: Relative permeability

ε': Real part of permittivity (F/m)

ε": Imaginary part of permittivity (F/m)

μ': Real part of permeability (H/m)

μ": Imaginary part of permeability (H/m)

Z_0: Characteristic impedance of free space ≈ 377 (Ω)

Z: Impedance of the material (Ω)

Γ: Reflection coefficient

T : Transmission coefficient

S_{11}: Reflection S-parameter

S_{21}: Transmission S-parameter

λ_0: Wavelength in free space (m)

λc: Cutoff wavelength of the waveguide (m)

$\lambda_0 g$: Guided wavelength in the waveguide (m)

γ: Propagation constant (1/m)

Λ: Auxiliary term related to γ (1/m)

n: Refractive index

d: Thickness of the sample (m)

ω: Angular frequency = 2πf (rad/s)

$f(\varepsilon_r, \mu_r)$: Error function

j: Imaginary unit : $j^2 = -1$

h: Height (mm)

b: Base (mm)

Table of Contents

ملخص	**iv**
ABSTRACT	**v**
RESUME	**vi**
List of figures	**vii**
List of tables	**x**
List of acronyms and symbols	**xi**
Table of Contents	**xiii**
General Introduction	**1**
Chapter1: OVERVIEW OF ANECHOIC CHAMBER	**3**
1.1 Introduction	3
1.2 Definition and purpose of AC	3
1.2.1 A brief history of AC	3
1.2.2 Introduction to AC	3
1.2.3 EM behavior inside AC	4
1.3 Structure and types of AC	5
1.3.1 Types of AC	5
1.3.1.1 Fully AC	5
1.3.1.2 Semi AC	6
1.3.2 Main components of AC	6
1.3.2.1 Chamber walls and shielding	6
1.3.2.2 Absorbing materials	7
1.3.2.3 Antenna positioners and measurement equipment	7
1.3.3 Shielding and isolation techniques	8
1.3.3.1 Faraday cages and RF shielding	8
1.3.3.2 Multi-layer shielding for enhanced protection	8
1.3.3.3 Measuring shielding effectiveness	9
1.4 Absorption phenomena in AC	9
1.4.1 Interaction of EM waves with materials	9
1.4.2 Mechanisms of EM waves absorption	10
1.4.2.1 Dielectric losses	10
1.4.2.2 Magnetic losses	11

1.4.2.3 Eddy current and conduction losses 11
1.4.2.4 Influence of material thickness on absorption efficiency 11
1.4.3 Factors influencing absorption efficiency 12
1.4.3.1 Material composition and electrical properties 12
1.4.3.2 Chamber geometry and absorber placement 12
1.5 Applications of AC 12
1.5.1 Antenna testing and characterization 12
1.5.2 EMC testing 13
1.5.3 Radar and stealth technology applications 13
1.5.4 Research and development in EM 13
1.6 Conclusion 14
CHAPTER2: ELECTROMAGNETIC ABSORBERS 16
2.1 Introduction 16
2.2 Definition and classification of absorbers 16
2.2.1 Absorber overview 16
2.2.2 Classification of absorbers 16
2.2.2.1 Classification by type of wave absorbed 16
2.2.2.2 Classification by absorption mechanism 17
2.2.2.3 Classification by material composition 17
2.3 Commercially available absorbers 18
2.3.1 Ferrite tiles 18
2.3.1.1 Structure and operating principle 18
2.3.1.2 Composition and physical configuration 18
2.3.1.3 Applications of ferrite tiles 19
2.3.2 Pyramidal absorbers 19
2.3.2.1 Structure, composition, and characteristics of pyramidal absorbers 19
2.3.2.2 Operating principle 20
2.3.2.3 Applications of pyramidal absorbers 21
2.4 Influence of material composition on absorption 21
2.4.1 Dielectric Materials 22
2.4.2 Magnetic materials 22
2.4.3 Composite materials 23
2.4.4 Comparison by material composition 23

2.5 Influence of geometry on absorption performance 23
2.5.1 Common absorbers geometries 24
2.5.1.1 Pyramidal absorbers 24
2.5.1.2 Wedge absorbers 24
2.5.1.3 Conical absorbers 25
2.5.2 Impact of geometry on wave interaction 25
2.5.3 Frequency dependent behavior 26
2.5.4 Performance metrics 26
2.6 Permittivity and permeability 29
2.6.1 Extraction of ε and μ from S-parameters 30
2.6.1.1 Nicolson Ross Weir (NRW) 30
2.6.2 Transmission/Reflection (T/R) 31
2.6.3 Robust inverse (Baker-Jarvis) 31
2.7 Conclusion 32
CHAPTER3: RESULTS and DISCUSSION 35
3.1 Introduction 35
3.2 Simulation setup 35
3.2.1 An overview of CST Studio Suite 35
3.2.2 Materials and dispersion models 35
3.2.3 Geometry and simulation matrix 36
3.3 Absorber shapes and results 36
3.3.1 Pyramidal absorber 36
3.3.1.1 Carbonyl iron based pyramidal absorber 38
3.3.1.2 NiZn ferrite based pyramidal absorber 40
3.3.1.3 Graphite based pyramidal absorber 41
3.3.1.4 Comparative analysis of the three materials: 43
3.3.2 Conical absorber 44
3.3.2.1 Carbonyl iron based conical absorber 46
3.3.2.2 NiZn ferrite based conical absorber 47
3.3.2.3 Graphite based conical absorber 49
3.3.2.4 Conical absorber: comparative analysis of the three materials: 50
3.3.3 Hybrid absorber 52
3.3.4 Rounded tip pyramidal absorber 54

3.3.4.1 NiZn ferrite based rounded tip vs standard tip 55
3.3.4.2 Graphite based rounded tip vs standard tip 55
3.3.5 Pyramidal vs conical absorbers: performance comparison 56
3.3.5.1 Carbonyl iron based comparison 56
3.3.5.2 NiZn ferrite based comparison 57
3.3.5.3 Graphite based comparison 57
3.3.5.4 Analysis 58
3.4 Realization and experimental validation 59
3.4.1 Waveguide design and simulation 60
3.4.2 Realization and measurement setup 61
3.4.2.1 Initial testing with analog instruments 62
3.4.2.2 VNA measurement 62
3.4.2.3 CST simulation of the graphite filled waveguide 63
3.5 Conclusion 65
General conclusion **66**
References **67**

General Introduction

The control and suppression of unwanted electromagnetic reflections is essential in areas such as antenna measurement, stealth technology, and electromagnetic compatibility testing. Anechoic chambers are specifically designed to provide controlled, reflection-free environments using broadband electromagnetic absorbers [1]. These absorbers rely on material losses and structural geometries to dissipate incident waves over a wide frequency range.

This study focuses on the design, simulation, and validation of absorber structure intended for use in 2-18GHz frequency band. Several geometries were explored using CST Studio Suite, including pyramidal and conical shapes, along with advanced variants such as hybrid structure and rounded-tip modifications. Three materials were tested (carbonyl iron, NiZn ferrite, and graphite) to evaluate their electromagnetic performance under identical geometric conditions.

To complement the simulation work, a measurement setup was developed using custom built waveguides and graphite powder. Experimental data was collected using both analog detector and vector network analyzer, allowing for direct comparison with simulated S-parameters.

This project is structured as follow:

Chapter 1 provides an overview of anechoic chamber, their functional role in electromagnetic testing and the importance of absorber design.

Chapter 2 presents a technical review of absorber materials and structures, including key electromagnetic properties and methods for extracting permittivity and permeability from S-parameter measurements.

Chapter 3 outlines the simulation methodology and result, followed by experimental validation. This includes material modeling, geometry simulation, shape optimization, and absorber comparisons. Its concludes with the experimental realization and validation of the graphite based absorber using waveguide measurements.

CHAPTER 1

OVERVIEW OF ANECHOIC CHAMBERS

1.1 Introduction

Anechoic chambers (AC) provide a controlled environment for electromagnetic (EM) testing and research, by eliminating reflections and external interference. These chambers are widely used in telecommunications, aerospace, automotive, and defense industries for testing antennas, electronic devices, and radar systems. This chapter introduces the purpose and structure of AC, covering their types, key components, and shielding techniques. It also explores wave absorption mechanisms and highlights their main applications, such as antenna testing, electromagnetic compatibility (EMC) compliance, and radar technology.

1.2 Definition and purpose of AC

1.2.1 A brief history of AC

AC were developed back in the mid-20th century by researchers who wanted to create controlled conditions for EM and acoustic wave studying.

- **World War II:** The first EM AC was developed for military radar research. Scientists required a way to evaluate aircraft radar cross sections (RCS) without interfering with external signals [2].
- **1950s and 1960s:** The telecommunications and aerospace industries used AC to test antennas, satellite components, and radio frequency (RF) systems. Over time, developments in absorbing material such as ferrite tiles and pyramidal absorbers significantly enhanced chamber performance, enabling operations over a wider frequency spectrum [2].
- **Present day:** AC are critical in telecommunications, automotive, aerospace, and defense industries, enabling applications such as EMC testing, antenna analysis, and stealth technology research [2].

1.2.2 Introduction to AC

AC as shown in Figure 1.1 is a specialized facility designed to eliminate reflections of EM or sound waves, creating a controlled testing environment. These chambers are used in research and development to ensure precise measurements free from external interference [1].

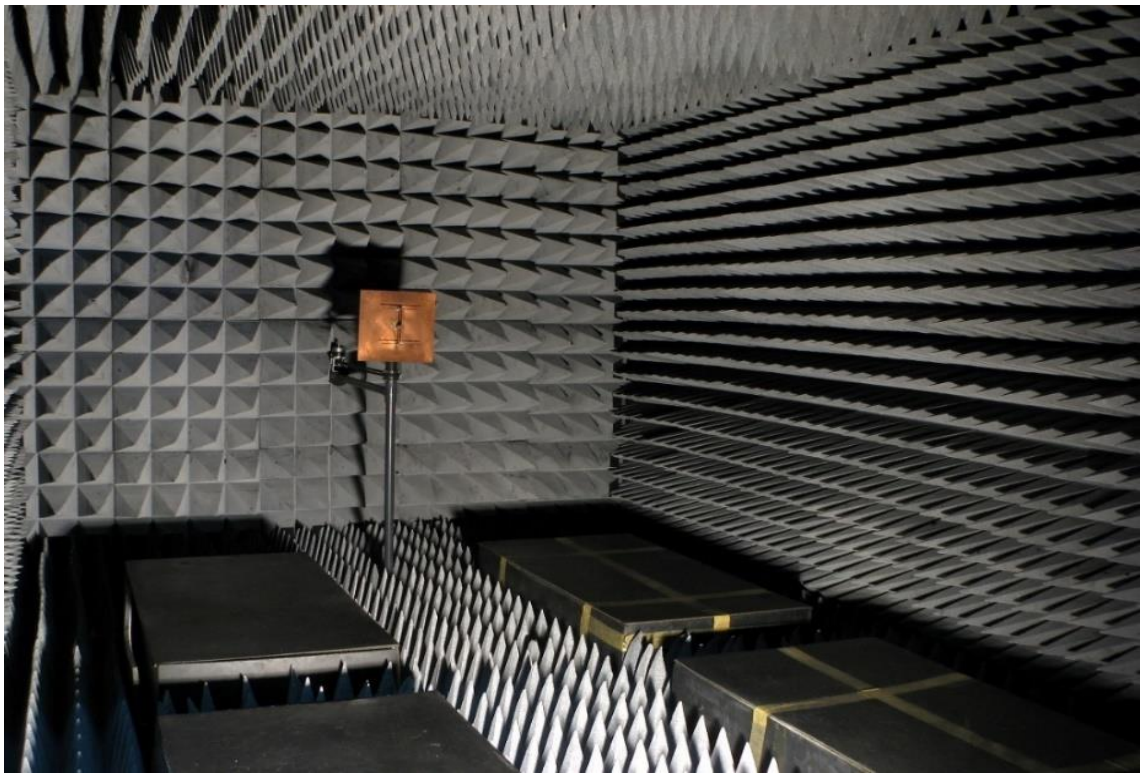


Figure 1.1: Radio frequency anechoic chamber**.**

There are three primary types of AC:

- **Acoustic AC:** Used for sound wave testing, commonly found in audio engineering, noise reduction studies, and acoustic research. Their Walls, ceiling, and floor are lined with sound absorbing materials to simulate a free-field environment.
- **EM chambers:** Designed for RF and microwave testing. They are critical in applications such as wireless communication, antenna characterization, radar testing, and material analysis. Their interior surfaces are lined with RF absorbers to prevent reflections and simulate open space conditions.
- **EMC chambers:** EMC chambers are specialized EM AC used to test the EMC and immunity of electronic devices. They help ensure that equipment complies with regulatory standards by evaluating emission levels and susceptibility. EMC chambers are vital in automotive, aerospace, medical, and consumer electronics industries.

1.2.3 EM behavior inside AC

AC function by absorbing incident EM waves to prevent reflections and external interference. This is achieved through:

- **Absorbing materials** such as pyramidal foam structures for high-frequency attenuation and ferrite tiles for low-frequency absorption.

- **Chamber geometry** optimized to reduce standing waves and enhance uniform field distribution.
- **Shielded enclosures** that block external electromagnetic interference (EMI), ensuring a stable testing environment.

The effectiveness of an AC depends on the placement and type of absorbers, as well as the frequency range of operation. Properly designed chambers allow engineers to conduct precise measurements without signal contamination.

1.3 Structure and types of AC

An AC is built to eliminate external interference and internal reflections, ensuring a controlled test environment. Its structure typically consists of a thick outer shell that provides isolation, often reinforced with a Faraday cage in EM chambers. Inside, the walls, ceiling, and sometimes the floor are lined with absorbing materials tailored to the frequency range of interest. In acoustic designs, this often includes fiberglass wedges, while EM chambers use RF absorbing foams or ferrite tiles. The floor may feature a raised metal mesh or platform for accessibility without affecting the absorber layout. Additional elements like floating floors, ventilated ducts with silencers, and heavy, sealed doors help maintain performance by minimizing vibration and leakage. The exact design depends on the chamber's intended application and operating frequency range.

1.3.1 Types of AC

1.3.1.1 Fully AC

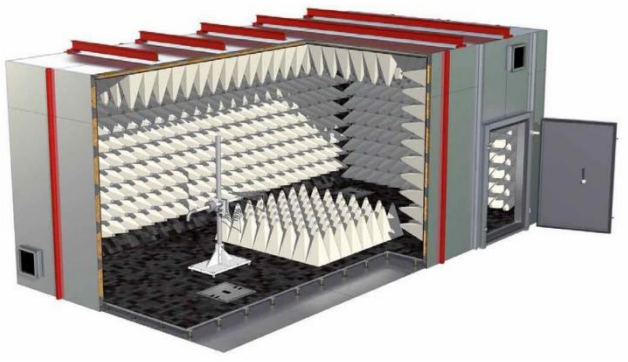


Figure 1.2: Fully anechoic chamber.

Fully AC are designed to eliminate EM reflections from all surfaces, creating an environment that mimics free space. As illustrated in Figure 1.2, the walls, ceiling, and floor are entirely covered with absorbers, ensuring that waves are absorbed regardless ensuring

One of the main considerations in fully AC is the floor design. Since the floor also needs to be non-reflective, a mesh or elevated platform is often used to allow personnel to move inside without disturbing the test conditions [3].

1.3.1.2 Semi AC

Semi-AC have a reflective floor, while the walls and ceiling remain covered with absorbing materials as shown in Figure 1.3. This setup is useful when testing vehicles, industrial equipment, and larger systems, where the test object rests on the ground, simulating real world conditions [3].

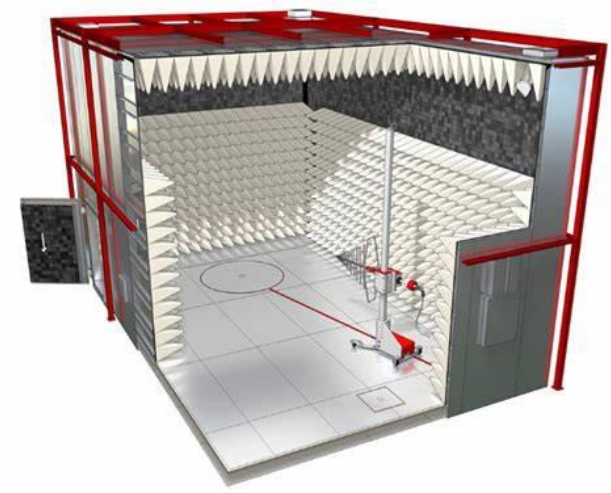


Figure 1.3: Semi-anechoic chamber.

These chambers are widely used for EMC testing, where devices are evaluated for radiated emissions and susceptibility to external EM fields. Unlike fully AC, they provide results that are closer to open-area test sites while still minimizing external interference.

1.3.2 Main components of AC

1.3.2.1 Chamber walls and shielding

The walls of an AC serve two key functions:

- Prevent external EMI from affecting test results.
- Ensure that waves generated inside the chamber do not escape, maintaining a controlled environment.

To achieve this, the walls are typically lined with high-conductivity metals, such as copper or aluminum, forming a shielded enclosure that reflects external signals [4].

1.3.2.2 Absorbing materials

Absorbing materials are essential in reducing EM wave reflections and within an AC, ensuring accurate and repeatable measurements. Their role is to attenuate incident energy and prevent it from reflecting back into the measurement zone, simulating free space conditions. The selection of absorbing materials depends on the operating frequency and the type of the test being conducted:

- **Ferrite tiles** are widely used for low frequency absorption, typically from 30 MHz to 1 GHz. These tiles exploit magnetic losses to dissipate energy and are effective in compact chamber designs.
- **Pyramidal foam absorbers** made from carbon impregnated polyurethane foam, are designed for high frequency applications, generally above 1 GHz. Their pyramidal shape increases the path length of waves, improving energy attenuation.
- **Hybrid absorbers** combine both ferrite and foam, offer broadband performance, covering both low and high frequencies, and are commonly used in modern EMC test chambers.

Principle performance parameters include the absorber's reflectivity, typically designed to achieve values of -30 dB or lower, to minimize unwanted reflections within the chamber. The power handling capacity of the absorbers must be adequate for the anticipated EM field strengths during testing. Ensuring correct placement, density, and orientation of the absorbers is essential to maintain field uniformity and to reduce residual reflections that could compromise measurement accuracy [1].

1.3.2.3 Antenna positioners and measurement equipment

For accurate measurements, AC incorporate various positioning and measurement systems, including:

- Motorized turntables, which rotate devices to capture radiation patterns from different angles.
- Antenna masts and positioning arms, allowing controlled adjustments of antenna height and orientation.
- Vector network analyzers (VNAs) and spectrum analyzers, which provide precise frequency response and signal characterization.

These components ensure that measurements are repeatable and aligned with industry standards [1]. An example setup to measure the radiation pattern of an antenna is shown in Figure 1.4.

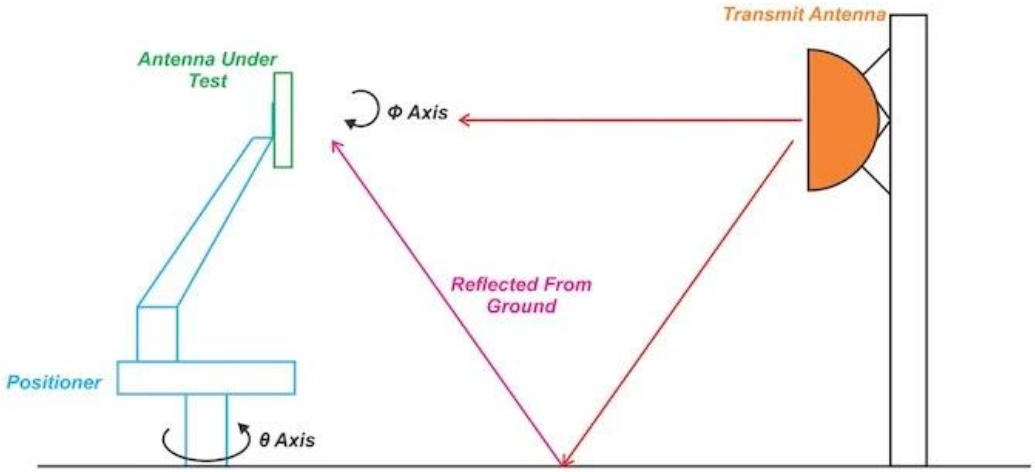


Figure 1.4: An example setup for antenna radiation measurement.

1.3.3 Shielding and isolation techniques

Shielding is essential in AC to block external EMI and preventing electronic eavesdropping, ensuring that signals generated inside the chamber remain isolated. RF shielded room forms the basis for a semi-AC. It's a well-sealed metal box, that offers electric and magnetic field shielding effectiveness over a given range of frequencies [4].

1.3.3.1 Faraday cages and RF shielding

Most AC are enclosed within a Faraday cage, a conductive enclosure that prevents EM signals from penetrating or escaping. These enclosures are typically constructed using:

- **Copper:** Offers high shielding efficiency;
- **Aluminum:** Lightweight and cost effective;
- **Steel:** Durable but has lower conductivity.

To further enhance shielding, additional components are integrated, such as:

- **Conductive gaskets:** Seal panel seams and prevent leakage;
- **Waveguide air vents:** Allow ventilation, while blocking high frequency interferences.

1.3.3.2 Multi-layer shielding for enhanced protection

Modern AC use multi-layer shielding to improve EM isolation. A typical configuration includes:

- **Metallic shielding (copper/steel):** Blocks low frequency EMI;
- **Conductive polymer coatings and foams:** Provides additional absorption;
- **Ferrite tiles:** Suppress high frequency interference.

This layered approach provides broadband shielding, making it suitable for environments requiring minimal noise interference [4].

1.3.3.3 Measuring shielding effectiveness

The effectiveness of AC shielding is assessed using the shielding effectiveness (SE) parameter, which quantifies the reduction of EM waves between an external source and the interior of the chamber. It is calculated as given in 1.1:

$$\mathbf{SE=20\ log\ \frac{E\ \mathit{incident}}{E\ \mathit{transmitted}}\ [dB]} \qquad \mathbf{1.1}$$

Where:

- **E** $\boldsymbol{incident}$: external field strength.
- **E** $\boldsymbol{transmitted}$ **:** internal field strength.

Regular testing and verification ensure that AC maintain optimal isolation and performance over time [5].

1.4 Absorption phenomena in AC

In AC, EM wave absorption is essential to prevent unwanted reflections and create a controlled testing environment. The efficiency of absorption depends on the material properties, geometry, and thickness of the absorbers [6].

1.4.1 Interaction of EM waves with materials

When EM waves encounter a material, they can be reflected, transmitted, or absorbed. For an AC to function effectively, it must maximize absorption while minimizing reflection and transmission.

- **Reflection** occurs when the wave encounters a boundary with a mismatched impedance, causing part of the energy to bounce back;
- **Transmission** happens when a portion of the wave passes through the material instead of being absorbed;
- **Absorption** converts EM energy into heat, reducing unwanted reflections.

To achieve efficient absorption, impedance matching is crucial. The closer the material's impedance is to free space, the better it can absorb incident waves instead of reflecting them.

1.4.2 Mechanisms of EM waves absorption

Absorption mechanisms vary based on the material's electrical and magnetic properties and the frequency range of operation. The most common mechanisms include dielectric losses, magnetic losses, eddy current dissipation, and resonance effects. Figure 1.5 demonstrates the different behaviors of the EM wave and material interactions.

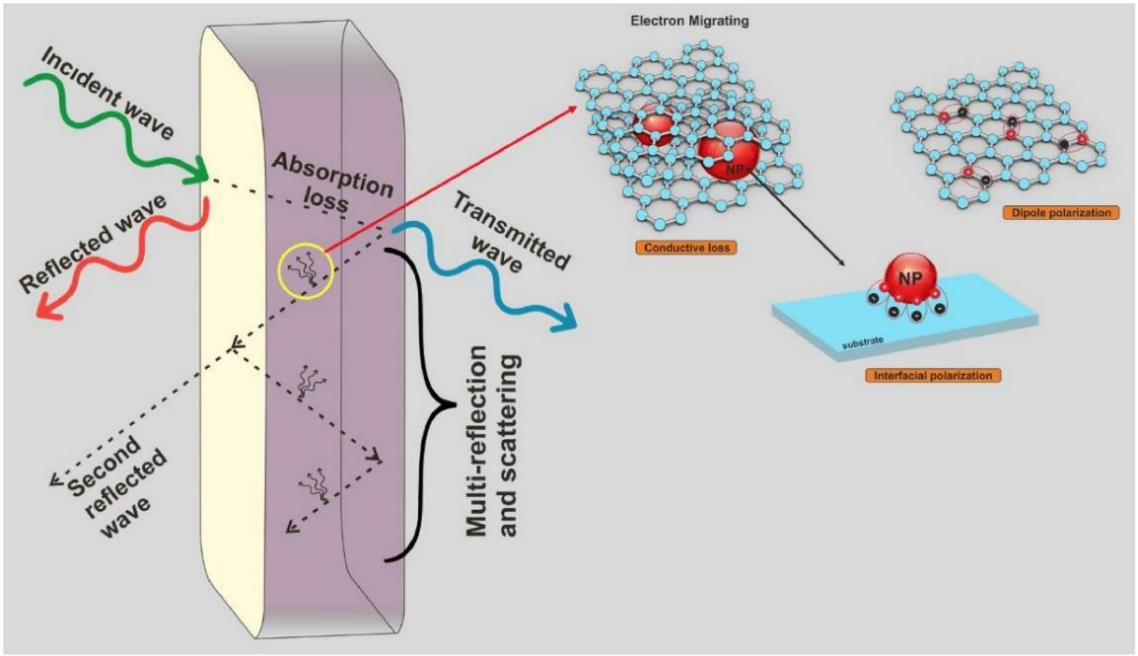


Figure 1.5: Schematic representation of the electromagnetic wave absorption and reflection.

1.4.2.1 Dielectric losses

Dielectric materials absorb EM waves by polarizing their molecular structure under an applied electric field which causes energy dissipation in the form of heat. The effectiveness of dielectric absorption depends on:

- **Permittivity (ε):** The complex permittivity ($\varepsilon_r = \varepsilon' - j\varepsilon''$) of the material determines its ability to store and dissipate electric energy. The imaginary part (ε'') represents the loss factor [7];
- **Operation frequency:** Dielectric losses are more significant at higher frequencies, where dipole relaxation effects occur;

- **Lossy dielectric fillers:** Materials like ceramics or conductive polymers enhances absorption by increasing the material's loss factor [7].

1.4.2.2 Magnetic losses

Magnetic absorbers, such as ferrites, dissipate energy through hysteresis and magnetic domain movement in response to an alternating magnetic field. These losses are influenced by:

- **Saturation magnetization:** Determines how effectively a material responds to a magnetic field. Higher values enhance absorption;
- **Resonance frequency:** Defines the frequency range where permeability is maximized;
- **Magnetic relaxation effects**: The microstructure of the material affects how quickly it can respond to changing magnetic fields, influencing energy dissipation [8].

1.4.2.3 Eddy current and conduction losses

When EM waves interact with conductive materials, they induce eddy currents, which generate heat and dissipate wave energy. The strength of eddy current losses depends on:

- Material thickness and conductivity
- Thin conductive layers enhance eddy current absorption;
- Highly conductive metals tend to reflect waves rather than absorb them.

Eddy current losses are more pronounced at higher frequencies, where skin depth decreases, leading to stronger surface currents [8] [9].

1.4.2.4 Influence of material thickness on absorption efficiency

The thickness of the absorber significantly impacts its ability to attenuate EM waves.

- **Thin absorbers:** Limited attenuation unless optimized through multi-layer configurations or metamaterial designs;
- **Thicker materials:** More effective at lower frequencies, where increased penetration depth enhances absorption;
- **Gradual impedance transition:** Using a tapered structure (pyramidal absorbers) improves impedance matching and minimizes reflections [9].

1.4.3 Factors influencing absorption efficiency

1.4.3.1 Material composition and electrical properties

The chemical and structural composition of an absorbing material defines its performance. Important parameters include:

- Relative permittivity and permeability;
- Electrical conductivity, which affects eddy current losses;
- Magnetic saturation and coercivity, which influence magnetic absorption.

1.4.3.2 Chamber geometry and absorber placement

Absorption performance is also influenced by chamber design and absorber arrangement:

- **Absorber orientation:** Pyramidal and wedge-shaped designs help direct reflections away from measurement areas;
- **Multi-layer stacking:** Combining materials with different properties broadens absorption bandwidth;
- **Placement of absorbers:** Strategic positioning minimizes standing waves and improves uniformity.

1.5 Applications of AC

AC are essential in fields where precise EM testing is required. They provide a controlled environment free from reflections and external interference, making them ideal for a wide range of applications, including antenna testing, EMC assessments, radar technology, and research in EM wave propagation [4].

1.5.1 Antenna testing and characterization

AC play a crucial role in antenna performance evaluation by allowing accurate measurement of key parameters such as:

- **Radiation patterns:** Mapping how an antenna transmits or receives signals in different directions;
- **Gain and efficiency:** Assessing how effectively an antenna radiates power;
- **Beam width and polarization:** Ensuring proper signal orientation and coverage.

These measurements are critical in industries such as wireless communications, satellite technology, and aerospace, where antennas must meet strict regulatory and operational standards.

1.5.2 EMC testing

EMC testing ensures that electronic devices do not generate excessive EMI and are immune to external EMI sources. AC provide the ideal setting for:

- **Radiated emissions testing:** Measuring unwanted EM noise produced by a device;
- **Radiated immunity testing:** Evaluating a device's ability to function correctly when exposed to external EM fields;
- **Compliance certification:** Ensuring adherence to international EMC standards.

This type of testing is essential in sectors such as automotive electronics, medical devices, consumer electronics, and industrial automation, where regulatory compliance is mandatory.

1.5.3 Radar and stealth technology applications

AC are widely used in military and defense applications, particularly for radar and stealth technology development. Their ability to create a reflection-free environment allows for:

- **RCS measurements:** Determining how much radar energy an object reflects, which is crucial in stealth aircraft and naval vessel design;
- **Radar system calibration:** Ensuring radar sensors operate accurately without interference;
- **Testing absorptive coatings and materials:** Evaluating advanced materials that minimize detectability by radar.

Such applications are critical in the aerospace, defense, and industries security, where stealth and radar performance directly impact operational effectiveness.

1.5.4 Research and development in EM

AC support cutting-edge research in EM by providing a stable, interference-free testing environment for:

- **EM wave propagation studies:** Analyzing how waves behave in different conditions;

- **Testing new absorbing materials:** Developing more efficient EM absorbers for improved chamber performance;
- **Wireless technology advancements:** Investigating new wireless communication protocols such as 5G, millimeter-wave, and terahertz technologies.

Their use in academic institutions, research labs, and technology companies helps drive innovation in telecommunications, materials science, and applied physics.

1.6 Conclusion

AC play a critical role in EM testing, providing a controlled, reflection-free environment for precise measurements. This chapter explored their design and function, covering the different types of chambers, their key components, and the shielding techniques used to prevent external interference. Additionally, we examined wave absorption mechanisms, highlighting how materials and chamber geometry influence performance.

These chambers are widely used in antenna characterization, EMC testing, radar applications, and EM research, ensuring compliance with industry standards and improving the reliability of modern electronic systems.

Since absorber materials directly impact chamber efficiency, the next chapter will focus on EM absorbing materials, their properties, and their role in optimizing chamber performance.

CHAPTER 2

ELECTROMAGNETIC ABSORBERS

2.1 Introduction

EM absorbers are essential elements in the design and functionality of AC. Their primary role is to suppress unwanted reflections of EM waves, ensuring a controlled test environment for accurate measurements. The efficiency of an absorber depends on several factors, notably its material composition and geometry. This chapter presents a detailed overview of absorber classifications, focusing on commercial solutions such as ferrite tiles and pyramidal foam, and explains how material properties and structural design influence performance across different frequency ranges. The discussion also includes recent advances in absorber technology and compares different absorber types based on their application domains and operating characteristics.

2.2 Definition and classification of absorbers

2.2.1 Absorber overview

Absorbers are essential elements in AC, designed to suppress unwanted EM wave reflections. They function by either converting the energy of incident waves into heat or dissipating it through their intrinsic electrical and magnetic properties. Depending on their composition and structure, absorbers can effectively limit wave reflection, transmission, and propagation across a defined frequency range [4].

2.2.2 Classification of absorbers

Absorbers can be classified according to the type of wave they are designed to attenuate, the physical mechanism by which they operate, and the materials used in their construction.

2.2.2.1 Classification by type of wave absorbed

- **Acoustic absorbers:** Employed in acoustic chambers to suppress sound reflections and minimize ambient noise levels. These include:
    - **Porous absorbers:** Typically made from open-cell foam or fiberglass; they attenuate sound by converting acoustic energy into heat through viscous and thermal losses;
    - **Resonant absorbers:** Utilize structures such as perforated panels or membrane-based systems that are tuned to absorb specific frequency bands;

- **Hybrid absorbers:** Combine porous and resonant elements to achieve broadband sound absorption across a wider range of frequencies [4].

- **EM absorbers:** Used in RF AC to reduce unwanted reflections of EM waves. Key types include:
  - **Ferrite tiles absorbers:** Ceramic based materials that offer efficient absorption at lower frequencies, typically from 30 MHz to 1 GHz;
  - **Pyramidal absorbers:** Constructed from carbon impregnated foam; these are effective at higher frequencies, generally above 1 GHz;
  - **Hybrid absorbers:** Integrate ferrite tiles with pyramidal foam layers to ensure wideband performance across both low and high-frequency ranges [4].

2.2.2.2 Classification by absorption mechanism

- **Dissipative absorbers:** Attenuate wave energy primarily through conversion into heat, using friction or molecular excitation;
- **Resonant absorbers:** Incorporate geometrically tuned structures that absorb energy at specific frequencies;
- **Impedance matching absorbers:** Designed to gradually match the impedance of free space to that of a lossy material, minimizing reflections and maximizing absorption [4].

2.2.2.3 Classification by material composition

- **Foam-based absorbers:** Used in both acoustic and EM applications. For instance, polyurethane foams are employed in acoustic treatments, while carbon-loaded foams serve RF absorption purposes;
- **Ferrite-based absorbers:** Employed mainly for low-frequency RF applications, these ceramic materials offer high magnetic losses to effectively dissipate EM wave energy;
- **Composite absorbers:** Engineered from a combination of different materials to achieve broadband absorption. A typical example is the hybrid RF absorber, which combines ferrite and foam layers for enhanced performance across a wide frequency range [4].

2.3 Commercially available absorbers

2.3.1 Ferrite tiles

2.3.1.1 Structure and operating principle

Ferrite tiles are square, rigid EM absorbers made from sintered ferrite materials, typically manganese-zinc or nickel-zinc compositions as illustrated in figure 2.1. These tiles are widely used for EMI suppression in the low-frequency range, particularly between 30 MHz and 1 GHz.

Their absorption mechanism relies on magnetic losses. When an incident EM wave strikes the ferrite surface, part of the wave energy is absorbed and dissipated as heat. This loss is primarily due to several internal magnetic phenomena, including eddy current loss, natural ferromagnetic resonance, domain wall motion, and exchange resonance. These processes convert the EM energy into thermal energy, reducing reflections and enhancing the performance of test environments such as AC. Ferrite tiles typically achieve absorption levels ranging from 10 dB to 25 dB, depending on frequency and tile configuration.

One of the main considerations in fully AC is the floor design. Since the floor also needs to be non-reflective, a mesh or elevated platform is often used to allow personnel to move inside without disturbing the test conditions [10].

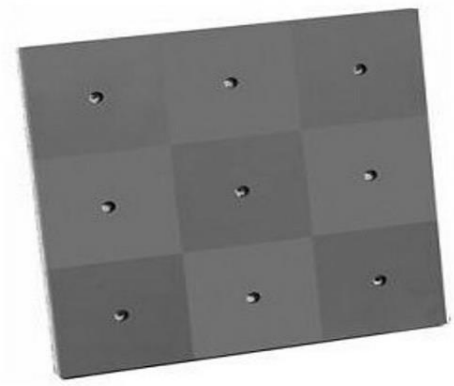


Figure 2.1: Ferrite tiles.

2.3.1.2 Composition and physical configuration

Ferrite tiles are EM absorbers manufactured from ceramic materials composed primarily of iron oxide, combined with metallic oxides such as nickel or zinc, the structure is illustrated in Figure 2.2, highlighting its composition. These materials are sintered to achieve the desired magnetic and structural properties. The tiles are generally produced in

square or rectangular shapes, with typical thicknesses ranging from a few millimeters to several centimeters. In practice, they are affixed to the interior surfaces of AC, including walls, ceilings, and floors, to mitigate reflections in the low-frequency range.

For applications requiring absorption above 1 GHz, ferrite tiles are often installed over a dielectric spacer of appropriate thickness. This configuration forms a composite absorber system, improving broadband performance by extending the effective frequency range and increasing attenuation efficiency [10] [11].

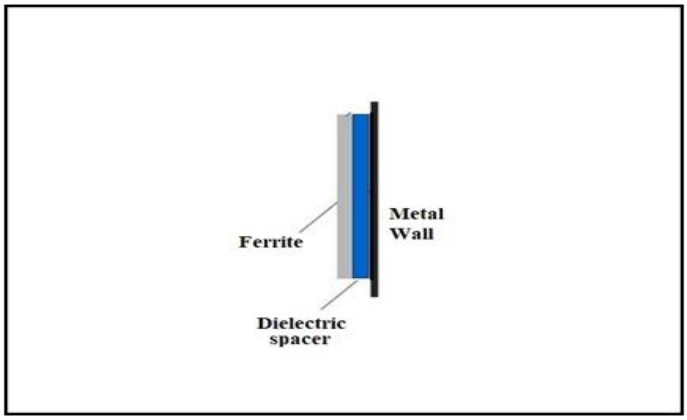


Figure 2.2: Mounted ferrite tile.

2.3.1.3 Applications of ferrite tiles

- Used in EMC testing environments to ensure compliance of electronic devices with EMC regulations by minimizing reflections and emissions;
- Enable accurate antenna performance evaluation by providing a controlled, reflection-free measurement environment;
- Applied in military and defense systems as part of stealth technology to reduce radar reflections and lower radar cross-section;
- Support testing of advanced wireless communication systems, such as 5G and satellite technologies, especially in the low-frequency range (30 MHz to 1 GHz) [10].

2.3.2 Pyramidal absorbers

2.3.2.1 Structure, composition, and characteristics of pyramidal absorbers

Pyramidal absorbers are RF absorbing structures made from carbon-loaded polyurethane foam, formed into pyramid shapes as shown in Figure 2.3. They are widely

used in RF AC, particularly for high-frequency applications, due to their broadband absorption properties and efficient reflection suppression.

- These absorbers typically operate effectively in the frequency range from 1 GHz up to 40 GHz, depending on their dimensions.
- The foam material is usually treated with carbon to introduce lossy characteristics, and may also be fire-retardant or coated to improve mechanical durability and safety.
- Principle advantages of pyramidal absorbers include:
    - Easy and flexible installation on the chamber's walls, ceiling, or floor;
    - High absorption performance across a wide frequency spectrum;
    - Effective suppression of reflections; allowing precise measurements in EM testing environments [6].

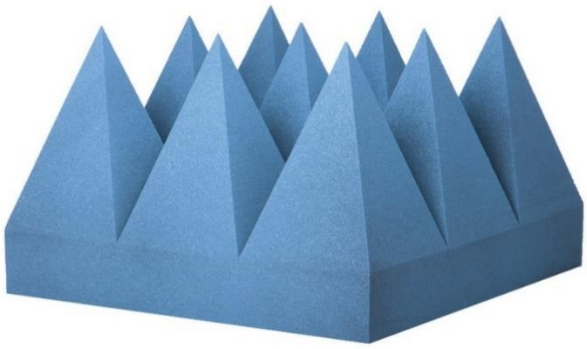


Figure 2.3: Foam pyramid absorbers.

2.3.2.2 Operating principle

The tapered geometry of pyramidal absorbers enables gradual impedance matching between free space and the absorbing material. As EM waves enter the pyramid, they experience a smooth transition in impedance, which minimizes reflection as the process is illustrated in Figure 2.4. Inside the absorber, according to Figure 2.5 the carbon-loaded foam dissipates the EM energy by converting it into heat. Additionally, the shape promotes

multiple internal reflections within the pyramid, further enhancing the overall absorption efficiency, especially at high frequencies [6].

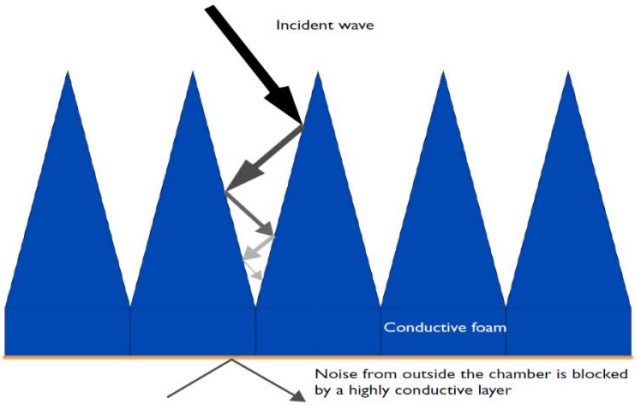


Figure 2.4: Reflections in pyramidal absorbers.

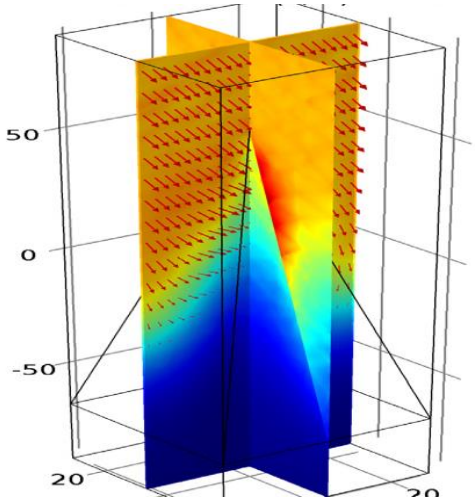


Figure 2.5: Transformation of energy into heat.

2.3.2.3 Applications of pyramidal absorbers

Pyramidal absorbers are commonly employed in RF AC for central purposes:

- Ensuring a low-reflection test environment for precise antenna pattern measurements;
- Verifying EMC performance of electronic devices;
- Supporting the development and testing of modern wireless communication technologies, by providing stable and controlled measurement conditions [10].

2.4 Influence of material composition on absorption

The EM properties of an absorbing material; whether dielectric, magnetic, or composite; play a key role in determining its absorption efficiency across specific frequency bands. Each

category interacts differently with incident waves, depending on whether the dominant mechanism is electric, magnetic, or a combination of both. The choice of material is closely tied to the application's frequency range, structural requirements, weight constraints, thermal stability, and manufacturing cost. Proper selection and engineering of the material composition are essential to achieve targeted performance in RF and microwave systems [6].

2.4.1 Dielectric Materials

- **Absorption mechanism:** Dielectric absorbers operate primarily through dielectric loss, which occurs when alternating electric fields cause dipole molecules within the material to oscillate. These repeated polarizations lag behind the field, dissipating energy as heat due to internal friction and relaxation processes. The mechanism becomes more pronounced at microwave and millimeter-wave frequencies [12].
- **Material properties**
  - **High permittivity (ε′):** Enhances interaction with the electric field and energy storage capacity;
  - **Moderate to high dielectric loss (ε″):** Enables efficient conversion of EM energy into heat;
  - **No magnetic response:** These materials interact solely with the electric component of the wave;
  - **Effective at high frequencies:** Typically used in the GHz range [12].

2.4.2 Magnetic materials

- **Absorption mechanism:** Magnetic absorbers interact with the magnetic field of EM waves. When exposed to time-varying fields, the magnetic domains undergo reorientation, producing **hysteresis losses**. Eddy currents are also generated, leading to additional energy dissipation through resistive heating. These mechanisms are particularly effective in the lower part of the RF spectrum [13].
- **Material properties:**
  - **High magnetic permeability (μ):** Enhances wave coupling with the magnetic field;
  - **Magnetic loss (μ″):** Measures the ability to dissipate magnetic energy;
  - **Saturation and hysteresis behavior:** Affects how energy is absorbed under high-intensity fields;

- **Best suited for low to mid-frequency operation**: Typically, from tens of MHz to several GHz [13].

2.4.3 Composite materials

- **Absorption mechanism:** Composite materials are designed to combine dielectric and magnetic loss mechanisms, creating multiple energy dissipation pathways. These include conduction loss, interfacial polarization, eddy current loss, and dipolar relaxation. The interface between different material phases enhances polarization, improving broadband absorption [14].
- **Material properties**
  - **Wideband frequency coverage:** Simultaneous electric and magnetic losses make them suitable across wide frequency spans;
  - **Lightweight and flexible:** Often more adaptable than ceramics or solid ferrites;
  - **Tunable properties:** Absorption behavior can be tailored by adjusting filler types, concentrations, and dispersion [14].

2.4.4 Comparison by material composition

The Table 2.1 represents a comparison between material composition of absorbers, including loss mechanism, frequency range.

Table 2.1: Comparison between material composition of absorbers.

Type	Loss Mechanism	Frequency Range	Examples
Dielectric	Dielectric loss	High frequencies	Conductive polymers, ceramics
Magnetic	Magnetic loss	Low to medium frequencies	Ferrites
Composite	Dielectric, magnetic, interfacial	Broadband	Ferrite and Carbon.

2.5 Influence of geometry on absorption performance

The geometry of EM absorbers used in AC is a determining factor in their performance across different frequency ranges. The shape of the absorber directly impacts critical

parameters such as impedance matching, EM wave interaction, and absorption efficiency. This section presents an analysis of commonly used absorber geometries, and explains their influence on wave behavior and frequency-dependent absorption characteristics [6].

2.5.1 Common absorbers geometries

2.5.1.1 Pyramidal absorbers

Pyramidal absorbers are among the most widely used geometries, particularly for broadband applications. Their tapered structure as evidenced in figure 2.6, facilitates a gradual impedance transition from free space to the absorber material, minimizing reflections at the interface. This geometry also increases the propagation path within the material, enabling multiple internal reflections and enhancing energy dissipation.

Due to these characteristics, pyramidal absorbers are effective over a wide frequency range and perform well across various angles of incidence [6].

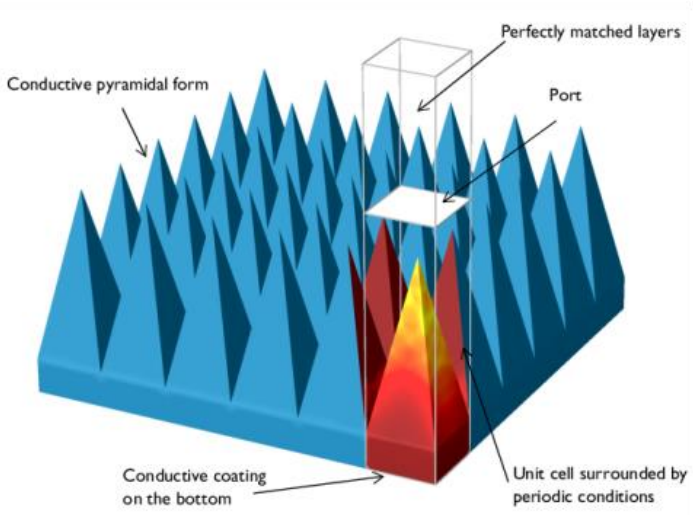


Figure 2.6: An infinite 2D array of pyramidal absorbers is modeled using periodic boundary conditions on the sides of one unit cell.

2.5.1.2 Wedge absorbers

Wedge absorbers are typically employed in setups where space constraints prevent the use of full pyramidal structures. Though they also offer a tapered profile for impedance transition, their performance is generally more directional. Energy dissipation occurs primarily through repeated reflections between the wedge faces as shown in Figure 2.7, but

edge diffraction effects can limit their efficiency at higher frequencies. Nonetheless, their compactness makes them suitable for applications requiring reduced volume [6].

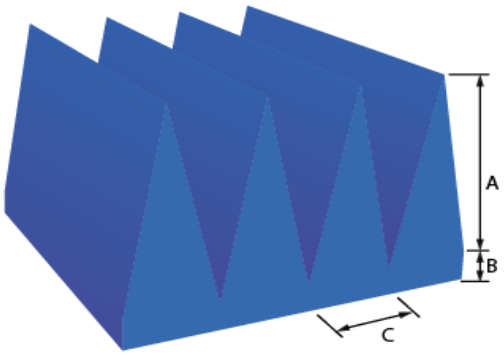


Figure 2.7: Foam based wedge absorber.

2.5.1.3 Conical absorbers

According to figure 2.8 conical absorbers are characterized by gradually tapered shape that ensures a smooth transition in impedance from free space to the absorber material. This geometric significantly reduces reflections and enables effective broadband absorption. The cone's continuous taper enhances energy dissipation by promoting progressive attenuation of incident waves, making it a suitable solution for wideband EMI mitigation [15].

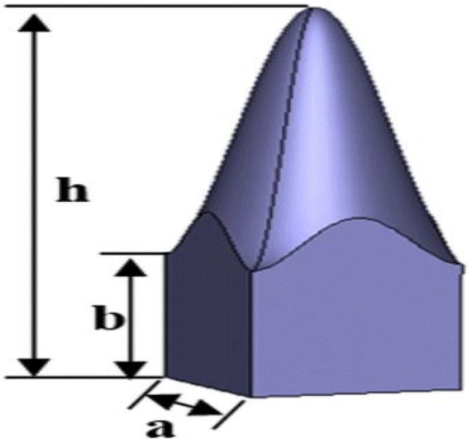


Figure 2.8: Conical absorber.

2.5.2 Impact of geometry on wave interaction

The physical shape of absorbers governs how EM waves interact with its surface and internal structure:

- **Impedance matching:** Tapered shapes such as pyramids and wedges provide a gradual transition from the impedance of free space to that of the absorber, which significantly reduces reflection;
- **Wave propagation path:** Longer path lengths inside the absorber (achieved via tall or tapered geometries) allow greater attenuation through successive reflections, thus improving absorption;
- **Surface scattering:** Geometries with irregular or non-planar surfaces enhance wave scattering, reducing coherent reflections and increasing overall absorption effectiveness [6].

2.5.3 Frequency dependent behavior

Absorber performance is inherently dependent on the operating frequency, which relates to the wavelength of the incident wave:

- **Low frequency operation:** At lower frequencies, where wavelengths are longer, effective absorption requires deeper penetration. Taller pyramidal structures are therefore more suitable due to their extended taper and longer propagation paths;
- **High frequency operation:** At higher frequencies, shorter wavelengths interact primarily with the absorber surface. As a result, smaller geometries such as shallow pyramids or conical profiles can achieve sufficient absorption while minimizing space usage [6].

2.5.4 Performance metrics

Several key metrics are directly affected by absorber geometry:

- **Reflectivity:** Pyramidal absorbers can achieve reflectivity levels below –30 dB across wide frequency bands, typically ranging from 2 to 18 GHz. Conical shapes, while more compact, also demonstrate good reflection loss performance due to their enhanced surface interaction;
- **Absorption bandwidth:** The bandwidth over which effective absorption is maintained is generally broader for pyramidal structures, though well optimized wedge designs can achieve similar results in a more compact form factor;
- **Sensitivity to angle of incidence:** Pyramidal and conical absorbers tend to maintain consistent performance across a wide range of incidence angles. In contrast, wedge absorbers may exhibit directional behavior, with performance varying depending on wave orientation and shape symmetry [6].

The geometry of an absorber has a direct impact on its EM performance. While pyramidal structures offer the most consistent broadband absorption**,** wedge and conical designs present compact alternatives with trade-offs in directionality and frequency range. The choice of geometry depends on specific testing needs, available space, and the frequency band of interest. The Table 2.2 below provides a comparative overview of typical absorber geometries.

Table 2.2: Comparative overview of typical absorber geometries.

Geometry	Description	Frequency Range	Absorption Efficiency	Thickness	Angle Sensitivity	Typical Use Cases
Wedge	Compact with directional properties; effective at high frequencies.	Narrowband to broadband	Medium (up to -20 dB)	Thin	Medium	Compact EMC setups, Industrial testing
Pyramidal	Gradual taper for impedance matching; affective at multiple angles.	Broadband (2-18 GHz)	High (up to -30 dB)	Medium	Low	EMC chambers, Antenna measurements
Conical	Compact absorber with a flared tip and large surface area for improved attenuation.	Broadband (multiple frequencies)	High (up to -30 dB)	Thin	Low	Portable chambers, High frequency tests

2.6 Permittivity and permeability

Permittivity and permeability are fundamental EM properties of materials. Permittivity (ε) describes a material's ability to store and transmit electric fields, influencing how electric energy propagates through it. Permeability (μ), on the other hand, indicates how easily a material can support the formation of magnetic fields, affecting the behavior of magnetic energy. Together, these parameters determine how EM waves travel, reflect, or get absorbed as demonstrated in Figure 2.9 [3].

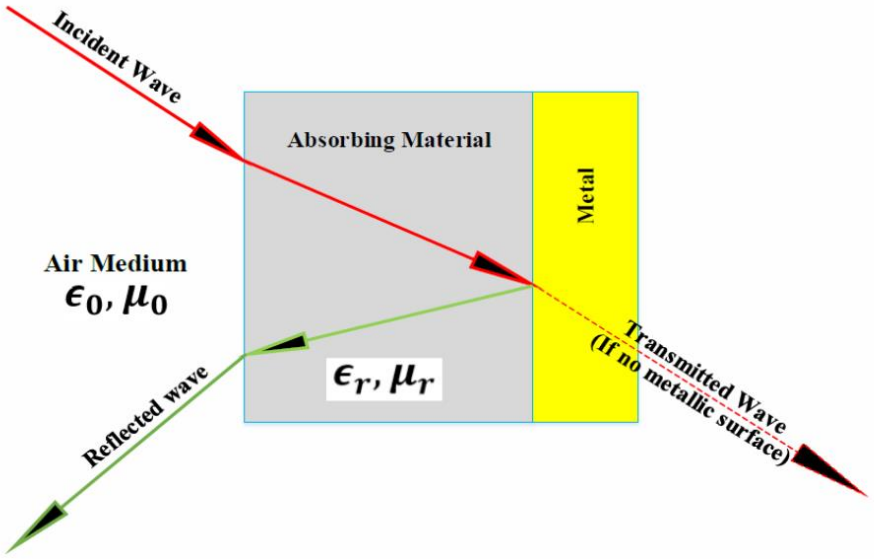


Figure 2.9: Basic characteristics of electromagnetic wave inside the anechoic chamber.

The operation of an EM absorber can be understood by examining the concept of impedance matching with free space. In a vacuum, the characteristics impedance is defined by the ratio of the electric to magnetic field magnitudes:

$$z_0 = \frac{E}{H} = \sqrt{\frac{\mu_0}{\varepsilon_0}} \approx 377\ [\Omega] \qquad 2.1$$

To ensure minimum reflection at the surface of an absorber, the wave impedance of the absorber Z_M must match that of the free space. The reflection coefficient Γ, which measures how much of the incident wave is reflected, is given by:

$$\Gamma = \frac{z_M - z_0}{z_M + z_0} \qquad 2.2$$

Perfect matching occurs when $\Gamma = 0$, which implies:

$$\frac{z_M}{z_0} = \sqrt{\frac{\mu_r}{\varepsilon_r}} = 1 \qquad 2.3$$

This condition is satisfied when the relative permittivity ε_r, and relative permeability μ_r of the absorber are equal. In practical absorbers, both ε_r and μ_r are complex:

$$\boldsymbol{\varepsilon_r = \frac{\varepsilon' - j\,\varepsilon''}{\varepsilon_0}},\ \boldsymbol{\mu_r = \frac{\mu' - j\,\mu''}{\mu_0}} \qquad \textbf{2.4}$$

Where the real parts ε' and μ' govern wave propagation, and the imaginary parts ε'' and μ'' account for energy loss. When $\varepsilon_r = \mu_r$, the wave entering the material experiences minimal reflection and is exponentially attenuated, allowing effective absorption of EM energy across the operating frequency band [3].

2.6.1 Extraction of ε and μ from S-parameters

Permittivity and permeability are key material properties that define how EM waves behave inside a medium. To extract them, S-parameters (S11, S21) are measured using a waveguide or a transmission line setup. These values are then used to calculate how the wave propagates through the material and how much of it is reflected or transmitted. The following methods are commonly used to determine ε and μ based on the measured S-parameters.

2.6.1.1 Nicolson Ross Weir (NRW)

This method estimates ε_r and μ_r of a material by analyzing its measured S-parameter in a waveguide. The material sample, of known thickness d, is inserted between two waveguides ports. The S-parameters reflect the combined effects of reflection and transmission, including multiple internal reflections [16].

- **Bulk reflection coefficient Γ:** The reflection coefficient is given by :

$$\boldsymbol{\Gamma = x \pm \sqrt{x^2 - 1}} \qquad \textbf{2.5}$$

$$\textbf{Where : } \boldsymbol{x = \frac{1-(S_{21}^2 - S_{11}^2)}{2S_{11}}} \qquad \textbf{2.6}$$

The appropriate root is selected to ensure a passive solution $|\Gamma| \leq 1$.

- **Bulk transmission coefficient T:** The transmission coefficient is obtained from:

$$\boldsymbol{T = \frac{S_{11} + S_{21} - \Gamma}{1 - (S_{11} + S_{21})\Gamma}} \qquad \textbf{2.7}$$

- **Propagation constant and auxiliary term Λ:** An auxiliary term Λ, related to the complex propagation complex, is defined by: $\frac{1}{\Lambda^2} = -\left[\frac{1}{2\pi d} ln\left(\frac{1}{T}\right)\right]^2$ [1/m] **2.8**

The logarithm is complex and multi valued; ambiguity is resolved using group delay considerations.

- **Permittivity ε_r:**

$$\varepsilon_r = \frac{\lambda_0^2\left(\frac{1}{\Lambda^2}+\frac{1}{\lambda_c^2}\right)}{\mu_r} \quad \textbf{2.9}$$

- **Permeability μ_r:**

$$\mu_r = \frac{\lambda_0 g}{\Lambda}\left(\frac{1+\Gamma}{1-\Gamma}\right) \quad \textbf{2.10}$$

2.6.2 Transmission/Reflection (T/R)

The T/R method also derives ε and μ from S-parameters by evaluating how a sample o known thickness modifies wave propagation. The method computes the complex propagation constant and the intrinsic impedance to infer material properties [17] [18].

- **Transmission coefficient T**:

$$T = \frac{S_{11}+S_{21}-\Gamma}{1-(S_{11}+S_{21})\Gamma} \quad \textbf{2.11}$$

- **Propagation constant γ**:

$$\gamma = \frac{1}{d}\ln\left(\frac{1}{T}\right) \text{ [1/m]} \quad \textbf{2.12}$$

- **Refractive index n**:

$$n = \frac{c\gamma}{j\omega} \quad \textbf{2.13}$$

This indicates the wave's phase velocity inside the material.

- **Impedance Z**:

$$Z = \sqrt{\frac{(1+S_{11})^2-S_{21}^2}{(1-S_{11})^2-S_{21}^2}} \text{ [}\Omega\text{]} \quad \textbf{2.14}$$

This represents the material's opposition to EM wave propagation.

- **ε_r and μ_r:**

$$\varepsilon_r = \frac{n}{Z}\ , \mu_r = nZ \quad \textbf{2.15}$$

2.6.3 Robust inverse (Baker-Jarvis)

This method is an iterative approach that extracts ε and μ from measured S-parameters using an inverse modeling process. The material is modeled as a slab, and wave interaction is evaluated through propagation and reflection inside the sample [17].

- **Propagation constant γ:**

$$\boldsymbol{\gamma = j\omega\sqrt{\mu\varepsilon}}\ [1/m] \quad \textbf{2.16}$$

This complex quantity combines both attenuation and phase shift.

- **Intrinsic impedance *Z*:**

$$\boldsymbol{Z = \sqrt{\frac{\mu}{\varepsilon}}}\ [\Omega] \quad \textbf{2.17}$$

- **Reflection coefficient Γ:**

$$\boldsymbol{\Gamma = \frac{z - z_0}{z + z_0}} \quad \textbf{2.18}$$

- **Transmission term T:**

$$\boldsymbol{T = e^{-\gamma d}} \quad \textbf{2.19}$$

- **S-parameters models**:

$$\boldsymbol{s_{11} = \Gamma\left(\frac{1 - e^{-2\gamma d}}{1 - \Gamma^2 e^{-2\gamma d}}\right)} \quad \textbf{2.20}$$

$$\boldsymbol{s_{21} = \frac{(1 - \Gamma^2)e^{-\gamma d}}{1 - \Gamma^2 e^{-2\gamma d}}} \quad \textbf{2.21}$$

- **Error function for optimization**:

$$\boldsymbol{f(\varepsilon_r, \mu_r) = \left|s_{11}^{meas} - s_{11}^{model}\right|^2 + \left|s_{21}^{meas} - s_{21}^{model}\right|^2} \quad \textbf{2.22}$$

Where:

meas: represents the measurable S-parameters

model: represents the theorical S-parameters

This error is minimized to retrieve the complex permittivity and permeability values that best fit the measure data.

2.7 Conclusion

The performance of EM absorbers is governed by a combination of material characteristics and geometric configuration. Dielectric, magnetic, and composite materials each offer unique absorption mechanisms and are selected based on their suitability for

specific frequency bands and mechanical constraints. Commercially available absorbers, such as ferrite tiles and pyramidal foams, are widely used in RF testing environments due to their reliability and broad coverage. Recent developments in advanced materials, including metamaterials, are expanding the capabilities of absorbers in high-performance applications. Finally, geometry plays a decisive role in optimizing absorption behavior; pyramidal, wedge, and conical structures each offer specific advantages in terms of bandwidth, reflectivity, and space efficiency. The following chapter will address simulation methodologies used to design and evaluate absorber performance, with a focus on CST Microwave Studio.

CHAPTER 3

RESULTS AND DISCUSSION

3.1 Introduction

This chapter presents the simulation and experimental evaluation of various EM absorber configurations. Multiple absorber geometries were tested including pyramidal, conical, hybrid, and rounded tip structures. Each shape was studied using a 3x3 matrix of base size and heights, and simulated with three materials: carbonyl iron, NiZn ferrite, and graphite. Performance was done across the 2-18GHz band using S-parameters, focusing on reflections reduction (S11).

After simulation based optimization, selected designs were compared to evaluate geometric influence. A final hybrid structure combining two materials was also introduced. Following the simulation campaign, experimental validation was carried out using custom built waveguides and graphite powder. Two measurement techniques were employed: analog and vector network analyzer (VNA).

3.2 Simulation setup

3.2.1 An overview of CST Studio Suite

CST Studio Suite is a 3D EM simulation software used in this work to model and analyze absorber structures over the 2–18 GHz range. It allows precise control of geometry, material properties, and excitation using waveguides and ports. The software is used to evaluate key performance metrics such as S11 and S21, helping validate absorber designs before experimental testing.

3.2.2 Materials and dispersion models

Three materials were defined in CST: carbonyl iron, NiZn ferrite, and graphite. Each was assigned appropriate complex permittivity and permeability values based on known EM behavior in the 2-18GHz range. For carbonyl iron and NiZn ferrite, constant values were used (see Figure 3.1), with dispersion modeling applied to better reflect frequency-dependent loss.

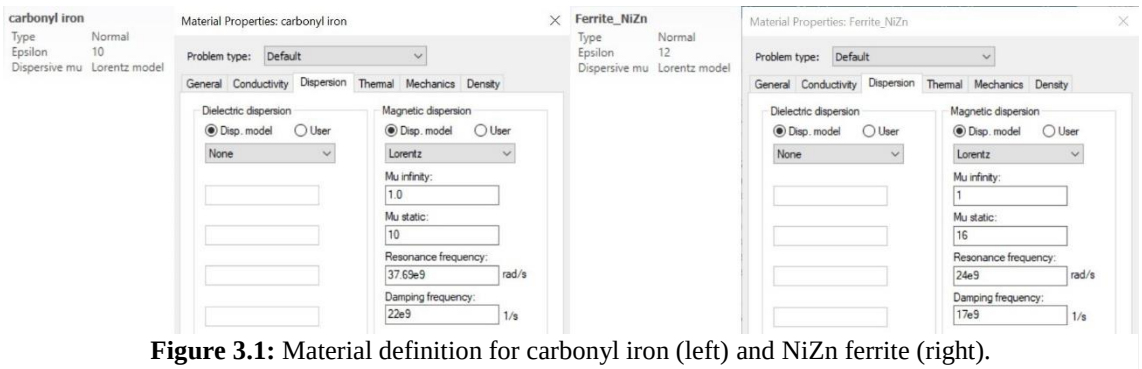


Figure 3.1: Material definition for carbonyl iron (left) and NiZn ferrite (right).

The graphite material was implemented as a high-loss dielectric using a constant complex permittivity (Figure 3.2). No magnetic response (permeability =1) was assumed for graphite, while NiZn ferrite and carbonyl iron included both dielectric and magnetic losses.

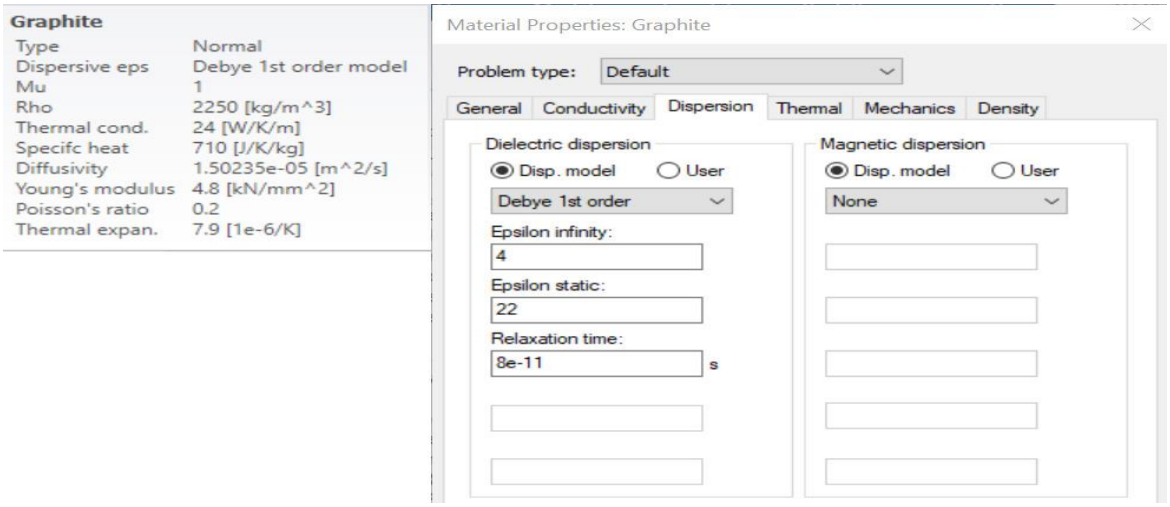


Figure 3.2: Material definition for graphite.

3.2.3 Geometry and simulation matrix

The simulated absorbers were modeled as a standalone geometry placed in front of a perfect electric conductor (PEC) backing. Two absorber shapes were studied: pyramidal and conical, with variations including rounded tips, hybrid structures. For each material, a 3x3 matrix of dimensions was tested combining three base sizes (30mm,50mm,80mm) and three heights (100mm, 180mm, 280mm) resulting in nine cases per shape.

3.3 Absorber shapes and results

3.3.1 Pyramidal absorber

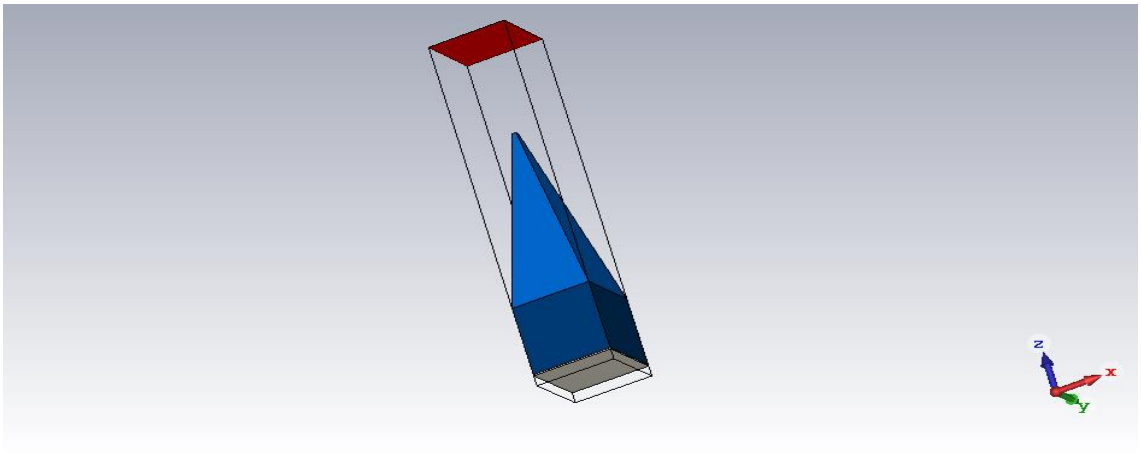


Figure 3.3: 3D geometry of the pyramidal absorber.

The figure below Figure 3.3 illustrates the 3D geometry of the pyramidal absorber used in the simulations.

The pyramidal absorber consists of a cubic base and four triangular faces that meet near the top. To prevent mesh singularities and ensure stable coupling in the time domain solver, a flat surface of 2.83mm diameter was introduced at the pyramid's tip as shown in Figure 3.4; this adjustment allows the excitation port to interact effectively with the absorber surface. Only one port was used in the simulation setup, the second port was replaced by a perfect electric conductor (PEC) plane positioned below the absorber, acting as a reflective boundary to redirect the incident wave energy toward the pyramid tip.

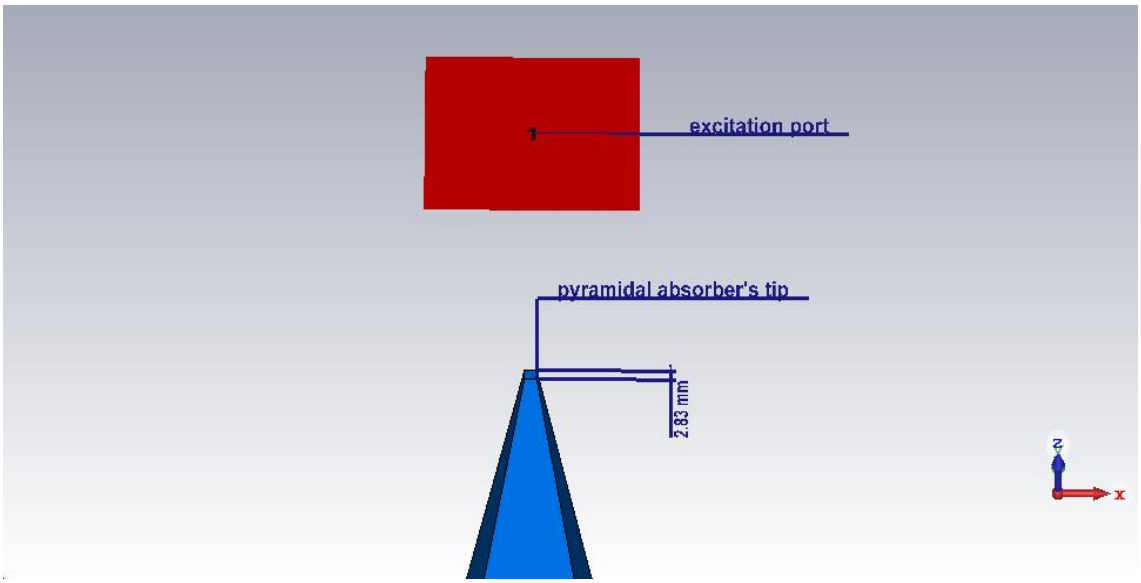


Figure 3.4: Close-up view of the pyramidal absorber tip and excitation port.

This model configuration was used to evaluate the effect of different height and base size combinations on absorption performance. Simulations were conducted separately for each material (Carbonyl iron, NiZn Ferrite, and Graphite), aiming to determine the optimal geometric parameters for broadband performance across the 2-18GHz range.

3.3.1.1 Carbonyl iron based pyramidal absorber

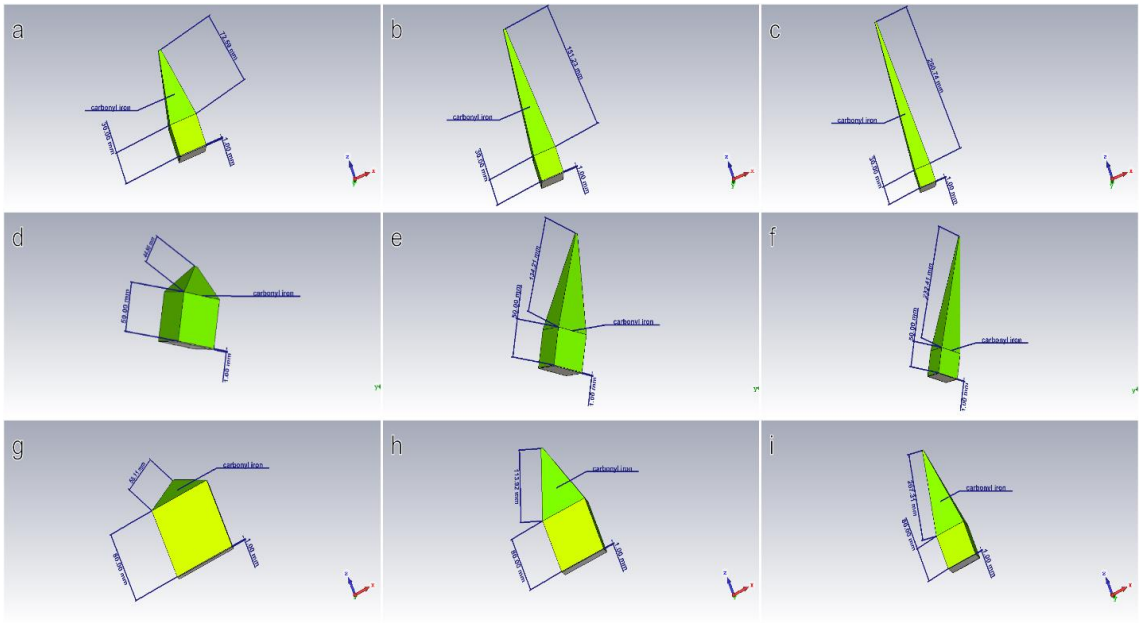


Figure 3.5: Carbonyl Iron pyramidal absorbers.

This section represents the simulation results of the pyramidal absorber made of carbonyl iron, tested with varying base sizes and pyramid heights as represented in Figure 3.5.

The full set of height and base size combinations tested for the carbonyl iron pyramidal absorbers is summarized in Table 3.1.

Table 3.1: Labeled configurations of carbonyl iron based pyramidal absorbers.

Base size (mm)	Height= 100mm	Height= 180mm	Height =280mm
30mm	a	b	c
50mm	d	e	f
80mm	g	h	i

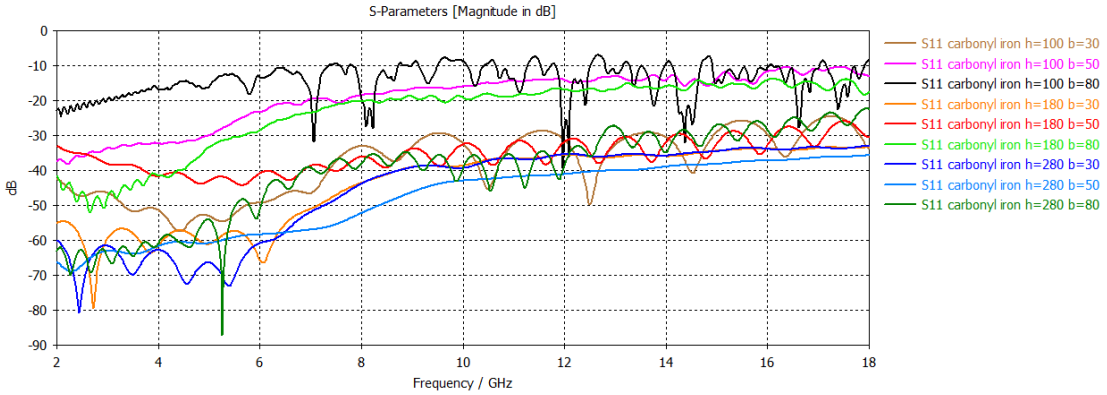


Figure 3.6: Simulated S11 curves for all carbonyl iron based pyramidal absorbers.

To evaluate the EM performance of the configurations, reflection coefficient (S11) curves were extracted over the 2-18GHz range for each case under identical simulation conditions.

The results in Figure 3.6 indicate that absorption improves with increasing height, particularly for narrow to moderate base sizes. Among the nine configurations, those with 280mm height consistently showed lower reflection across a wider frequency range. Overall, height had a strong impact than base size on performance.

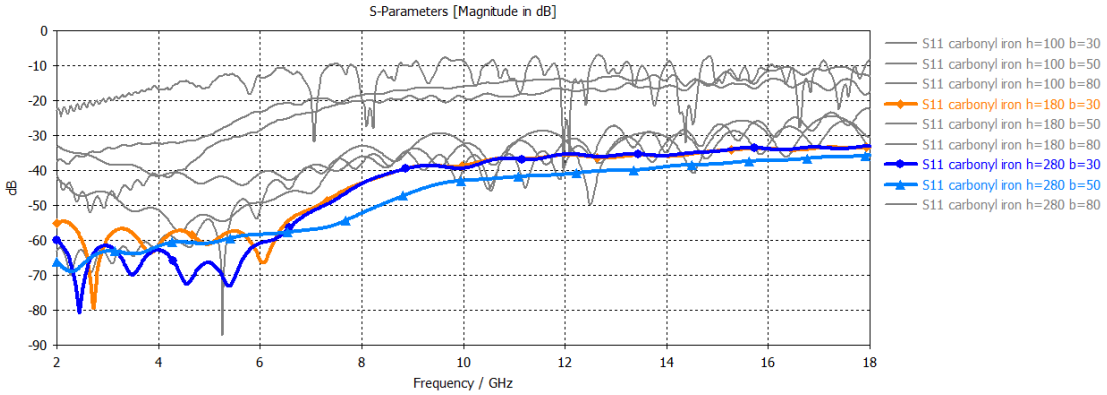


Figure 3.7: Reflection coefficient S11 curves of the three best performing configurations.

The absorber with h=280mm and b=30mm exhibited the broadest and deepest absorption band below -30dB as shown in Figure 3.7. The two other high performing geometries (h=280mm b=50mm; h=180mm b=30mm) followed similar trends, confirming the effectiveness of tall, narrow structures for broadband performance.

Based on the S11 results, the carbonyl iron absorber with 280mm height and 30mm base achieved the most effective broadband absorption. To evaluate the influence of material properties, the same geometric configurations were simulated using NiZn ferrite, as detailed in the next section.

3.3.1.2 NiZn ferrite based pyramidal absorber

This section represents the simulation results of the NiZn ferrite based pyramidal absorbers, tested over varying base sizes and pyramid heights.

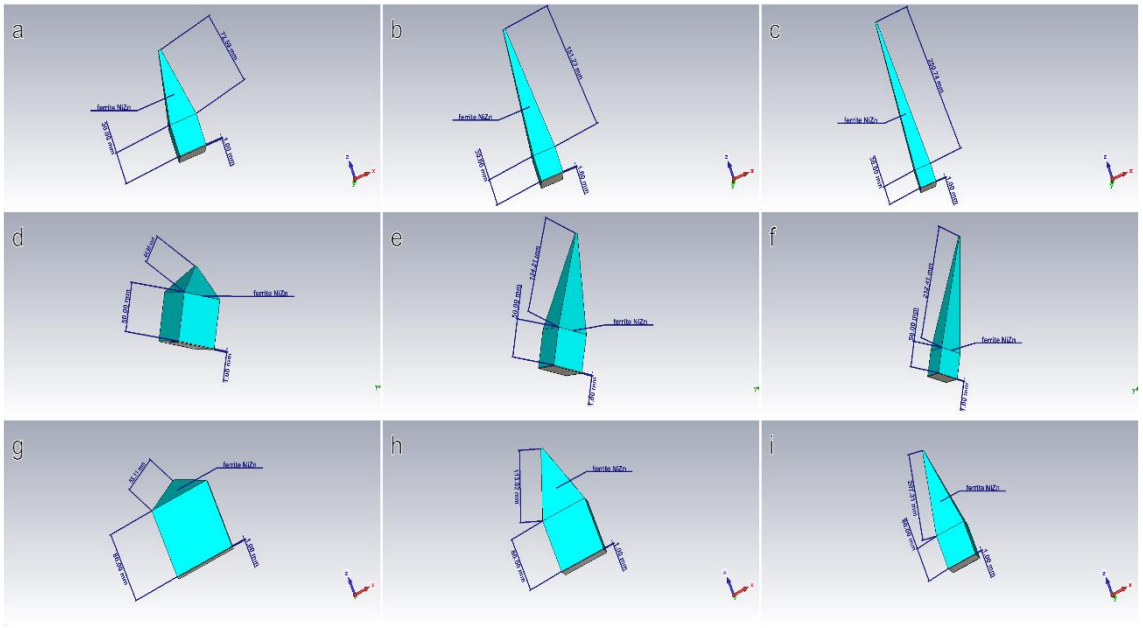


Figure 3.8: NiZn ferrite pyramidal absorbers geometries combined.

The pyramidal absorbers simulated in this section use identical geometric configuration to those in the previous carbonyl iron analysis. A total of nine geometries were tested using NiZn ferrite as shown in Figure 3.8, combining three base sizes with three total heights. The summary of the labeled configurations is presented in Table 3.1.

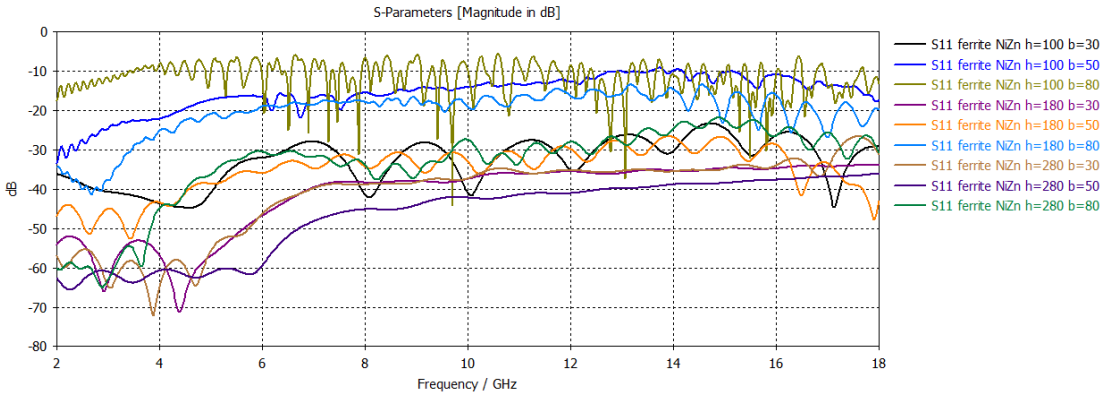


Figure 3.9: Simulated S11 curves for all NiZn ferrite based pyramidal absorbers.

The reflection coefficient (S11) curves for all configurations using NiZn ferrite are shown in Figure 3.9. These results were obtained under the same simulation settings used for carbonyl iron to permit direct comparison.

From the S11 results, three configurations demonstrated the most favorable broadband absorption performance:

- S11 NiZn ferrite h=180 b=30;
- S11 NiZn ferrite h=280 b=30;
- S11 NiZn ferrite h=280 b=50.

These results follow the trends observed with carbonyl iron as highlighted in Figure 3.10.

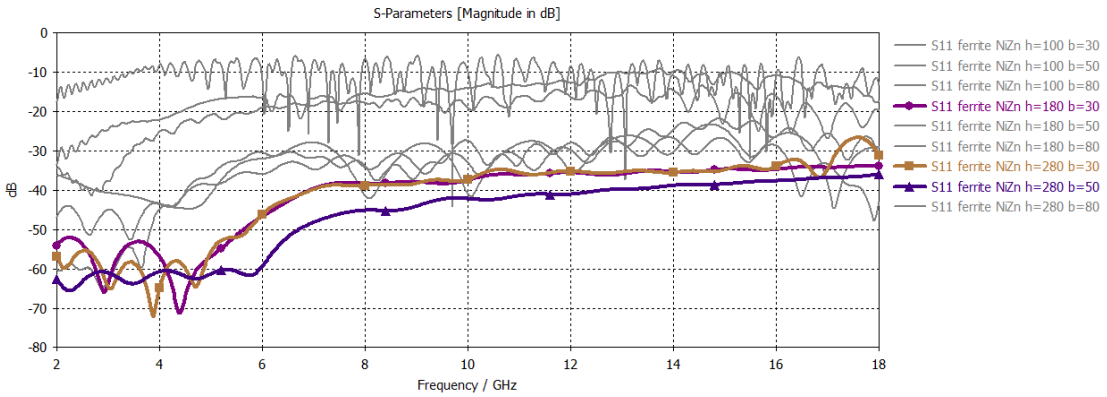


Figure 3.10: Best performing NiZn absorbers based on S11 results.

The combination of moderate base (b=50) and maximum height (h=280) leads to one of the best performances.

3.3.1.3 Graphite based pyramidal absorber

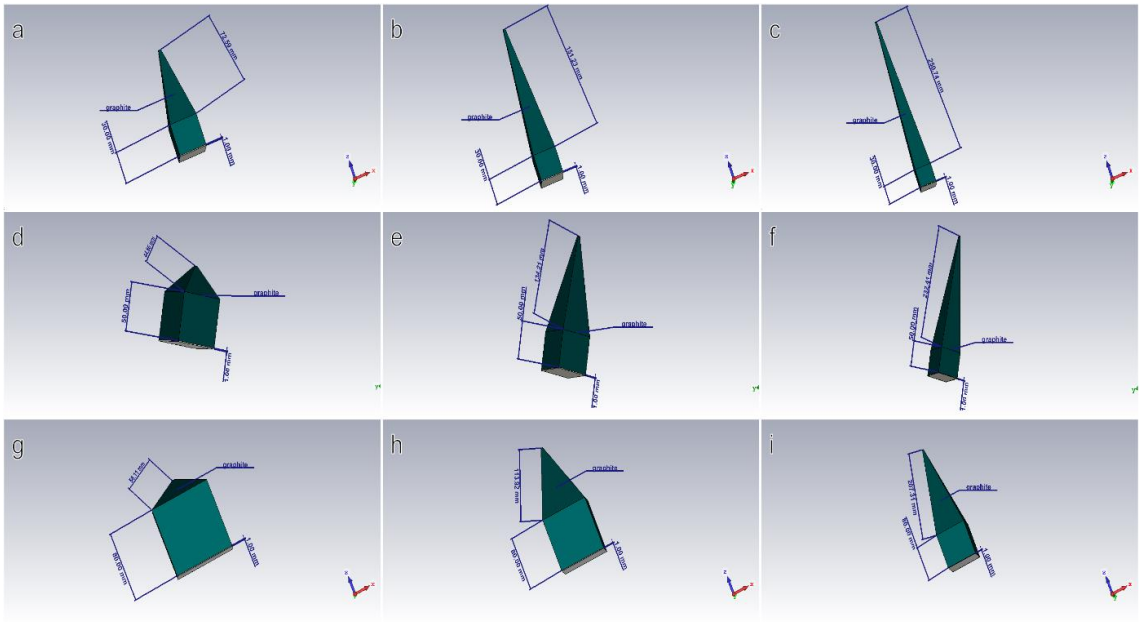


Figure 3.11: Pyramidal absorber geometries with graphite.

In this section, the same nine pyramidal absorber configurations were simulated using graphite as the material. Base sizes of 30mm, 50mm, and 8àmm were combined with heights of 100mm, 180mm, and 280mm as illustrated in Figure 3.11.

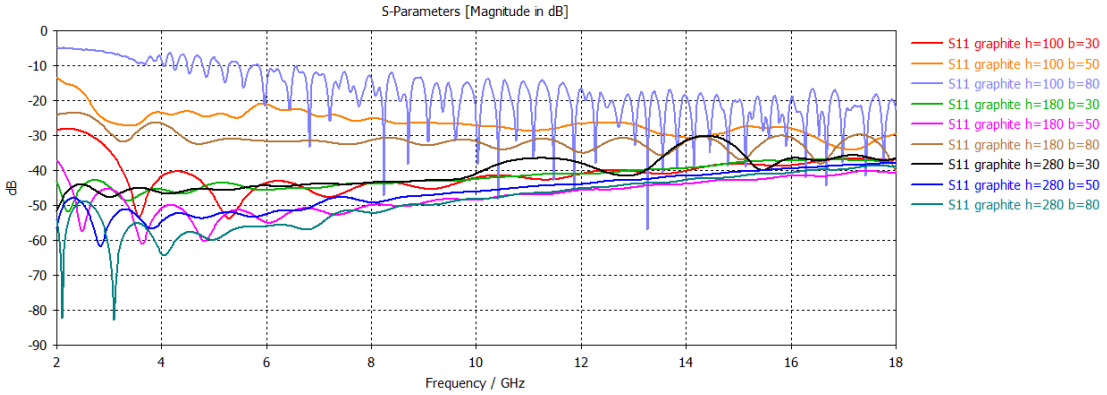


Figure 3.12: S11 curves for the graphite pyramidal absorbers.

The S11 performance of the graphite absorbers is presented in figure 3.12. As with the previous materials, all simulations were conducted under the same conditions across the 2-18GHz.

Similar to previous materials, higher absorber heights tend to reduce reflection across the band. However, graphite has a slightly delayed absorption at lower frequencies and stronger attenuation at higher frequencies.

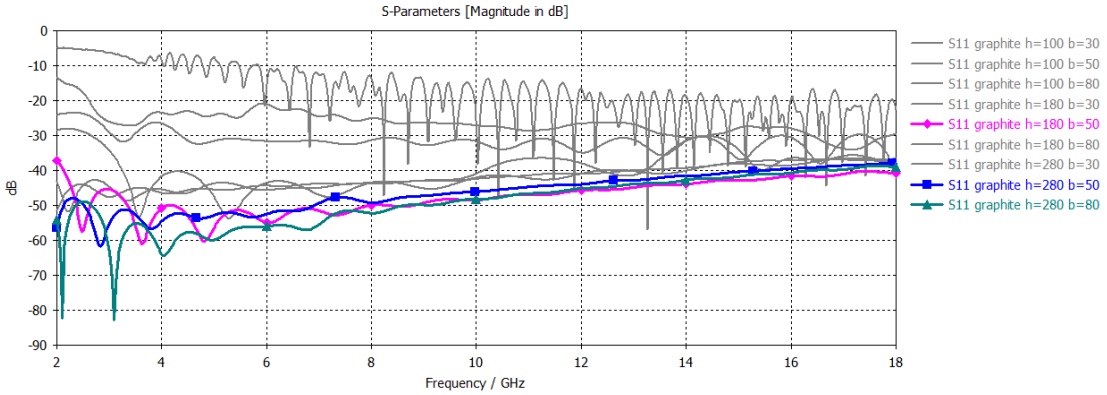


Figure 3.13: S11 curves for the three best performing graphite absorber geometries.

The overall trend confirms that increasing height and selecting suitable base dimensions improves absorption performance.

The three best configurations are shown in Figure 3.13. The absorber with h=180mm and 50mm base demonstrated the best broadband performance above 10GHz. Other top performing structures included (h=280mm b=80mm; h=280mm b=50mm), which provide effective absorption over wide frequency ranges.

3.3.1.4 Comparative analysis of the three materials:

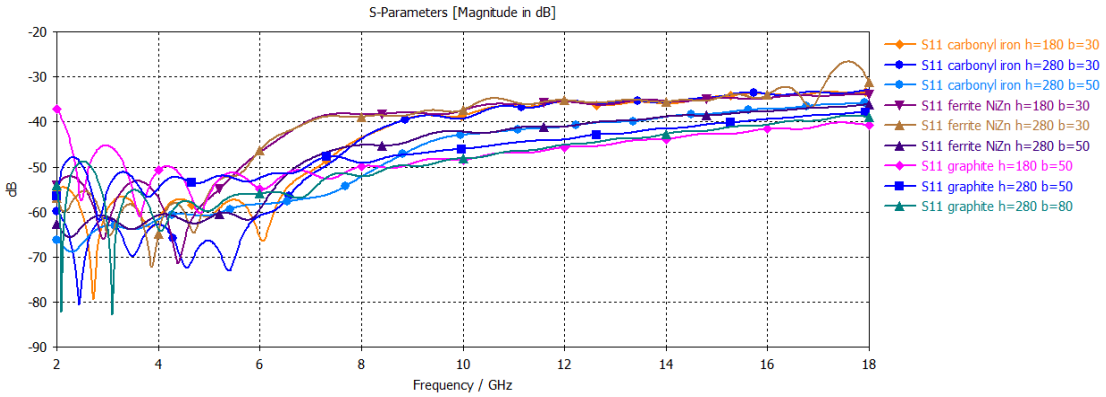


Figure 3.14: S11 curves of the best absorber configurations: three per material.

This section compares the most effective pyramidal absorber configurations for each tested material based on their S11 reflection characteristics. Figure 3.14 presents combined plot of the nine best performing absorbers.

The comparative analysis below highlights the relative performance at 2GHz, 8GHz and the 10-18GHZ high frequency region.

1. **Performance at 2GHz:**

   Figure 3.15 show the best reflection coefficient at 2GHz. At this low frequency, carbonyl iron (h=280mm, b=50mm) achieved the lowest S11, indicating superior absorption compared to ferrite and graphite.

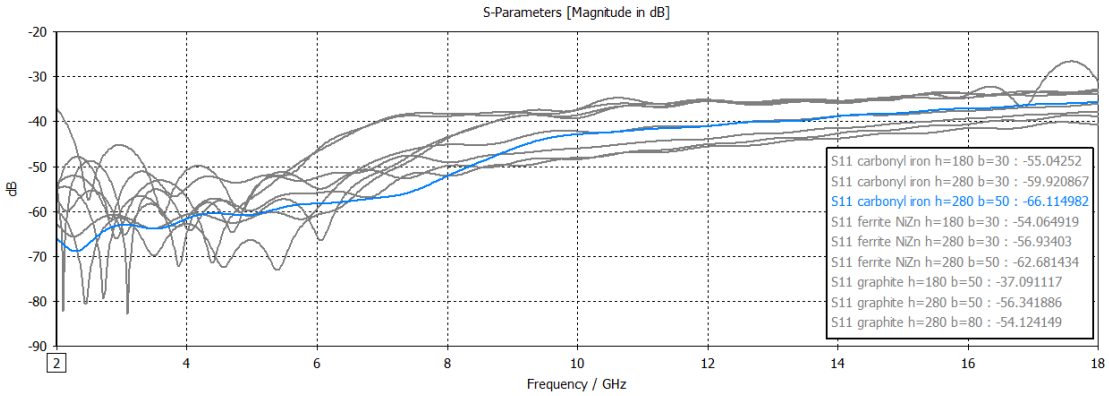


Figure 3.15: S11 curves comparison at 2GHz.

2. **Performance at 8GHz:**

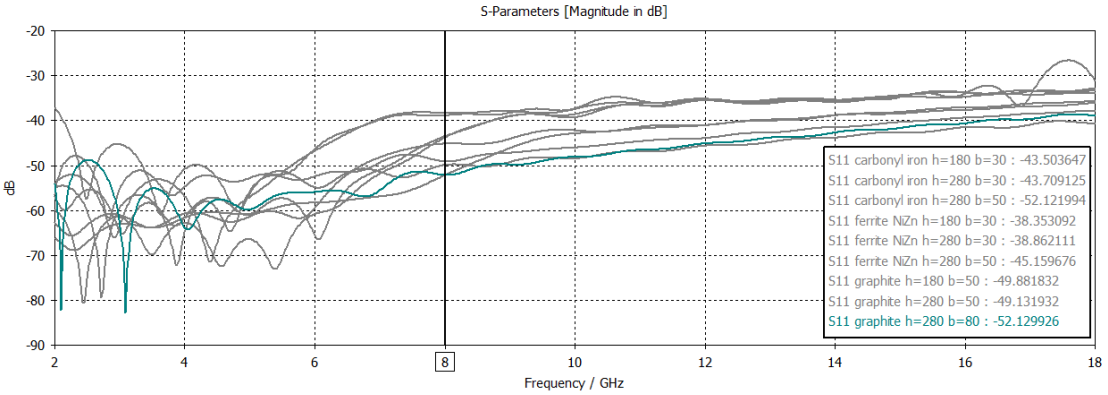


Figure 3.16: S11 curves comparison at 8GHz.

At mid-band, the reflection response (figure 3.16) highlights graphite (h=280mm, b=280mm) as the most affective material. The steep dip in S11 indicated strong absorption at this frequency, outperforming carbonyl iron and ferrite.

3. Performance at 10GHz:

As shown in figure 3.17, graphite (h=180mm, b=50mm) maintained the lowest reflection across the high frequency band [10-18GHz], confirming its effectiveness for wideband high frequency absorption.

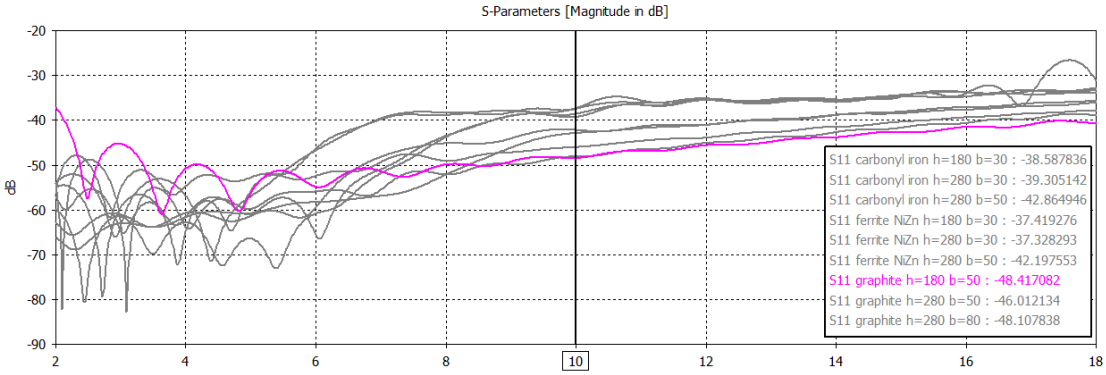


Figure 3.17: S11 curves comparison at 10GHz and beyond.

These comparisons show that carbonyl iron performs better at low frequencies <8GHZ, while graphite dominates the higher frequency range >8GHz, making it a suitable choice for broadband applications when designed with appropriate dimensions.

3.3.2 Conical absorber

Figure 3.18 presents the conical absorber geometry used in the simulation.

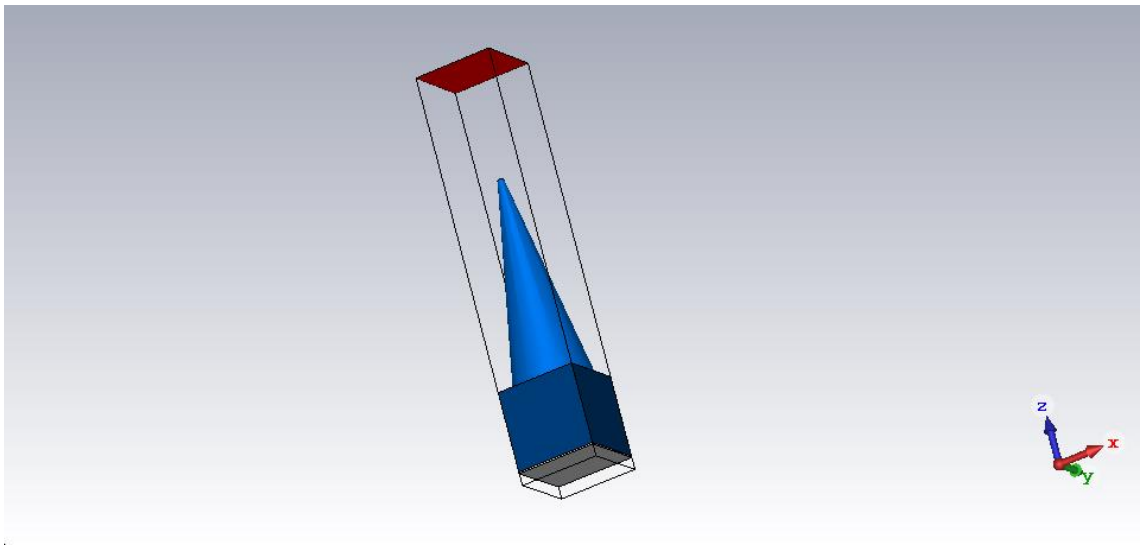


Figure 3.18: 3D geometry of the conical absorber.

The conical absorber follows the same design logic as the pyramidal one, with adjustments to the shape. It consists of a smooth conical body mounted on a rectangular base. To prevent meshing issues at the tip, a flat surface of 2.83mm diameter was added as highlighted in Figure 3.19, just as in the pyramidal case. The structure is excited from the top using a single waveguide port, while the bottom is closed with a PEC boundary to reflect incident fields toward the absorber's tip.

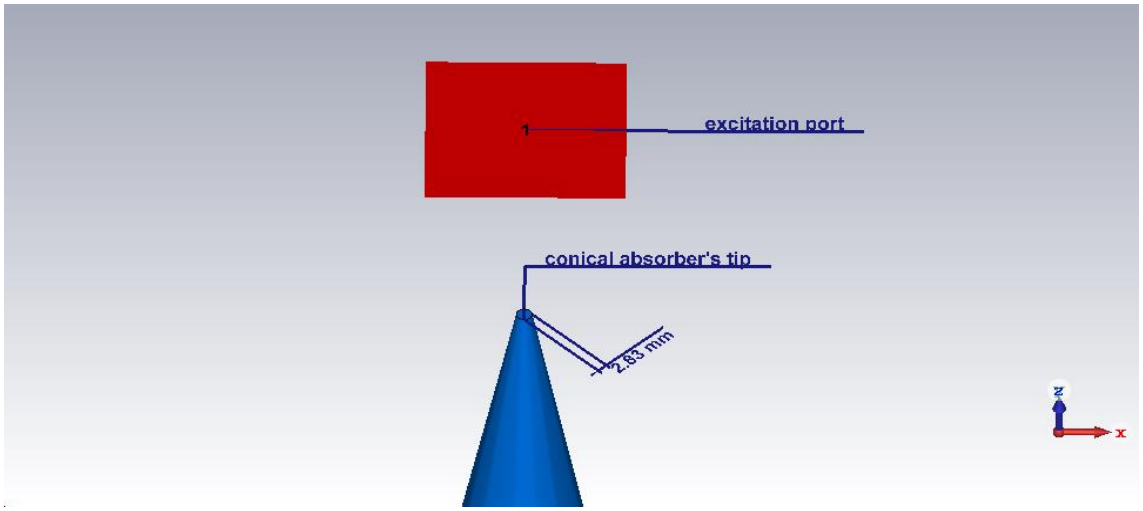


Figure 3.19: Close-up view of the conical absorber tip and excitation port.

The following section present the simulation results for the conical absorber using the same evaluation procedure applied to the pyramidal design.

3.3.2.1 Carbonyl iron based conical absorber

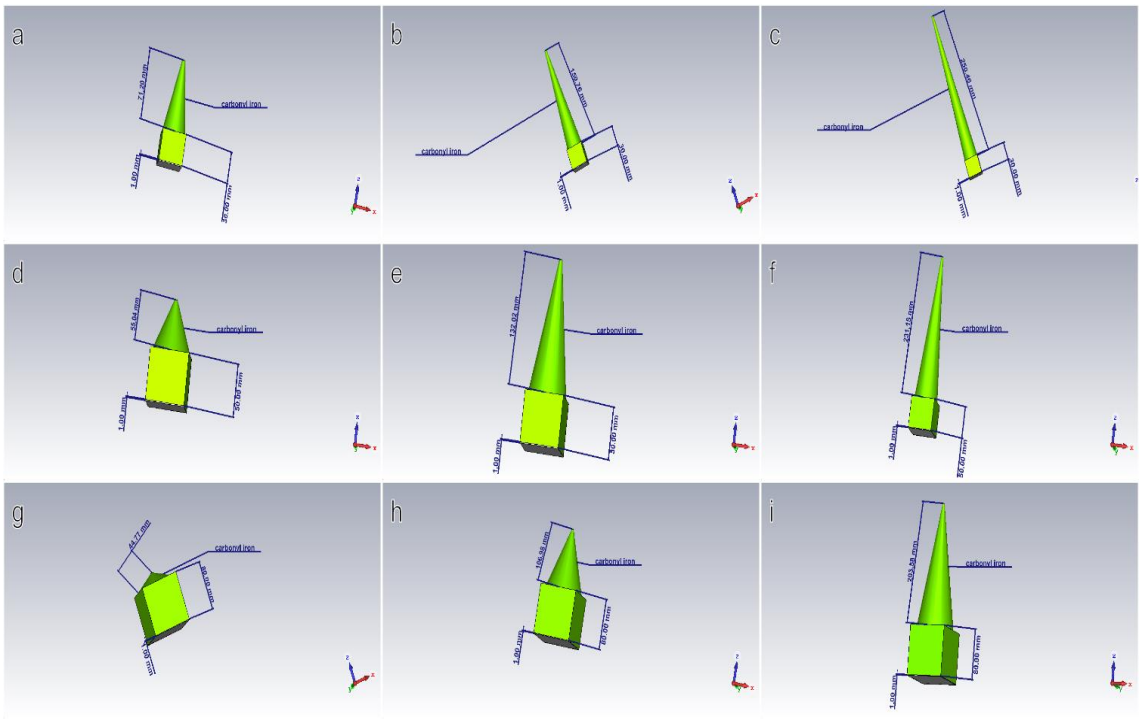


Figure 3.20: Carbonyl iron conical absorbers with all height base combinations.

Figure 3.20 presents the nine carbonyl iron based conical absorber geometries, covering all height-base combinations used in the simulations.

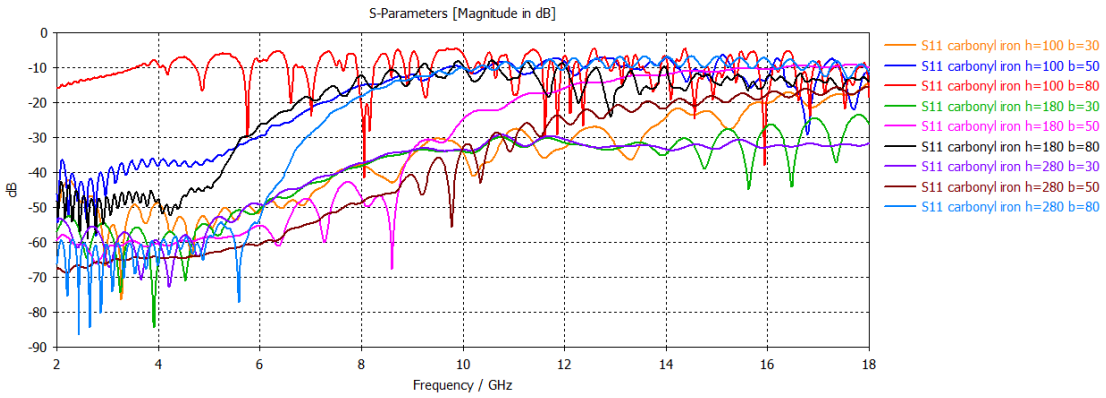


Figure 3.21: S11 curves for the nine carbonyl iron conical absorber configurations.

The tested geometries follow the same base-height combinations previously listed in Table 3.1, allowing for consistent comparison across different absorber shapes. The reflection coefficient (S11) results for all nine carbonyl iron absorbers are shown in Figure 3.21. Each curve corresponds to a different height-base configuration, as previously described.

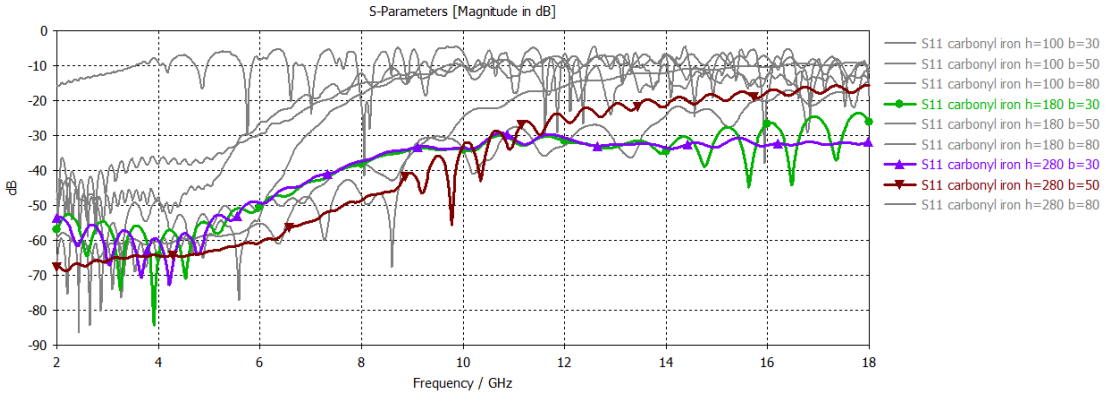


Figure 3.22: S11 curves of the top three performing conical absorbers.

The results show that increasing the absorber height generally tend to perform better, especially in the lower frequency range.

Among the nine configurations, three geometries exhibited the best performance based on broadband absorption. The corresponding S11 responses are shown in Figure 3.22.

The absorber with h=280mm and b=30mm stands out with the most stable and broadband absorption across the entire 2-18GHz range. The h=180mm b=30mm variant follows a similar trend but exhibits more oscillations, the h=280mm b=50mm shows the strongest absorption below 10GHz, but its performance drops significantly beyond that point, making it more suitable for low frequency applications.

3.3.2.2 NiZn ferrite based conical absorber

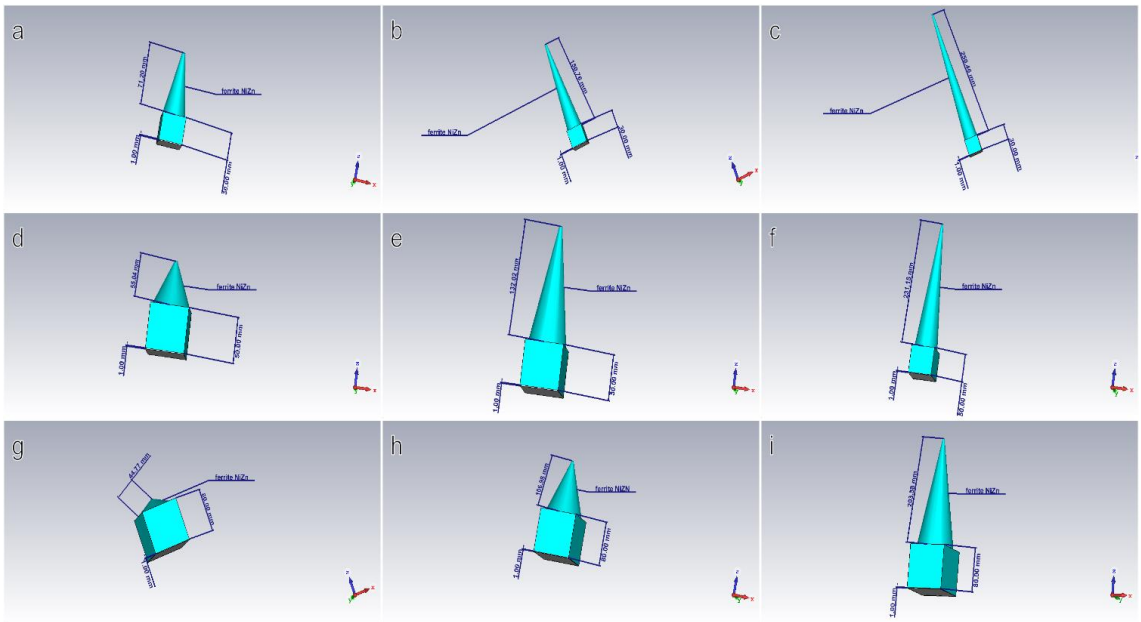


Figure 3.23: NiZn ferrite conical absorbers geometries combines.

This section presents the results of the NiZn ferrite based conical absorbers using the same 3x3 height-base configuration and simulation setup described previously (Figure 3.23).

The simulated S11 curves for all nine NiZn ferrite based conical absorbers are shown in Figure 3.24.

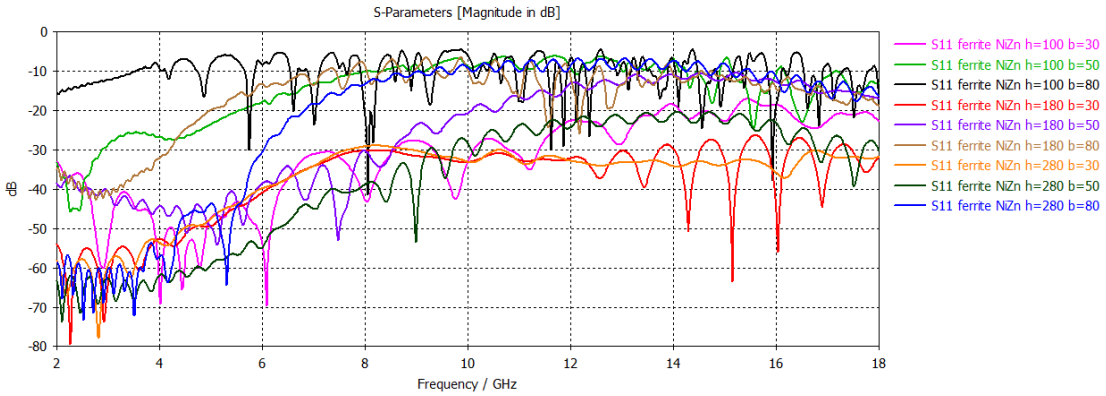


Figure 3.24: S11 results for the nine NiZn ferrite conical absorbers.

As with previous materials, the trends reveal a strong dependence on absorber height, with improved low frequency absorption observed for taller structures.

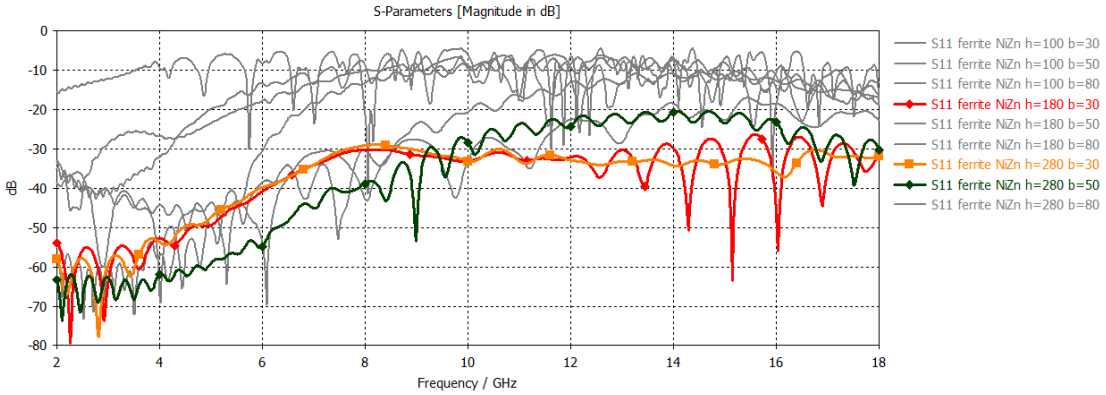


Figure 3.25: Top performing NiZn ferrite absorbers.

The 280x50mm absorber shows the best performance below 10GHz before slightly rising. The 180x30mm and 280x30mm configurations exhibit nearly identical behavior, with the latter showing slightly more oscillations. All three converge around -20dB as shown in Figure 2.25, indicating good broadband absorption.

3.3.2.3 Graphite based conical absorber

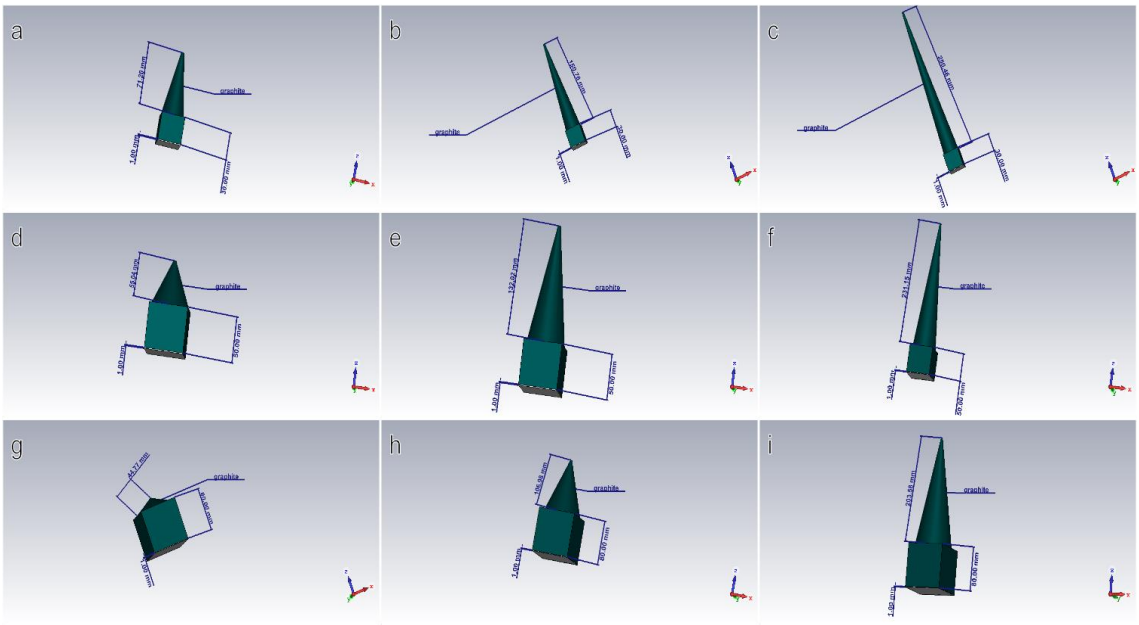


Figure 3.26: Conical absorber geometries with graphite.

This section includes the analysis of graphite based conical absorbers under the same height-base previously detailed, outlined in Figure 3.24.

As illustrated in Figure 3.27, several graphite based configurations demonstrate strong absorption performance.

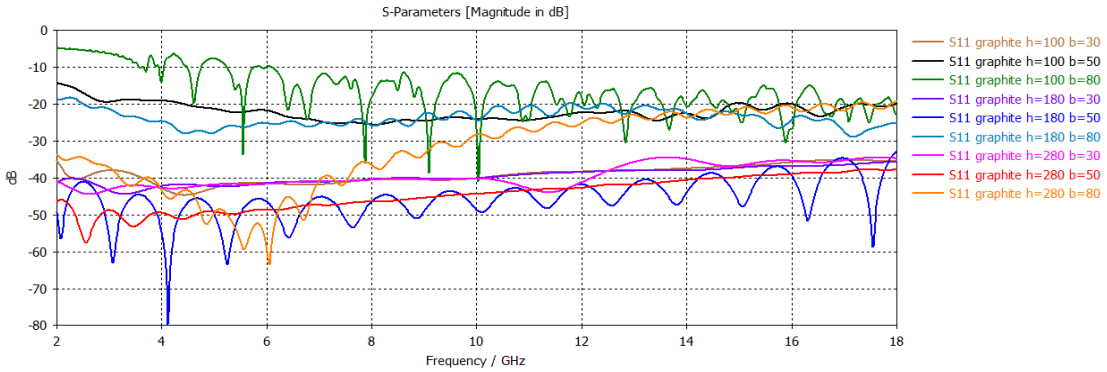


Figure 3.27: S11 results of the graphite based conical absorbers.

Among the three top performing graphite based conical absorbers, as illustrated in Figure 3.28 the 280mm height, 50mm base configuration stands out the most effective. It maintains reflection losses mostly below -40dB throughout the entire band. The 180x30mm case also performs very well, with the smoothest curve among the three. In contrast, the 180x50mm configuration, despite being affective, shows noticeable oscillations across the band, making the absorption behavior less stable.

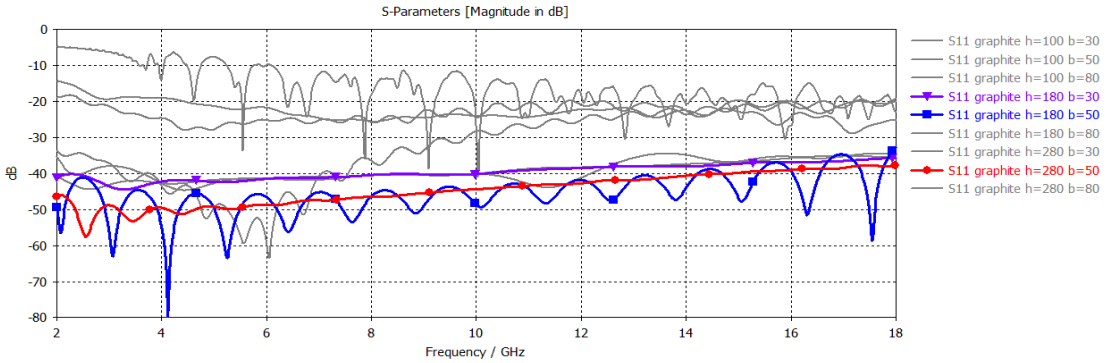


Figure 3.28: Top three S11 curves for graphite based conical absorbers.

3.3.2.4 Conical absorber: comparative analysis of the three materials:

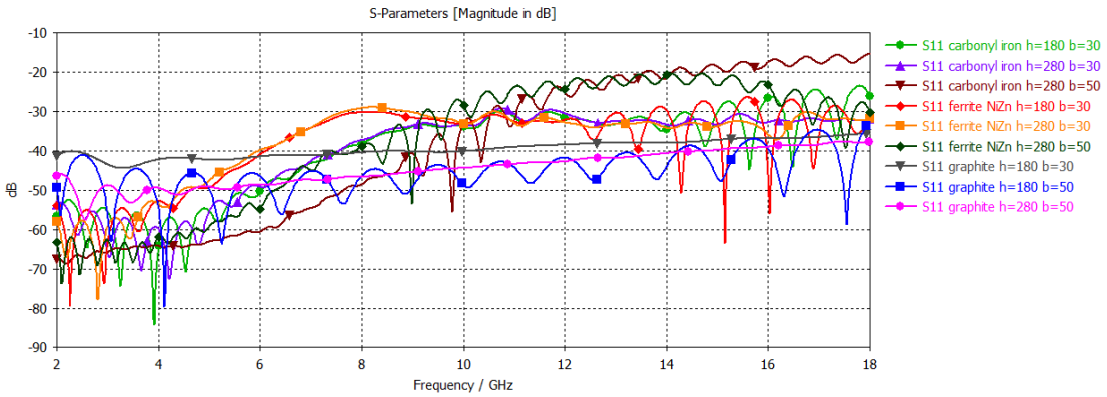


Figure 3.29: S11 curves of the best pyramidal absorber configurations: three per material.

This section compares the absorption performance of the three conical absorber materials based on their top performing S11 responses. Figure 3.29 presents combined plot of the nine best performing absorbers.

The comparison is made at four representative frequency positions: 2GHz, 8GHz, 14GHz, and 18GHz, covering the full operational bandwidth.

1. **Performance at 2GHz and 8GHz:**

   At both 2GHz and 8GHz, the configuration carbonyl iron based conical absorber with h=280mm and b=50mm demonstrated the most effective EM absorption, showing the lowest S11 values across the compared materials. Figure 3.30 illustrates the comparative performance at these two frequencies.

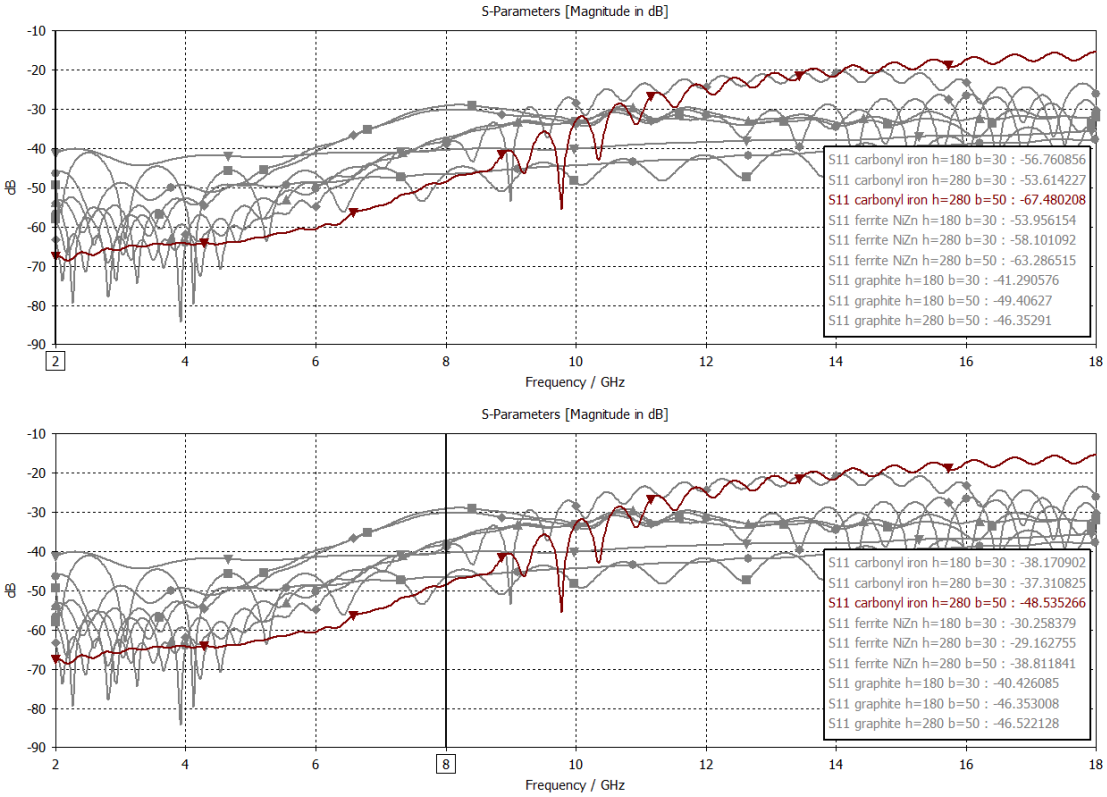


Figure 3.30: S11 curves response at 2GHz (top) and 8GHz (bottom).

2. Performance at 14GHz:

Figure 3.31 show the S11 performance of the top absorber configurations at 14GHz, where the graphite based absorber with dimensions 180mm x 50mm clearly outperforms the others, achieving the lowest reflection level.

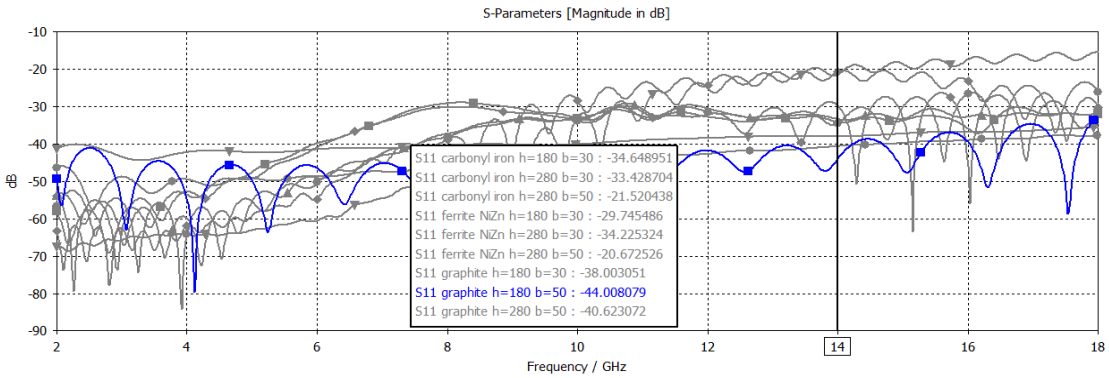


Figure 3.31: S11 curves response at 14GHz.

3. Performance at 18GHz:

At 18GHz, the graphite 280x50mm absorber shows the best absorption, with a smooth S11 curve below -35dB, as seen in Figure 3.32.

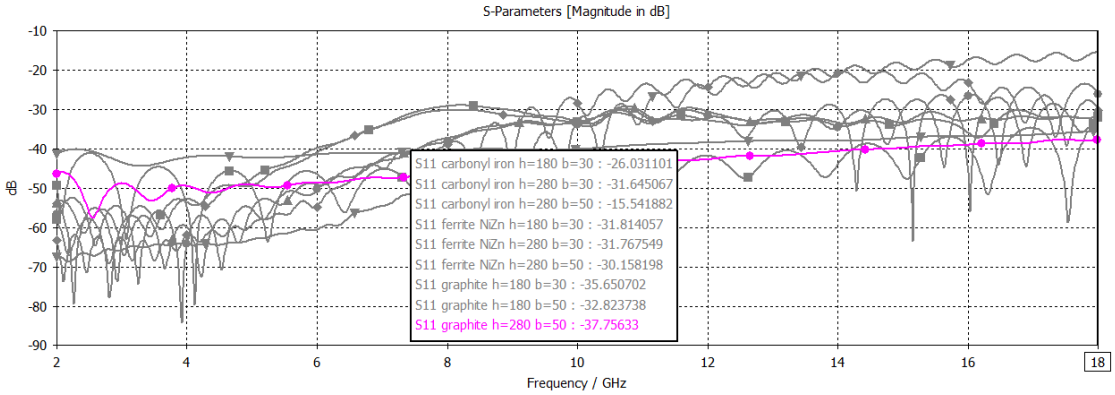


Figure 3.32: S11 curves response at 18GHz.

The comparative analysis of the top performing conical absorber configurations shows that graphite performs better at higher frequencies, especially above 10GHz. Carbonyl iron and NiZn ferrite give better results at lower frequencies, but graphite ensures deeper and more stable absorption over the broader band.

3.3.3 Hybrid absorber

This section introduces a hybrid pyramidal absorber composed of two stacked sections: carbonyl iron at the top and NiZn ferrite at the bottom as shown if Figure 3.33. The total height is 180mm with a 50mm base. This geometry was developed after thorough testing to combine the complementary absorption characteristics of both materials.

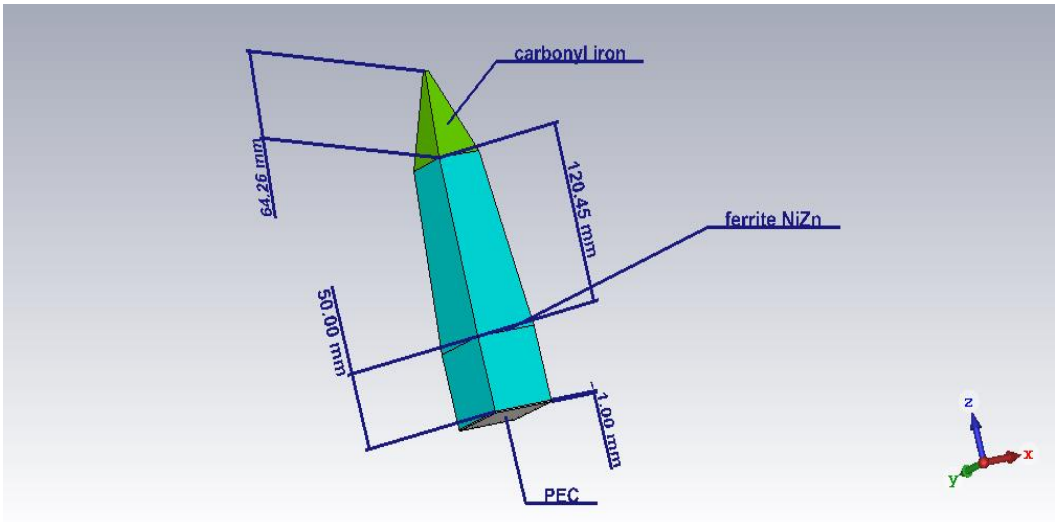


Figure 3.33: 3D geometry of the hybrid pyramidal absorber.

This hybrid absorber combines carbonyl iron and NiZn ferrite within a single pyramidal structure. Earlier tests of both materials at 180mm height and 50mm base revealed complementary performance, each material compensating where the other declined. To

exploit this, a dual section pyramid was built: a 60mm carbonyl iron top and a 120mm NiZn ferrite base, designed with different apex angles to form a continuous shape.

To better understand the individual absorption characteristics of each material, Figure 3.34 displays the S11 responses of carbonyl iron and NiZn ferrite absorbers, both using the same geometry (180mm height, 50mm base). The plots illustrate how each material performs better in different frequency range.

As shown in Figure 3.34, NiZn ferrite performs better from 2-4GHz, while carbonyl iron dominates between 4-8GHz. In the mid band, both behave similarly, with carbonyl iron slightly ahead overall. NiZn ferrite regains advantage at 16-18GHz. Both maintain S11 below -25dB across the entire range.

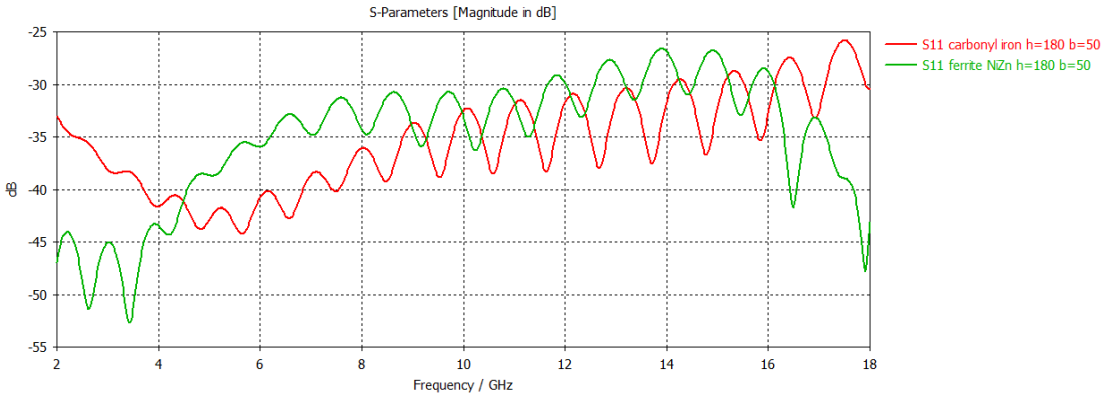


Figure 3.34: Comparison of S11 curves for carbonyl iron and NiZn ferrite absorbers.

Compared to the individual absorbers, as illustrated in Figure 3.35, the hybrid structure outperforms both in terms of consistency and depth of absorption. While NiZn ferrite and carbonyl iron each dominate in specific bands, the hybrid maintains strong performance across the full 2-18GHz range, with most of the curve staying below -35dB.

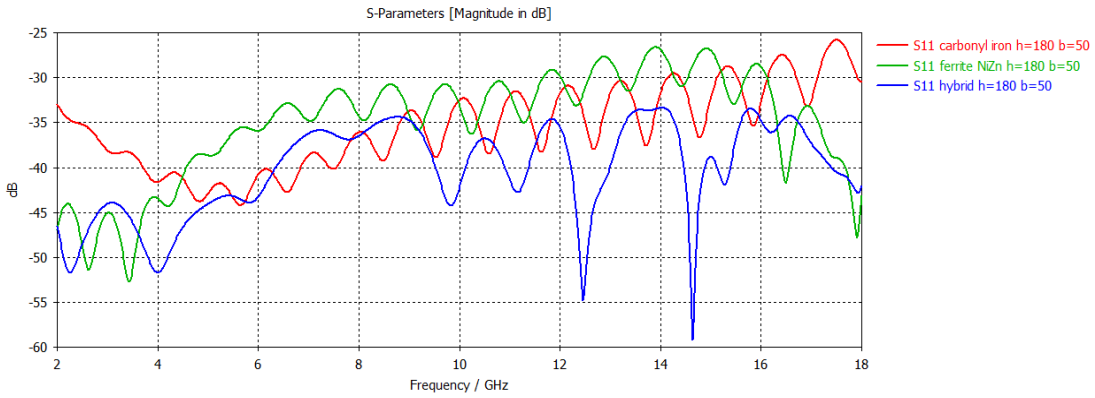


Figure 3.35: Comparison between S11 performances of NiZn ferrite, carbonyl iron, and hybrid pyramidal absorbers.

This confirms that combining the two materials in a dual pyramidal geometry successfully merges their best characteristics, resulting in broadband absorption with minimal reflection and reduced oscillations.

This result confirms the effectiveness of the hybrid design, which successfully combines the most favorable characteristics of both materials. The structure maintains excellent absorption throughout the 2-18GHz range, validating the design approach and material pairing.

3.3.4 Rounded tip pyramidal absorber

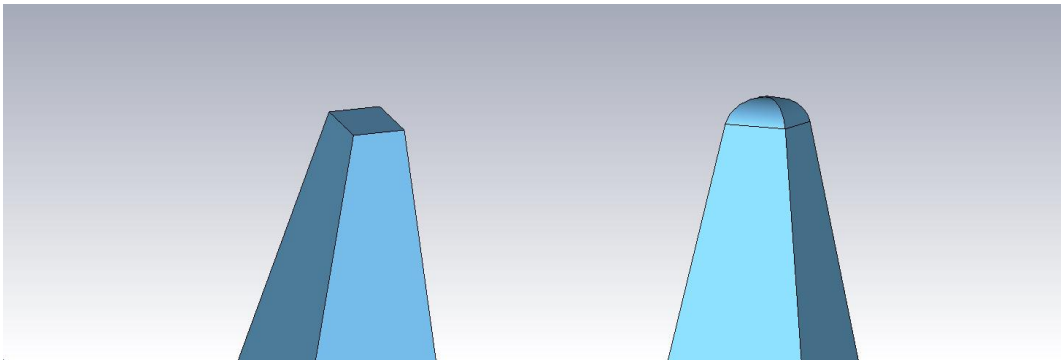


Figure 3.36: Geometrical comparison between standard tip (left) and rounded tip (right) pyramidal absorbers.

To evaluate the influence of the apex shape on absorber performance, this sections compares standard pyramidal structures with modified versions featuring a rounded tip. The geometry as represented in Figure 3.36, remains unchanged except for the apex region, allowing for an isolated assessment of this specific design variation.

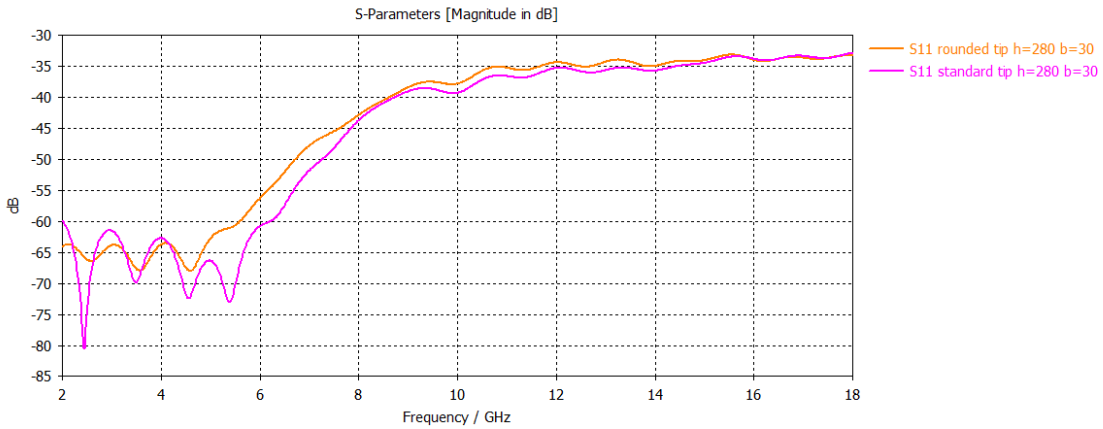


Figure 3.37: S11 comparison carbonyl iron based pyramidal absorber : rounded tip vs standard tip.

As shown in figure 3.37, both curves maintain strong absorption below -30 dB across the band. The rounded tip structure shows slightly reduced oscillations in the lower frequency range, but the standard tip performs marginally better.

3.3.4.1 NiZn ferrite based rounded tip vs standard tip

Figure 3.38 compares the two tip geometries for the NiZn ferrite absorber. Similar to carbonyl iron, both structures perform comparably.

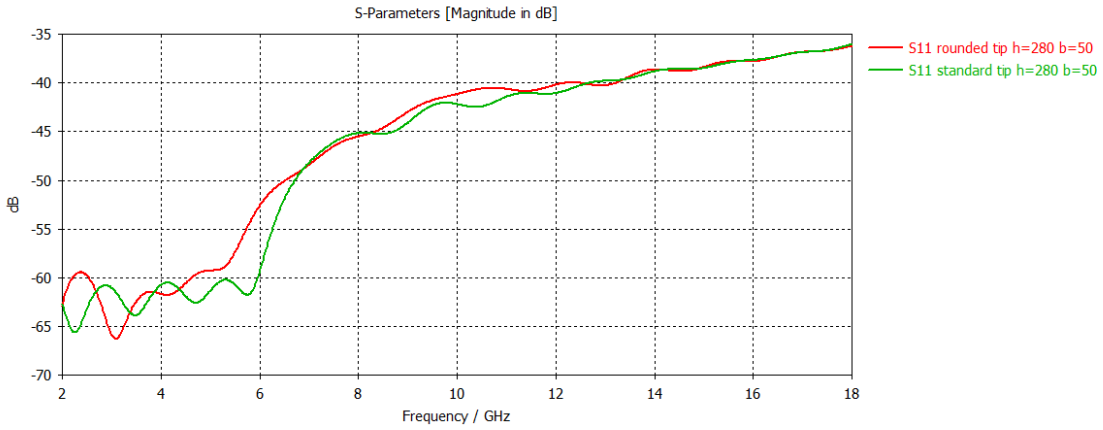


Figure 3.38: S11 comparison NiZn based pyramidal absorber : rounded tip vs standard tip.

3.3.4.2 Graphite based rounded tip vs standard tip

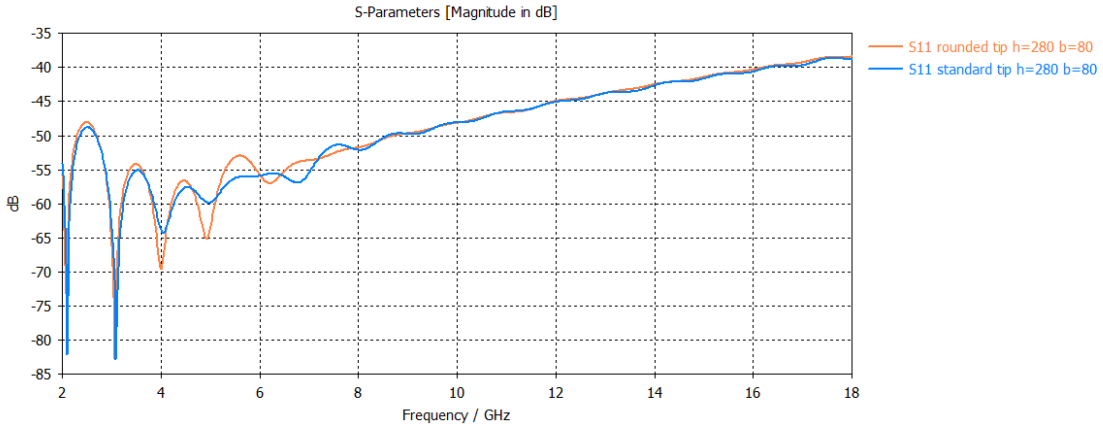


Figure 3.39: S11 comparison graphite based pyramidal absorber : rounded tip vs standard tip.

As illustrated in Figure 3.39, both curves are closely matched, but the standard tip demonstrates a slightly smoother response across the band. Oscillation levels are nearly identical, indicating minimal impact from the rounded modification in this case.

Across all three materials, modifying the pyramidal tip to a rounded shape had a minimal effect on overall performance. While the rounded tip slightly reduced oscillations at low frequencies in some cases, the standard tip consistently delivered better or equivalent absorption, making it the more reliable design choice.

3.3.5 Pyramidal vs conical absorbers: performance comparison

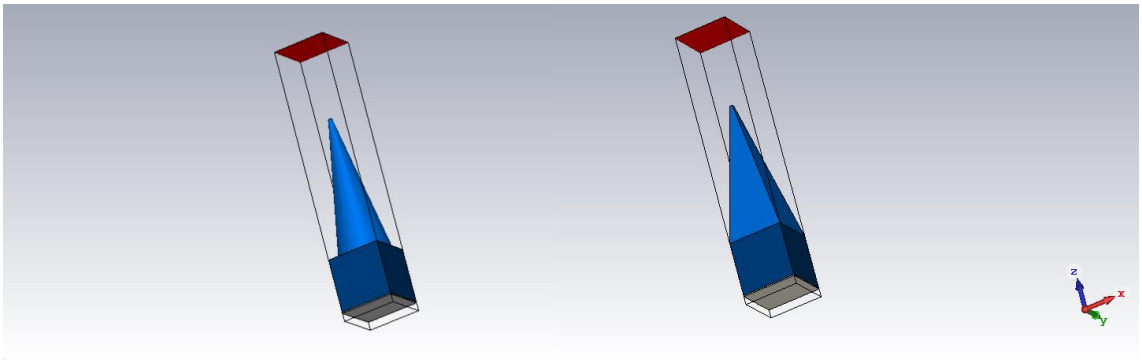


Figure 3.40: Geometry comparison between conical (left) and pyramidal (right) absorber structures.

Figure 3.40 presents a visual overview of pyramidal and conical absorbers respective geometries. The shapes differ primarily in taper profile, which impacts their impedance matching and absorption behavior.

To evaluate the effect of absorber geometry, this section compares he best performing pyramidal and conical structures for each material. All compared configurations share the same total height (280mm), while base dimensions vary slightly depending on the optimal configuration.

3.3.5.1 Carbonyl iron based comparison

Figure 3.41 presents the reflection coefficients of the top performing pyramidal and conical absorbers based on carbonyl iron. Both structures have a height of 280mm, with base sizes of 30mm for the conical shape and 50mm for the pyramidal.

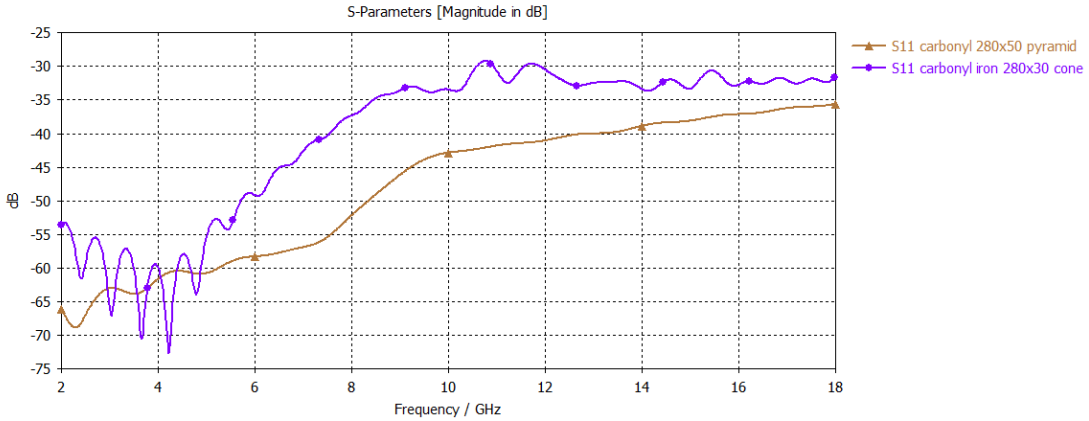


Figure 3.41: Comparison of top performing pyramid, conical absorbers carbonyl iron based.

The pyramidal absorber clearly outperforms the conical design across the entire 2-18GHz band. It maintains lower reflection levels, with smoother performance and fewer oscillations. The conical absorber, although still efficient, exhibits higher reflection.

This confirms that, for carbonyl iron, the pyramidal geometry provides more stable and broadband absorption characteristics.

3.3.5.2 NiZn ferrite based comparison

Figure 3.42 shows the reflection coefficient comparison between the top performing pyramidal and conical absorbers made of NiZn ferrite. Both have a height of 280mm, with base sizes of 30mm for the conical shape and 50mm for the pyramidal.

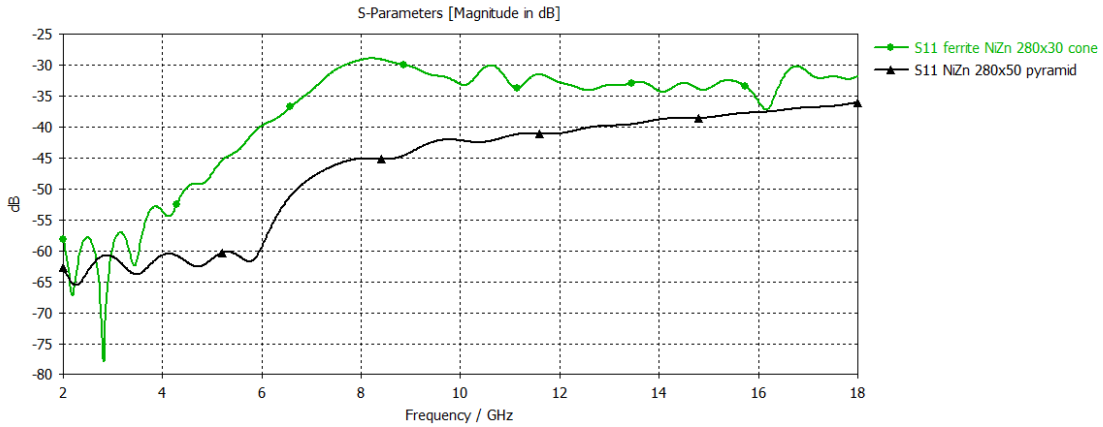


Figure 3.42: Comparison of top performing pyramid, conical absorbers NiZn ferrite based**.**

As observed, the pyramidal absorber demonstrates superior performance over the full frequency range. These results confirm that the pyramidal geometry delivers better broadband absorption than the conical one.

3.3.5.3 Graphite based comparison

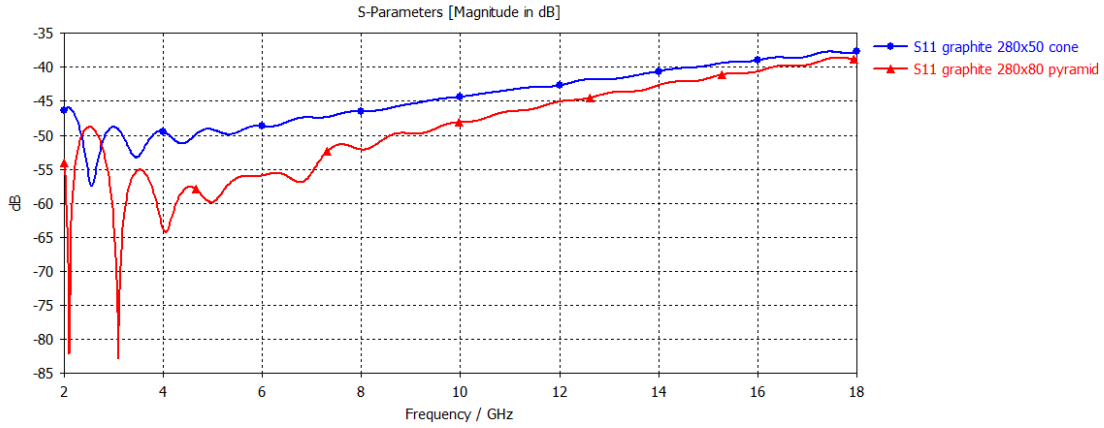


Figure 3.43: Comparison of top performing pyramid, conical absorbers graphite based**.**

Figure 3.43 presents the S11 comparison between the top performing pyramidal and conical absorbers using graphite. Both absorbers have the same 280mm height, with the pyramidal base of 80mm and 50mm for the conical.

Once again, the pyramidal absorber outperforms the conical one. Overall, graphite based absorbers benefit significantly from the pyramidal shape.

3.3.5.4 Analysis

As summarized in Table 3.2, the comparative analysis of pyramidal and conical absorber designs across all three materials (carbonyl iron, NiZn ferrite, and graphite) shows a clear and consistent trend: the pyramidal shape delivers superior absorption performance in each case. The pyramidal absorber maintained lower S11 values all across the 2-18GHz range, with better stability and reduced oscillations. While conical absorbers can be effective, especially with careful parameter tuning, pyramidal structures offer more reliable and broadband performance for the tested configurations. This makes the pyramidal design the more favorable choice for broadband absorber applications in this frequency range.

Table 3.2: Summary of top performing configurations by shape and material.

Material	Shape	Height(mm)	Base(mm)	Min S11(dB)	Notes
Carbonyl iron	pyramidal	280	50	-66 dB	Smooth curves
	conical	280	30	-53dB	Slightly higher oscillations
NiZn ferrite	pyramidal	280	50	-63dB	Good low-frequency response
	conical	280	30	-58dB	Noisier
Graphite	pyramidal	280	80	-82dB	Best performance across full band
	conical	280	50	-57dB	Higher S11

These results not only confirm the simulation trends but also highlight the more robust and stable response of pyramidal structures, especially at higher frequencies.

3.4 Realization and experimental validation

In this part, we used waveguides to test the EM absorption performance of graphite powder. The material was first delivered in solid rod form, then crushed into powder as shown in Figure 3.44, so it could be used in the test setup. A custom PLA holder was printed 3D printed to contain the powder between two waveguides operating from 10-20GHz during measurement. The following figures (Figure 3.44, 3.45 and 3.46) show the graphite in both forms, the PLA frame, and the waveguide used.

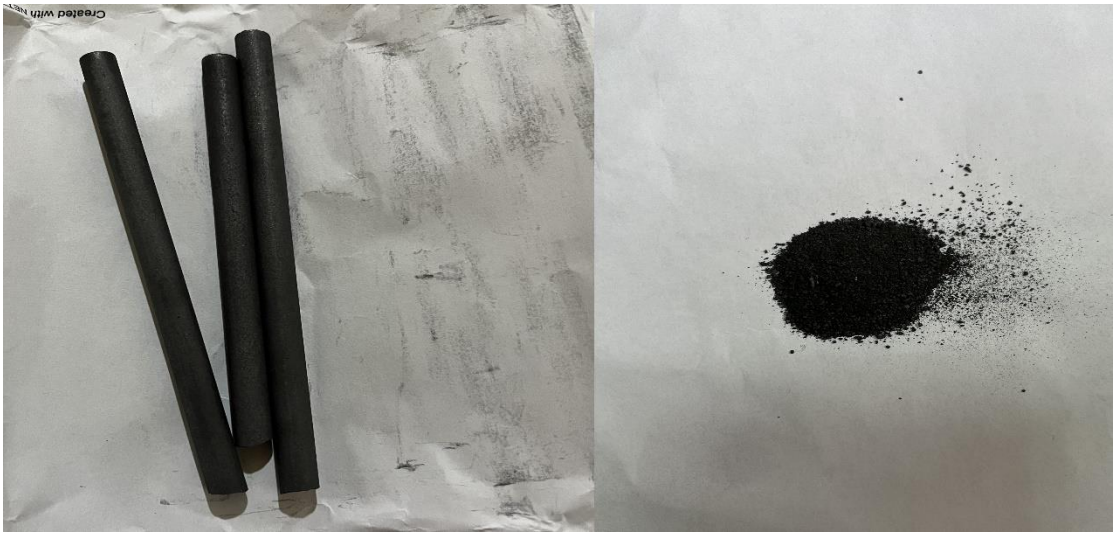


Figure 3.44: Graphite in its two forms.

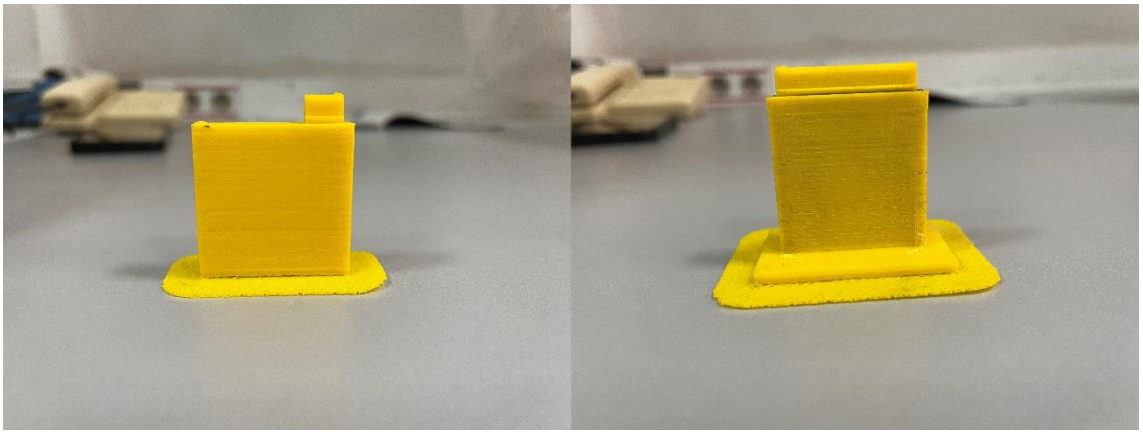


Figure 3.45: Graphite holder.

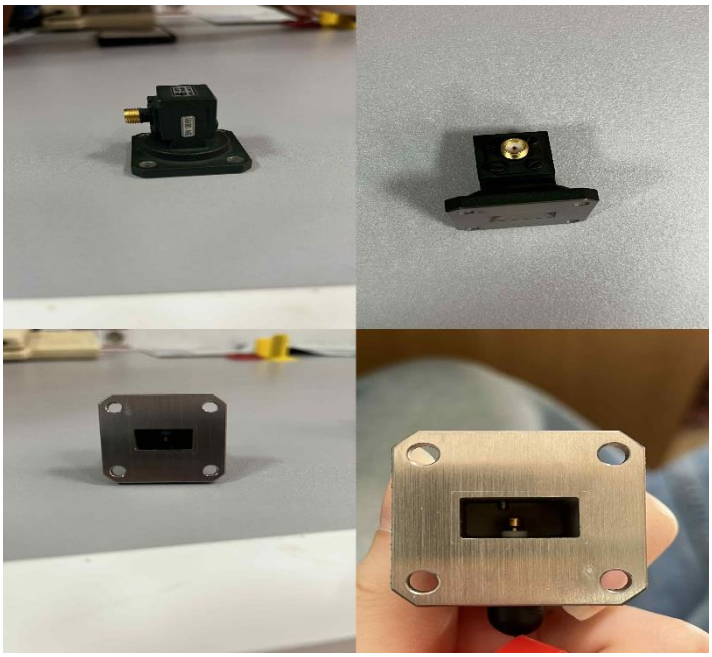


Figure 3.46: Multiple side views of the waveguide.

3.4.1 Waveguide design and simulation

A rectangular waveguide was designed using CST Studio Suite to serve as a test fixture for material characterization. The design ensures propagation of TE_{10} mode over a usable portion of 2-18GHz band, while the structure does not support the full frequency range, the effective operating band is sufficient for evaluating attenuation behavior. To evaluate the attenuation performance of the absorbers, two identical rectangular waveguides were used, the overall geometry is shown in Figure 3.47, with two ports were placed on top of SMA connectors, allowing signal excitation and reception as provided in Figure 3.48.

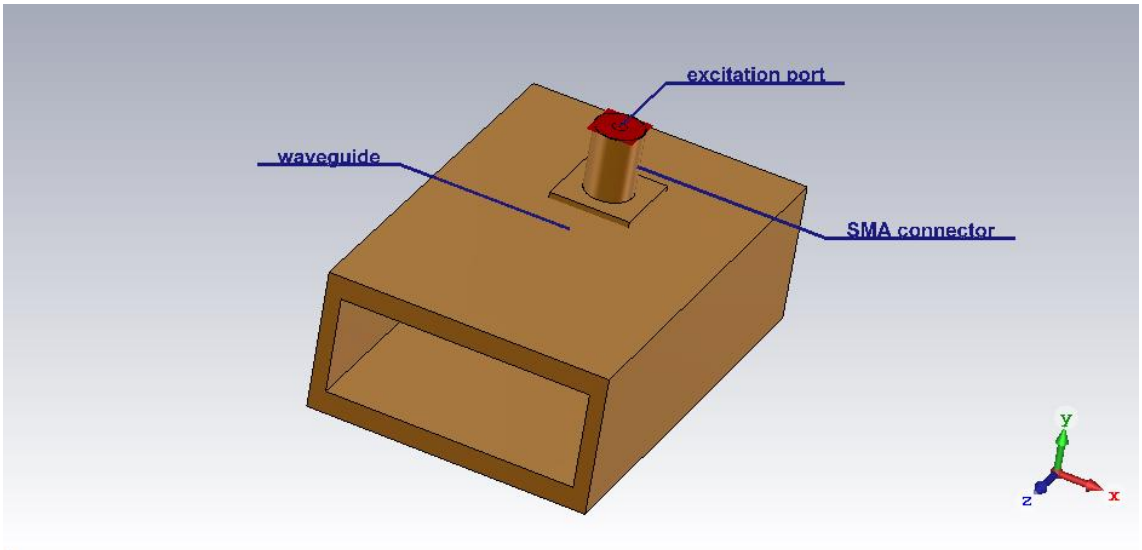


Figure 3.47: Full 3D view of the waveguide model used for simulation.

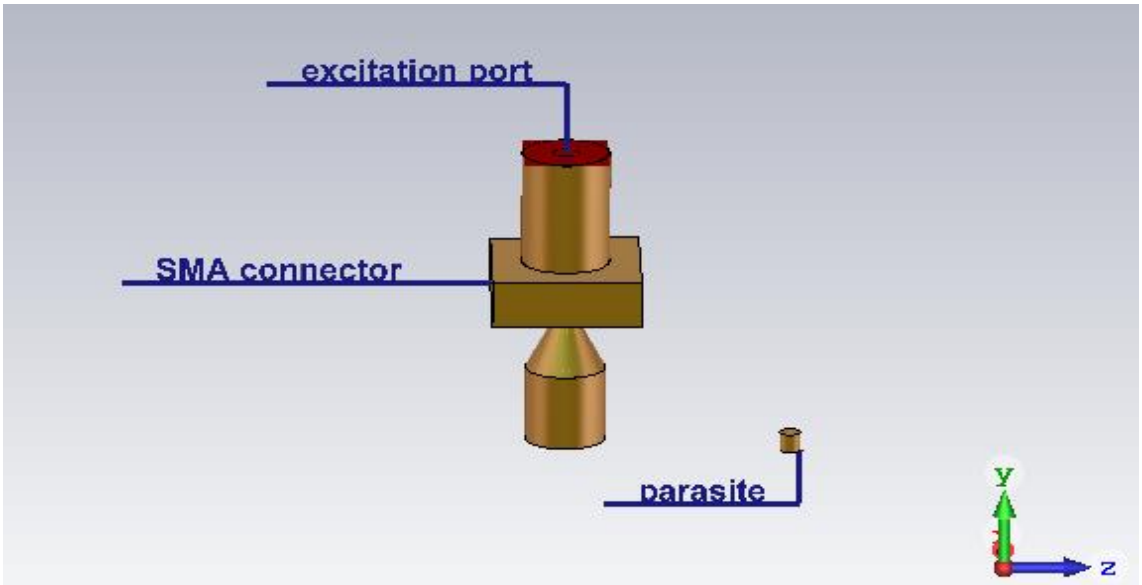


Figure 3.48: Close-up view of the SMA connector.

The simulated S-parameters of the empty waveguide are shown in Figure 3.49. the S11 remains low over the usable frequency range, indicating good impedance matching and minimal reflections at the input port. S21 shows high transmission, confirming stable propagation through the structure and proper alignment of the waveguide ports. These results validate the waveguide's stability for material attenuation measurements.

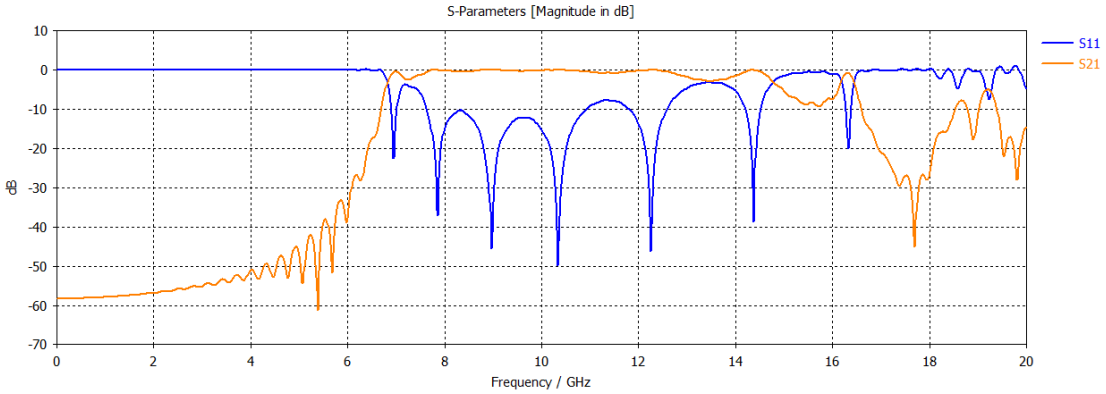


Figure 3.49: Waveguides S11 and S21 results.

3.4.2 Realization and measurement setup

After completing the design and simulation stages, practical measurements were conducted to evaluate the EM behavior of graphite powder. The testing phase included an initial analog check to verify the waveguide setup, followed by characterization using a VNA. To complement the physical tests, the same setup was modeled in CST for simulation based comparison. This combined approach ensures both experimental validation and simulation consistency.

3.4.2.1 Initial testing with analog instruments

In the initial phase, attenuation measurements were performed using a continuous wave signal generator and a spectrum analyzer to validate the general setup and ensure correct port alignment. The generator is connected to one waveguide port to transmit signal, while the analyzer is connected to the opposite end to record the received power. The absorber powder was placed between the two waveguides as shown in Figure 3.50. No detailed results are presented here, as this step served only as a preliminary check before proceeding to final measurements with a VNA.

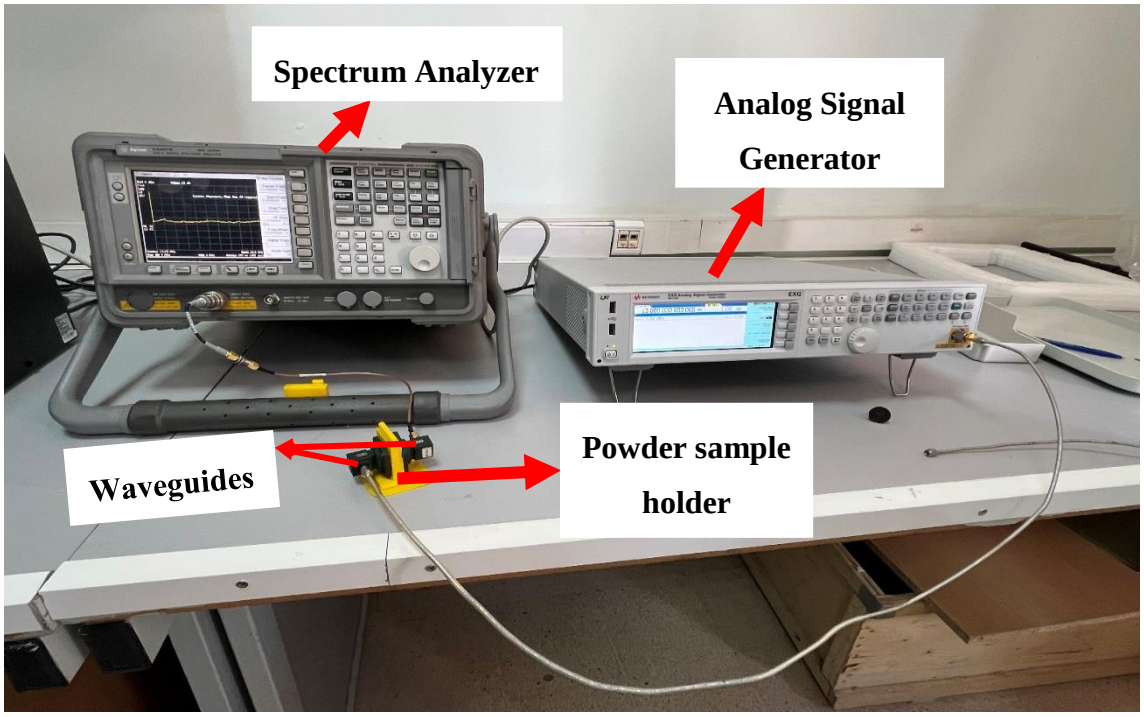


Figure 3.50: Analog measurement setup.

3.4.2.2 VNA measurement

The graphite powder was tested using a VNA over the 2-20GHz band. Two measurements were performed: first with an empty PLA holder, then with another one filled with graphite. Both configurations were placed between two waveguides, replicating the setup previously described. The physical setup of both tests are shown in Figure 3.51.

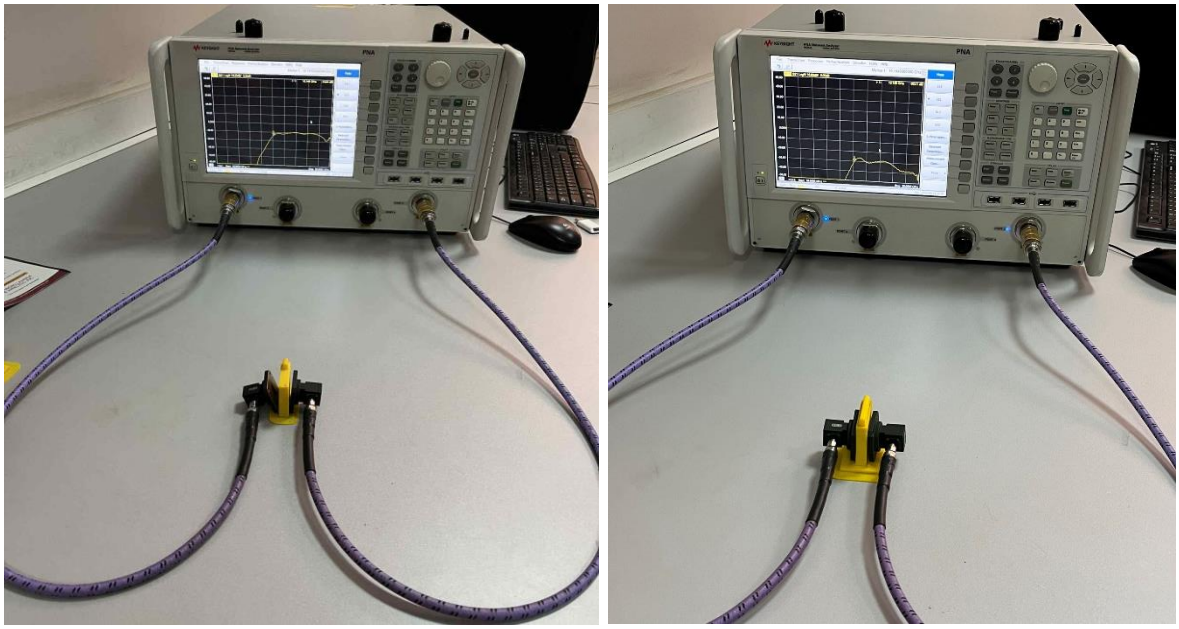


Figure 3.51: VNA measurement setups : empty PLA holder (left), graphite filled holder (right).

S-parameters data were exported in Excel format and processed using a simple MATLAB script to generate the reflection and transmission plots. Figure 3.52 shows the S-parameter curves of the empty holder, which introduces low attenuation and minimal reflection.

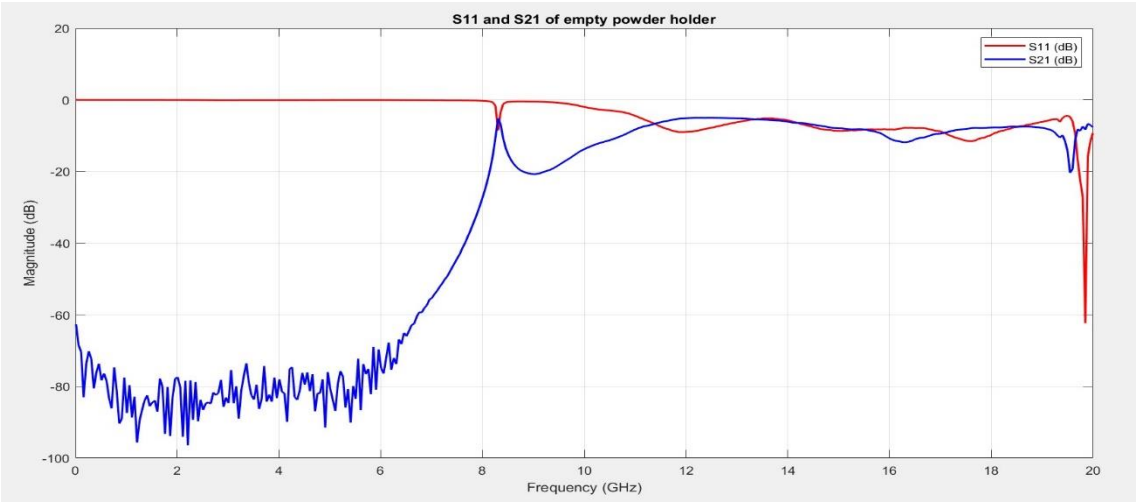


Figure 3.52: Measured S11 and S21 for the empty PLA holder.

3.4.2.3 CST simulation of the graphite filled waveguide

To replicate the VNA measurement, a solid graphite block was modeled directly between two waveguides, as shown in Figure 3.53.

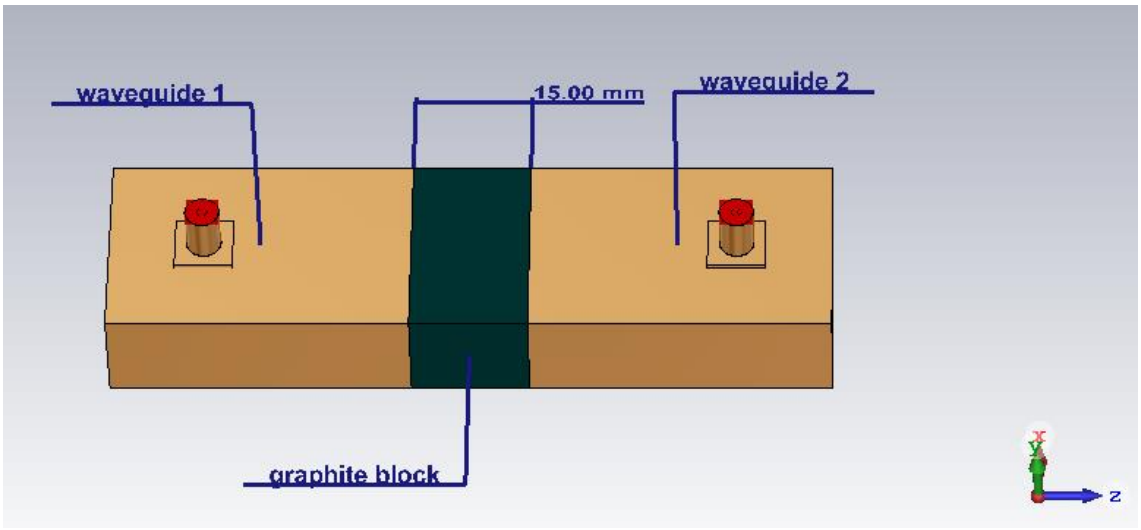


Figure 3.53: CST model of the graphite block between waveguides.

The graphite material was defined using frequency dependent complex permittivity and permeability, consistent with the values used in previous absorber simulations.

This section as shown if Figure 3.54 compares the simulated and experimental S-parameters of the graphite filled waveguide structure to assess the reliability of the CST model in replicating real measurement behavior.

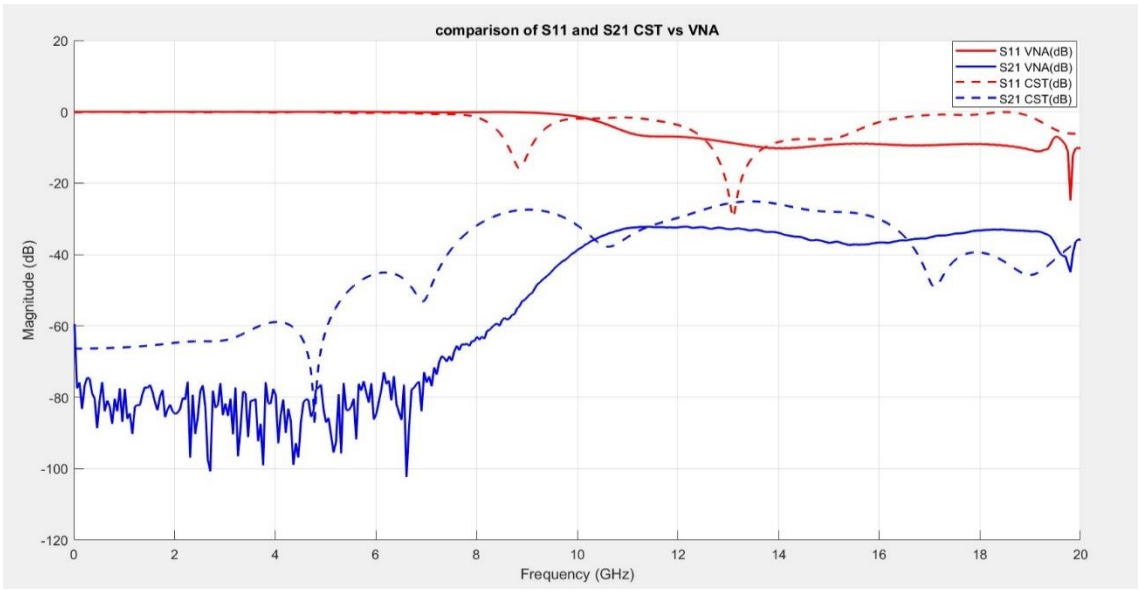


Figure 3.54: Comparison of S11 and S21 CST vs VNA.

The simulation closely matches the measured results. Both S11 values remain near 0dB, indicating strong reflection, and S21 values are mostly below -30dB, confirming high attenuation. This consistency validates the EM behavior modeled in CST. Overall, the comparison demonstrates that the CST model successfully captures the dominant EM

behavior of the graphite filled waveguide, validating both simulation fidelity and material choice.

3.5 Conclusion

The simulation results confirmed the strong influence of both material choice and geometry on absorber performance. The hybrid absorber successfully combined the strengths of carbonyl iron and ferrite, achieving low reflection levels across the full frequency range. Rounded tip designs showed minimal performance differences compared to standard tip, with slightly reduced oscillations.

Among the studied materials, graphite showed superior behavior at higher frequencies, while NiZn ferrite and carbonyl iron offered better absorption in the lower band. Geometrically, pyramidal structures consistently outperformed conical ones.

Finally, experimental measurements on a graphite filled waveguide structure validated the simulation trends. The results from VNA technique aligned with expectations, confirming the material's high absorption and supporting the simulated models.

General conclusion

This project addressed the design, simulation, and experimental validation of broadband electromagnetic absorbers intended for use in anechoic chambers and radio-frequency testing environments. The work began with a technical review of anechoic chambers and the role of absorbers in minimizing reflections. A detailed review of material properties was also provided, including methods of extracting permittivity and permeability.

Using CST Studio Suite, several absorber geometries were simulated across the 2-18GHz band, including pyramidal, conical, hybrid, and rounded tip designs. Three materials were studied using a consistent 3x3 matrix base sizes and heights. The results showed that absorber performance is strongly influenced by geometry and material type, with pyramidal shapes and graphite based configurations achieving the lowest reflection levels, particularly at higher frequencies.

The final part of the study involved experimental validation using a graphite filled waveguide structure. Vector network analyzer measurements confirmed the trends observed in simulation, validating the model and confirming the practical effectiveness of graphite.

While the final test used bare powder due to time constraints, future work could involve embedding the material in a polymer or resin matrix to eliminate air gaps and improve stability. Other possible extensions include testing material mixtures, or optimizing the internal structure.

References

[1] S. Khadka, *Evaluation of Radio Anechoic Chamber*, 2017.

[2] Y. Kotsuka, *Electromagnetic Wave Absorbers: Detailed Theories and Applications.*, United Kingdom: Wiley, 2019.

[3] Q. Xu et H. Yi , Anechoic and Reverberation Chambers: Theory, Design, and Measurements. Anechoic and Reverberation Chambers, United Kingdom: Wiley, 2018.

[4] A. Awastchi, J. Apruv et . D. Rahul, «analysis of different absorbers used in designing of an anechoic chamber,» *international research journal of engeering and technology (IRJET)*, 2025.

[5] P. F.Wilson et M. T.Ma, *A Study of Techniques for Measuring the Electromagnetic Shielding Effectiveness of Materials*, NBS .

[6] V. RODRIGUEZ, Anechoic range design for electromagnetic measurements, BOSTON/LONDON: Artech house, 2019.

[7] C. Liu, D. Yu, D. W. Kirk et Y. Xu, «Electromagnetic wave absorption of silicon carbide based materials,» *RSC Advances*, vol. 7, pp. 595-605, 2017.

[8] Y. Du, Y. Liu, A. Wang et J. Kong , «Research progress and future perspectives on electromagnetic wave absorption of fibrous materials.,» *iScience*, vol. 26(10), n° %1107873, 2023.

[9] B. Zhao, J. Deng, R. Zhang, L. Liang, B. Fan, Z. Bai, G. Shao et C. B. Park, «Recent Advances on the Electromagnetic Wave Absorption Properties of Ni Based Materials,» *Engineered Science*, vol. 3, pp. 5-40, 2018.

[10] E. T. -E. Directory, «EMC directory,» 30 january 2025. [En ligne]. Available: https://www.emc-directory.com/community/what-are-ferrite-tiles-construction-working-principle-and-applications. [Accès le 2025].

[11] D. Weston, Electromagnetic Compatibility: Principles and Applications, Second Edition, Revised and Expanded, USA: marcel dekker, 2001.

[12] X. C. Tong, Advanced materials and design for interference shielding, CRC Press, 2016.

[13] A. Goldman, handbook of modern ferromagnetic materials, NEW YORK: Springer science+business media , 1999.

[14] R. Benzerga, M. Badard, A. Sharaiha, C. Le Paven-Thivet et C. Méjean, «Rigid composite materials for anechoic chamber application,» *ELSEVIER,* vol. 96, n° %12, pp. 94-99, 2017.

[15] R. VICENTE, «A cone shaped taper anechoic chamber for antenna measurements in the 200 MHz to 18GHz frequency range,» chez *Antennas and Propagation & USNC/URSI National Radio Science Meeting*, Chicago, 2012.

[16] A. Natã Vicente, . G. Maciulis Dip et C. Junqueira, «The step by step development of NRW method,» chez *International Conference on Microwave and Optoelectronics (IMOC),* NATAL,BRAZIL, 2011.

[17] J. Baker-Jarvis, . M. D. Janezic, J. H. Grosvenor, R. G. Geyer et Jr, Transmission/Reflection and Short-Circuit Line Methods for Measuring Permittivity and Permeability, WASHINGTON: U.S. GOVERNMENT PRINTING OFFICE, 1993.

[18] Guerrieri, S. Kim et J. R, *Low-loss complex permittivity and permeability determination in transmission/reflection measurements with time-domain smoothing,* 2015.

[19] L. H. Hemming, Electromagnetic Anechoic Chambers: A Fundamental Design and Specification Guide, United States: IEEE press, 2002.

[20] D. Casillo, «isotechinc,» 2025. [En ligne]. Available: www.isotechinc.com.


Guide du projet
Pour obtenir un diplôme/startup
Dans le cadre de l'Arrêté Ministériel 1275
Décembre
2022
CNCSIIU
MHESR
ALGERIA

information's Card

about the supervision team and project team

1. Supervision team :

	Name	Specialty
supervisor	Dr MENASRI Wahiba	electrical engineering
Co supervisor	Dr ZOUBIRI Bachir	electrical engineering



2. Working team

	Name	Specialty
Student 1	LAROUSSI Manel	Telecommunications systems
Student 2	BENKESSIRAT Khadidja	Telecommunications systems



Index

Content

table of content

1. Project presentation 8
1.1 project idea: 8
1.2 Proposed value of project 8
1.3 Project team 9
1.4 Objectives of project 9
1.5 Planning of project 9
2. Innovative aspects 12
2.1 Nature of innovations: 12
2.2 Areas of Innovation: 12
3. Strategic Market Analysis 14
3.1 Market segment: 14
3.2 Marketing strategy: 14
4. Production plan 16
4.1 Production process 16
4.2 Supply and Procurement 16
4.3 workforce 17
4.4 key partners 17
5. Financial plan 19
5.1 Costs and Charges 19
5.1.1 Initial Production Costs 19
5.1.2 Equipment cost: 19
5.1.3 Operating cost 21
5.1.4 Unit price for each material: 21
5.1.5 12 months treasury plan (in Algerian Dinar - DA) 22
6. Tests and results and perspectives: 25
6.1 preparing materials and tests: 25
6.2 perspectives: 26

List of tables :

Table 1 : Project planning..... 10
Table 2: Materials cost. 19
Table 3: Equipment cost..... 20
Table 4: Operating cost. 21
Table 5: Unit price for each material..... 21
Table 6: Ferrite and graphite treasury plan. 22
Table 7: carbonyl iron treasury plan..... 23

List of figures :

Figure 1: The nature of innovation..... 12
Figure 2: Machine Zünd G3 Cutter..... 19
Figure 3: Machine Tormach 1100MX. 20
Figure 4: Material preparation and tests..... 25

Introduction

To enable students with innovative projects to develop their work, facilitate the design and drafting of their patents, and enable them to move from a simple idea to a complete invention, with details and information clarifying the innovative aspects of the project, its attractiveness, and the integrity of the logical sequence of ideas, the National Commission for Coordination, Monitoring of Innovation, and University Incubators has developed this document, which serves as a guide for students to write their dissertations in accordance with the provisions of Ministerial Decree No. 1275 Diploma – Startup.

The necessary presentations and explanations in the guide are illustrated through a very simple example to facilitate understanding of the different steps. This example relates to a project to produce natural juice from fruit that has not been subjected to pesticides or chemical fertilizers.

First axis:

Project presentation



1. Project presentation

1.1 project idea:

This project was inspired by a practical laboratory session conducted with Dr. Rebiai, where electromagnetic wave experiments yielded inaccurate results due to unwanted reflections in the testing environment. The incident highlighted the critical role of anechoic chambers. every anechoic chamber contains absorbers in its walls, its design has an important role to ensure reliable measurements. In response, this study focuses on the design, material selection, and geometrical optimization of electromagnetic absorbers operating over a broad frequency range (2–18 GHz)**.** The aim is to develop compact, efficient absorber models that can significantly minimize reflections across this wideband spectrum, improving the fidelity of measurements in educational and professional testing environments.

-Our offers:

- Manufacturing and installation of absorbers in labs or client rooms;
- A dedicated testing room available for paid use;
- Clients will need to replace absorbers after their lifetime.

Note: This is a paid service neither the products nor the testing access is free.

1.2 Proposed value of project

This project brings strong added value to the Algerian market, both academically and industrially. Currently, there is a noticeable lack of accessible anechoic testing environments in most universities and research institutions across the country. Laboratories often struggle with inaccurate measurements due to reflection problems, and importing absorbers is costly and not adapted to local needs.

Our project offers a local and practical solution, with the following benefits:

- Improved research quality in telecommunications, electronics, and antenna testing;
- Support for academic labs by providing treated environments or installation services;
- Creation of new market opportunities for manufacturing and technical services related to absorbers.

1.3 Project team

The project team is composed of the following members:

Student 01: LAROUSSI Manel has completed training in the field of telecommunication systems;

Student 02: BENKESSIRAT khadidja has completed training in the field of telecommunications systems.

1.4 Objectives of project

The main objectives of this project are:

- Design and develop electromagnetic absorbers that work efficiently across a wide frequency range (2–18 GHz);
- Reduce reflection problems in measurement environments to ensure accurate experimental results;
- Create a treated testing space accessible to students, researchers, and professionals;
- Offer installation services for clients who want to set up their own anechoic environments;
- Promote local production of absorbers to reduce reliance on imports;
- Support scientific research and education in Algeria with practical, affordable solutions;
- Build the foundation for a future business around absorber manufacturing and service.

1.5 Planning of project

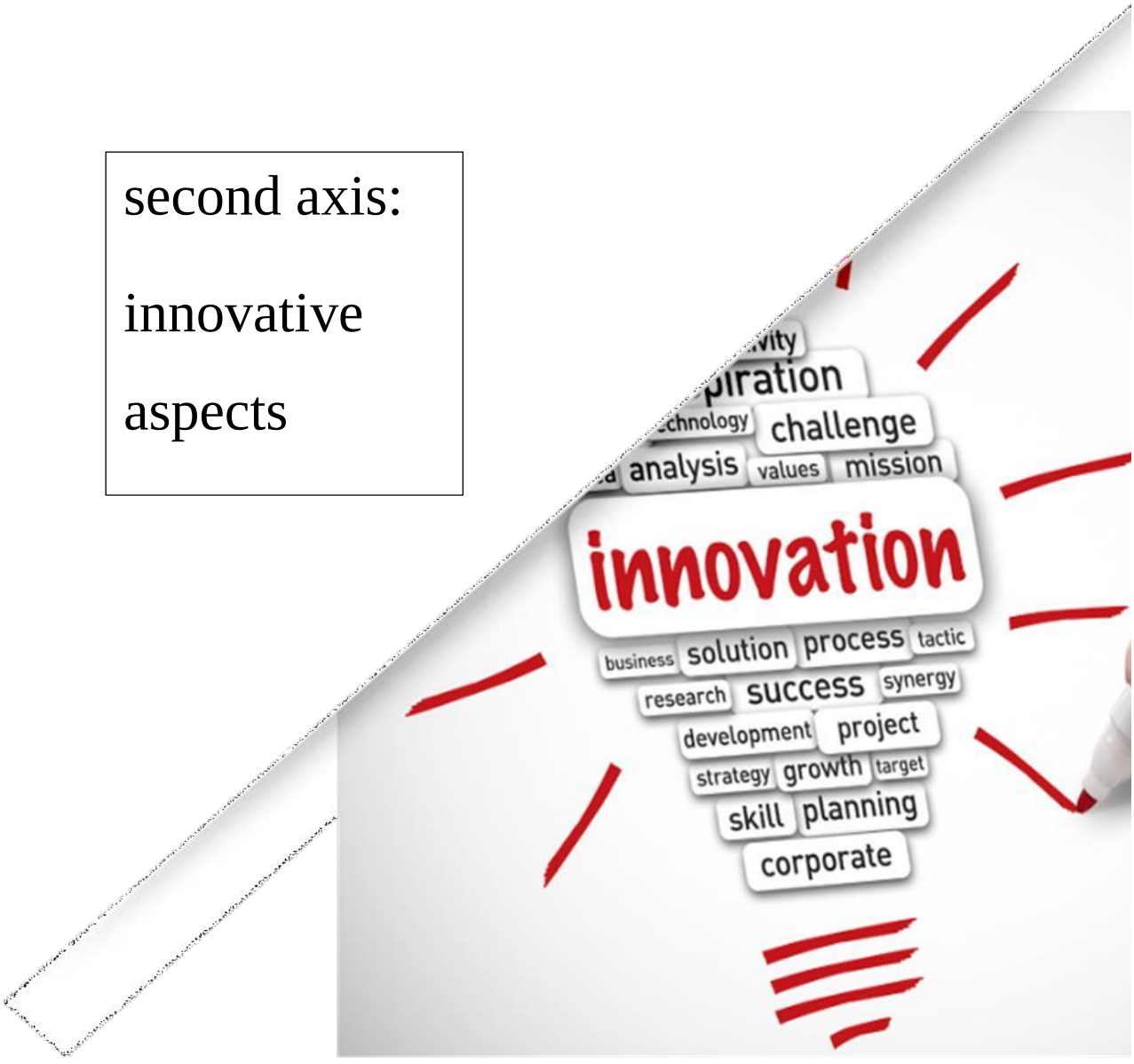
Table 1 represents the planning of the project from the beginnings of researches to the final step (tests of materials):

Table 1 : Project planning.

			1	**2**	**3**	**4**	**5**
1	Research and initial analyses	Study of materials, absorber types	✔	✔	✔	✔	
2	simulation	Designs tested and optimized using simulation tools.		✔	✔	✔	✔
3	tests	Tests of Materials					✔

second axis:

innovative aspects



2. Innovative aspects

2.1 Nature of innovations:

The nature of the innovations adopted in the project must be specified according to the proposals given in the following diagram as shown in figure 1:

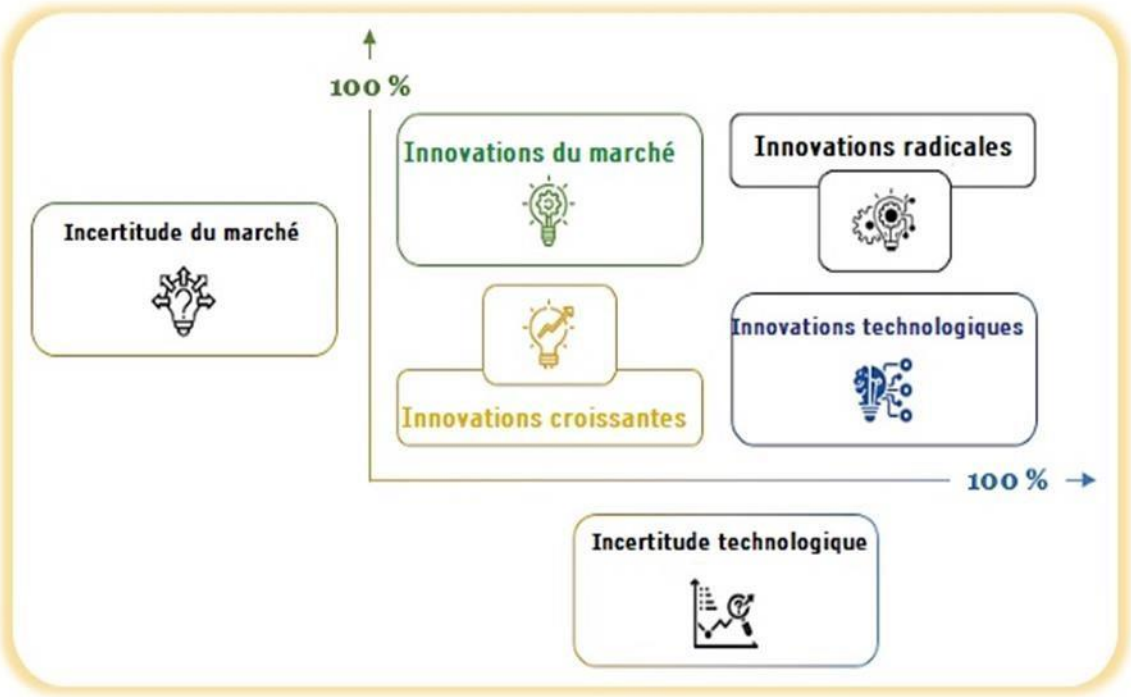


Figure 1: The nature of innovation

Our project represents a radicale innovation

2.2 Areas of Innovation:

The innovative aspects of the example presented are:

- Wideband absorber design covering 2–18 GHz, which is uncommon in local solutions;
- Compact and optimized geometry for better space efficiency;
- Flexible installation options adapted to client needs and room sizes;
- Dual-purpose approach both a functional testing room and a commercial service;
- First local initiative of its kind in Algeria for electromagnetic absorber manufacturing and installation.

third axis:

Strategic Market Analysis



3. Strategic Market Analysis

3.1 Market segment:

This project targets several key sectors in Algeria:

- Universities and Engineering Schools For academic research, and practical lab work;
- Research Centers and Laboratories For electromagnetic compatibility (EMC), antenna, and RF testing;
- Telecommunication Companies For equipment testing, network optimization, and R&D;
- Defense and Aerospace Sectors Where controlled electromagnetic testing is critical;
- Private Clients and Industrial Firms Interested in customized absorber installations for specific testing needs.

3.2 Marketing strategy:

The project will be presented as a local, reliable, and practical solution for electromagnetic absorber needs. It offers an alternative to expensive imported products, with designs made to suit local labs and testing rooms. To reach the right audience, the following methods will be used:

- Direct contact with universities, companies, and labs;
- Brochures and presentations sent to institutions;
- Participation in fairs, university events, and tech exhibitions;
- Word of mouth and recommendations from early clients.

fourth axis:

production plan



4. Production plan

4.1 Production process

The production of the electromagnetic absorbers goes through three main steps:

- **Materials preparation :**
  - Choosing the right materials (foam, ferrite, or composites) depending on how the absorber should perform;
  - Cutting and mixing the raw materials;
  - Preparing the base with the right size and thickness.
- **Shaping and Forming :**
  - Giving the absorber its final shape (pyramid, cone, or another form);
  - Making sure the shape is clean and accurate for better absorption;
  - Using tools like molds or CNC machines to keep the shape consistent.
- **Finishing and Testing :**
  - Adding any surface treatment if needed (for strength or heat resistance);
  - Checking the product visually and physically;
  - Testing a few samples in the lab to see how well they absorb signals;
  - Getting everything ready for delivery and installation.

4.2 Supply and Procurement

- The main raw materials used in this project are foam, ferrite, and magnetic composites**,** which are essential for the absorber structure. Since these materials are not available locally, they will be imported from international suppliers, especially during the first few months of the project.
- Suppliers will be chosen based on quality, technical compatibility, and cost**,** to make sure the absorbers perform well across the full 2–18 GHz frequency range.

4.3 workforce

- The project is expected to create about 2 direct jobs in the first year of production;
- the technical team will include 2 engineers in charge of design and simulation, and 1 technician responsible for manufacturing and installation work and 1 security stuff.

4.4 key partners

- Material suppliers are among the most important partners, since the project depends heavily on the quality of their components.
- University incubators will also play a key role by providing support for development, testing, and technical advice during the early stages.
- Finally, funding organizations will be essential in helping launch the project and supporting its growth over time.



fifth axis:

Financial plan



5. Financial plan

5.1 Costs and Charges

5.1.1 Initial Production Costs

The table 2 define the basic material costs needed to produce the first absorber units:

Table 2: Materials cost.

Raw Materials	Quantity	Total Price (DA)	Unit Price
Graphite Powder	50 kg	500,000	10,000 DA / kg
Carbonyl iron.	50 kg	750,000	15,000 DA / kg
Ferrite Powder	50 kg	500,000	10,000 DA / kg
Binders	50 liters	150,000	3,000 DA / liter

5.1.2 Equipment cost:

figure 2 represents the machine Zünd G3 Cutter



Figure 2: Machine Zünd G3 Cutter.

Figure 3 represents the machine Tormach 1100MX



Figure 3: Machine Tormach 1100MX.

Table 3 show the machines and tools cost required to begin manufacturing

Table 3: Equipment cost.

Equipment	Estimated Price (DA)	Notes
Zünd G3 Cutter	1,500,000	For precision cutting of materials
Tormach 1100MX (CNC Milling Machine)	2,000,000	For Mold fabrication (pyramids)
Molds for pyramid shaping	100,000	Reusable molds
Worktables & assembly Tools	60,000	Manual Tools, benches, etc.
Safety gear & ventilation system	40,000	For a safe working environment

5.1.3 Operating cost

These are the ongoing costs to maintain the production facility like shown in the table 4:

Table 4: Operating cost.

Cost Item	Months 1–2 (DA)	Months 3–12 (DA)
Technician salary	35,000	35,000
Direct workers (2 × 30,000)	0	60,000
Security staff	20,000	20,000
Electricity & Water	30,000	30,000
Maintenance & Insurance	9,000	9,000
Taxes & Admin Fees	10,000	10,000
Workshop Rent (Loyer)	50,000	50,000
Depreciation (Zünd G3 + Tormach)	38,690	38,690
Total Operating Cost	187,690	247,690

5.1.4 Unit price for each material:

Table 5 represents the unit price for each material with 25% of a profit margin:

Table 5: Unit price for each material.

Materials Type	Unit Price (DA)
Ferrite/Graphite	8,300
Carbonyl Iron.	11,425

5.1.5 12 months treasury plan (in Algerian Dinar - DA)

- **Ferrite tile or graphite**:

Table 6 describes the ferrite and graphite treasury plan

Table 6: Ferrite and graphite treasury plan.

Month	Income (DA)	Material Cost (DA)	Op Cost (DA)	Net Cash-Flow (DA)	Cumulative Balance (DA)
1	0	500,000	187,690	−687,690	−687,690
2	0	0	187,690	−187,690	−875,380
3	0	0	247,690	−247,690	−1,123,070
4	830,000	500,000	247,690	+82,310	−1,040,760
5	830,000	0	247,690	+582,310	−458,450
6	830,000	0	247,690	+582,310	+123,860
7	830,000	500,000	247,690	+82,310	+206,170
8	830,000	0	247,690	+582,310	+788,480
9	830,000	0	247,690	+582,310	+1,370,790
10	830,000	500,000	247,690	+82,310	+1,453,100
11	830,000	0	247,690	+582,310	+2,035,410
12	830,000	0	247,690	+582,310	+2,617,720

- **Carbonyl iron**

Table 7 defines the carbonyl iron treasury plan

Table 7: carbonyl iron treasury plan.

Month	Income (DA)	Material Cost (DA)	Op Cost (DA)	Net Cash-Flow (DA)	Cumulative Balance (DA)
1	0	750,000	187,690	−937,690	−937,690
2	0	0	187,690	−187,690	−1,125,380
3	0	0	247,690	−247,690	−1,373,070
4	1,142,500	750,000	247,690	+144,810	−1,228,260
5	1,142,500	0	247,690	+894,810	−333,450
6	1,142,500	0	247,690	+894,810	+561,360
7	1,142,500	750,000	247,690	+144,810	+706,170
8	1,142,500	0	247,690	+894,810	+1,601,000
9	1,142,500	0	247,690	+894,810	+2,495,810
10	1,142,500	750,000	247,690	+144,810	+2,640,620
11	1,142,500	0	247,690	+894,810	+3,535,430
12	1,142,500	0	247,690	+894,810	+4,430,240

-The primary funding source for this project is a loan or support program from the Ministry of Higher Education and Scientific Research**.** Additional support may come from university incubators or startup programs, especially for acquiring high-tech equipment like the Zünd G3 and Tormach 1100MX.

Sixth axis :

Tests, results and perspectives





6. Tests and results and perspectives:

6.1 preparing materials and tests:

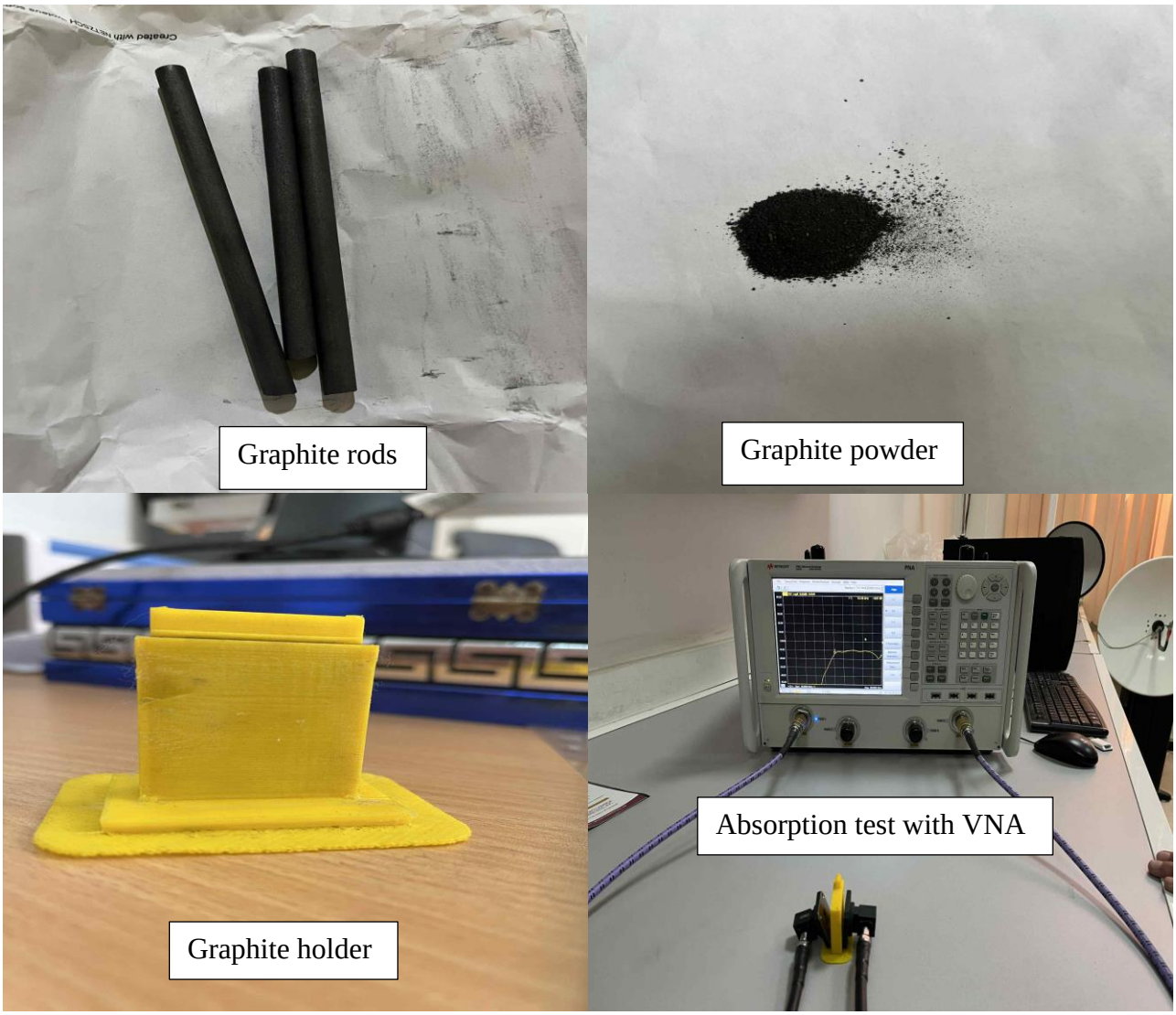
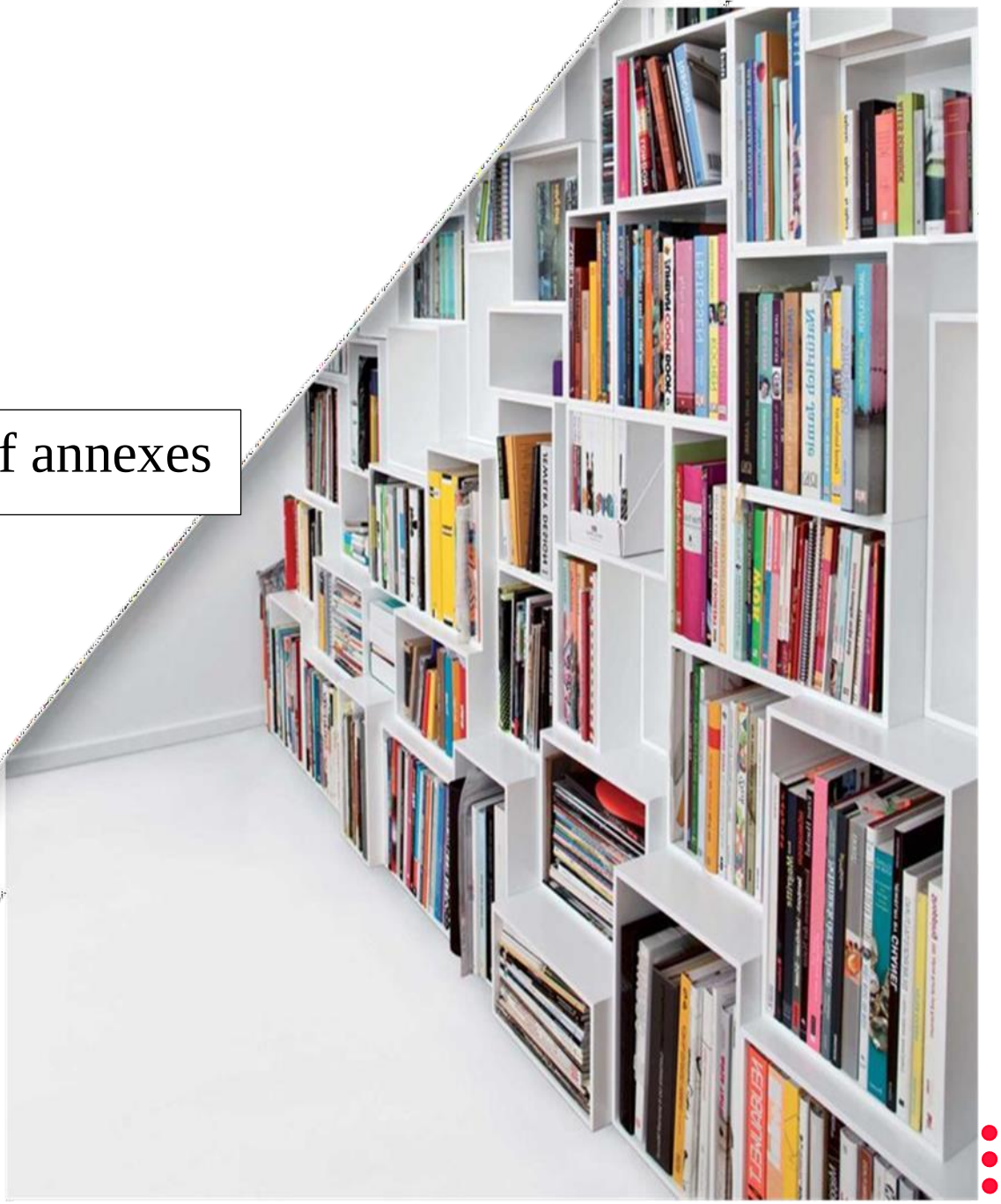


Figure 4: Material preparation and tests.

6.2 perspectives:

This project aims to provide a practical solution to improve electromagnetic testing environments by designing and producing efficient absorbers. As part of our work, we tested the material used to evaluate its performance. In the future, we plan to manufacture the pyramidal absorbers locally, which can support research, education, and industry in Algeria while reducing reliance on imported products. The project also has the potential to grow into a service or business that offers absorber production, installation, and access to treated testing spaces.

List of annexes



Business Model Canvas

Key Partners

- Raw-material suppliers
- University incubator
- Funding agencies/ministry
- Logistics and shipping partners

Key Activities

- Simulation-based absorber design & optimization
- Material preparation & manufacturing
- Anechoic testing of prototypes
- Client installation & after-sales service

Key Resources

- Project team (students, supervisors) • Equipment: Zünd G3, Tormach 1100MX, molds
- Production/test space
- Material suppliers (ferrite, graphite, composites)

Value Propositions

- Wideband absorbers (2–18 GHz) in compact, optimized geometries
- Local manufacturing, installation & maintenance
- Paid access to a dedicated test room

Customer Relationships

- On-site installation & maintenance support
- Training on product use
- Loyalty built through regular testing and absorber replacements

Channels

- Direct outreach to universities/labs
- Fairs, conferences & brochures
- Professional website
- Referrals via incubator and partner networks

Customer Segments

- Universities & research labs
- Telecommunications companies
- R&D, defense & aerospace centers
- Industrial clients requiring anechoic testing environments

Cost Structures

- Fixed monthly costs: salaries, utilities, rent, insurance, machine depreciation
- Variable costs: material cost per absorber unit

Revenue Streams

- Sale and installation of absorbers
- Paid usage of the test room
- Maintenance contracts and periodic absorber replacement services

